Dynamics of the Hadley cell and its implication for solar energy resources over South Africa.

BY

DAWN DUDUZILE MAHLOBO
(1513523)

School of
Geography, Archaeology and Environmental Studies

Submitted to the Faculty of Science, University of the Witwatersrand, Johannesburg, in partial fulfilment of the requirements for the degree of Doctor of Philosophy

(Geography and Environmental Science)

Supervisors: Prof. Stefan Grab
Dr. Thando Ndarana
Prof. Francois Engelbrecht
March 2019

Declaration

I declare that this thesis is my own, unaided work except where acknowledged. It is being submitted for the Degree of Doctor of Philosophy in the University of the Witwatersrand, Johannesburg. It has not been submitted before for any degree or examination in any other University.

_____

Dawn Duduzile Mahlobo

15 July 2019

Dedication

In memory of my late father, Rev Robert Hlatshwayo

Acknowledgements

I would like to express my sincere gratitude to my supervisors, Dr Thando Ndarana, Prof. Stefan Grab and Prof. Francois Engelbrecht for their guidance, input and support in making this academic journey a success. I'm thankful to the National Research Foundation for funding the study. I also acknowledge the European Centre for Medium-Range Weather Forecasts (ECMWF), South African Weather Service, Council for Scientific and Industrial Research, Department of Energy as well as Stats South Africa for the data used in the study. I am greatly indebted to my husband Khumbuza who have been a pillar of strength throughout the study. My children Nolizwi, Makabongwe and Zethembiso are acknowledged for making this experience worthwhile. I'm grateful to my mom Esther for her encouragement, friendship and consistent prayers. I would like to extend my gratitude to all my friends, sisters and brother. Lastly all glory belongs to God; You always exceed my expectations as you have said it in Ephesians 3:20.

Abstract

This study was inspired by the need to investigate interactions between the Hadley cell, total cloud cover as well as sunshine duration over South Africa and how the Hadley cell impacts energy generation in South Africa. To diagnose the local Hadley circulation two methods are used; first the zonally averaged mass stream function, and second the stream function vector method. The two methods are applied to the ERA-Interim reanalysis data for the period 1980–2015, to calculate both the climatology and trends of the Hadley cell. Both diagnostics advocate downwards massflux being dominant over the subtropics, particularly over South Africa, yet the strength of Hadley is seasonal. Contrasts have been found between linear trends of the two diagnostics. Zonally symmetric diagnostics indicate strengthening of the Hadley cell, particularly in the subtropics of the Southern Hemisphere in winter and weakening in summer. The zonally asymmetric results indicate maximum strengthening of the Hadley over South Africa to be in spring and weakening in summer. Furthermore, maximum decrease in cloud cover and increase in sunshine duration over South Africa is in spring, implying more opportunities for solar energy generation. The causality between the Hadley cell and cloud cover as well as sunshine duration was further explored. Granger causality between the Hadley cell and cloud cover as well as the Hadley cell and sunshine duration was analysed by means of a bivariate vector autoregressive model. Suitability of the time series was tested by means of a Dickey Fuller test and both time series failed the stationary test. To attain stationarity, the time series were first differenced. The presence of Granger causality was established between the two time series, with causal direction predominantly from the Hadley cell to cloud cover. Areas of strong causality are found over the north-western parts of South Africa. However, weak causality from cloud cover to the Hadley cell does exist, with vertical velocity being the main variable responsible for this causality, and hence indirectly affects cloud cover to Hadley cell causality. Granger causality has also been established between the Hadley cell to sunshine duration and no causality from sunshine duration to the Hadley cell was established. The behaviour of the Hadley cell, rainfall and temperatures over South Africa under the RCP 8.5 scenario and its implication to energy generation was examined. The statistical downscaled data from a regional climate model CCAM is used. The Hadley cell has been strengthening and is projected to strengthen for all seasons except DJF. Consequently, rainfall is projected to decrease during all seasons. In DJF, rainfall is projected to decrease only over the western parts, while it is expected to increase over the central and eastern regions of South Africa. Mean temperatures are projected to increase during all seasons. Changes in the Hadley cell, rainfall and temperature, have strong implications to the electricity generation in South Africa. A further advantage in understanding the Hadley cell is that it could also be used to locate areas with solar potential in South Africa.

Table of Contents

Page No.

Dedication ii

Acknowledgements iii

Abstract iv

Table of Contents v

List of acronyms vii

Chapter1: Introduction 1

Project research questions 5

Objectives of the research questions 6

Thesis outline 8

Chapter2: Preface 11

Paper 1: Integrated climatology and trends in the subtropical Hadley cell, sunshine duration and cloud cover over South Africa 12

Chapter 3: Preface 55

Paper 2: Granger causality of the local Hadley cell and cloud cover over South Africa 56

Chapter 4: Preface 96

Paper 3: Granger causality of the local Hadley cell and sunshine duration over South Africa 97

Chapter 5: Preface **119**

Paper 4: Link between the local Hadley circulation and energy generation in South Africa **120**

Chapter 6: Summary **152**

List of acronyms

- ACCESS1-0 Australian Community Climate and Earth System Simulator
- ADF Augmented Dickey Fuller
- ACCESS1-0 Australian Community Climate and Earth System Simulator
- AIC Akaike Iinformation Criteria
- BIC Bayesian Information Criteria
- CCAM Conformal-Cubic Atmospheric Model
- CCSM Community Climate System Model
- CNRM–CM5 National Centre for Meteorological Research Coupled Global Climate Model, version 5
- COLs Cut-Off-Lows
- CSIR Council for Scientific and Industrial Research
- CSP Concentrated Solar Power
- DEA Department of Environment Affairs
- DoE Department of Energy
- DJF December January February
- DWA Department of Water Affairs
- ECMWF European Centre for Medium-Range Weather Forecasts
- ERA-Interim European Centre for Medium-Range Weather Forecasts Interim Reanalysis
- EC Eastern Cape
- GAU Gauteng
- GCMs Global Climate Models
- GDP Gross Domestic Product
- GFDL-CM3 Geophysical Fluid Dynamics Laboratory Coupled Model
- GGP Gross Geographic Product

- GHGs Green House Gases
- HC Hadley Cell
- HCE Hadley Cell Edge
- HCI Hadley Cell Intensity
- IPP Independent Power Producers
- IRP Integrated Resource Plan
- ITCZ Inter-Tropical Convergence Zone
- JJA June July August
- KZN KwaZulu-Natal
- LEAP Long-range Energy Alternatives Planning
- MAM March April May
- MPI-ESM-LR Max Planck Institute Coupled Earth System Model
- MPU Mpumalanga
- NC Northern Cape
- NAO North Atlantic oscillation
- NCAR National Centre for Atmospheric Research
- NRF National Research Foundation
- NW North West
- PV Photovoltaic
- RCM Regional Climate Model
- RCP Representative Concentration Pathway
- REF Reference
- REIPPP Renewable Energy Independent Power Procurement Programme
- REN Large scale Renewables
- REN_PV_embedded Renewables plus embedded PV

- SAWS South African Weather Service
- SEI-B Stockholm Environment Institute, Boston
- SH Southern Hemisphere
- SON September October November
- SSTs Sea Surface Temperatures
- TARWS Total Actual Renewable Water Resources
- TCC Total Cloud Cover
- TED Technology and Environmental Database
- TTTs Tropical-Temperate Troughs
- UNEP United Nations Environment Programme
- VAR Vector Autoregressions
- WC Western Cape
- WEAP Water Evaluation and Planning
- WMO World Meteorological Organisation

Chapter 1
Introduction

1 Background

The Hadley cell is defined by Wallace and Hobbs (2006), and many other systematics reviews of atmospheric processes, as a large scale atmospheric circulation that is caused by differential heating of the earth's surface. Unlike the Ferrell cell poleward of it, it is a thermally direct circulation that is characterised by ascending and descending branches in the tropical and subtropical regions, respectively. Because air is warm and moist near the equator; it rises and diverges polewards in the upper troposphere and subsides in the subtropics within the cell. This situates it in tropical-subtropical belt in each hemisphere (Ceppi and Hartman, 2013) and renders it the most protruding feature of the atmospheric circulation (Kang and Lu, 2012). Therefore, its meridional extent characterizes the climates of the tropical and subtropical regions. On average, the subsiding branch of the Hadley cell is dry, warm and cloud free. This causes arid and semi-arid climates in the subtropical regions. This has important implications for the solar energy resource along the subtropical belts, and over South Africa in particular.

The Hadley cell boundaries are characterized by a pole-ward extent of subsidence in the subtropical zones as well as the location of subtropical jets boundaries (Seidel et al., 2008). The subtropical jet, which is a thermally driven jet stream, is a boundary between regions of small total ozone in the tropics and higher values in the mid-latitudes (Hudson et al., 2003). The Hadley cell plays an integral role in the context of climate change and associated changes in the atmospheric circulation. Several studies have shown that the Hadley cell has progressively been widening (Johanson and Fu, 2009; Choi et al., 2014; Hu and Fu, 2007; Lu et al., 2007). As a consequence, the subtropical jets have been shifting poleward and the cell has widened by about 3 degrees of latitude since 1979 (Johanson and Fu, 2009). The widening of the Hadley cell has been confirmed by many other studies (e.g. Hu and Fu, 2007) using the poleward shift of outgo-

ing long wave radiation contours at the boundaries of the tropics and a poleward displacement of subsidence in the subtropical dry zones as indicators of these changes. Complementary to these observed changes in the Hadley circulation, Seidel and Randel (2007) showed that increased frequency of higher subtropical tropopause heights and the widening of the subtropical dry zones may have detrimental effects to precipitation and moisture budget in these regions. These changes have largely been attributed to increases in the concentrations of greenhouse gases (GHGs) in the atmosphere (Lu et al., 2007). It is expected that as GHG concentrations continue to increase into the future under various scenarios (IPCC, 2007), the changes discussed above will persist, depending on the prevailing GHG reality. In addition to this meridional expansion, some studies have suggested that the descending branch is strengthening (Engelbrecht et al., 2011; Loeb et al., 2014; Grenfell, 2003) and will continue to do so in future. As it is well known in meteorology and climatology, in as far as atmospheric motion is concerned, clouds form as a result of rising air parcels which cool adiabatically and moisture condenses. Descending motion leads to less cloud formation. Therefore, the broadening and strengthening of the descending branch of the Hadley cell will lead to broader subtropical regions of cloudless skies and higher frequencies of cloudless days.

Clouds play an integral role in the earth's atmosphere and they involve a wide range of space and time scales (Bergman and Salby, 1996; Salby, 1991). They interact strongly with long wave and short wave radiation, which affects the distribution of surface and atmospheric heating. This, in turn, modulates atmospheric motions (Bergman and Salby, 1996). Through their characteristics and movement, clouds can also be seen as indicators of atmospheric motion as well as contributors to atmospheric and oceanic energetics (Bergman and Salby, 1996; Bergman and Salby 1997; Warren et al., 1986). For this reason, the effects of cloud cover should not be separated from atmospheric circulation changes (Lau and Crane, 1995; Young et

al., 2012), through the changes in the Hadley cell.

A number of studies on cloud cover climatologies and trends have been documented. Wang and Key (2003), (2005a) and (2005b) investigated trends in cloud and radiation properties over the Arctic, a cooling trend was found in winter and a warming trend dominated in spring, summer and autumn. On the other hand, an increased total cloud cover for the period 1950-1980 was found by Karl and Steurer (1990). A non-linear relationship exists between cloud cover and solar radiation in fact; cloudiness is the key regulator of solar radiation in the atmosphere and contributes substantially to multidecadal changes in downward solar flux (Norris and Wild, 2007).

Global solar radiation could be estimated from cloud cover (Lorente et al., 1996; Hamdy, 2007). Under cloudy conditions, the incoming solar radiation is reduced at the surface but in some instances, clouds may cause the radiation levels to exceed the expected clear sky value (Pfister et al., 2003). Although some studies state that increase in low level cloud cover is usually associated with reductions in solar flux (Abakumova et al., 1996; Qian et al., 2006); other studies showed similar trends for the occurrence of surface solar radiation under both cloudy and clear sky conditions (Liepert, 2002; Wild et al., 2005). Solar radiation that reaches the surface has a strong longitudinal gradient and so does sunshine duration; since sunshine duration can be used to estimate solar radiation (Falayi et al., 2008). South Africa has abundant sunshine (Kruger and Esterhuyse, 2005); since it is located on the subtropical belt, where the Hadley cell descending branch is located. This study was inspired by the need to investigate more about the interactions, between the Hadley cell, total cloud cover as well as sunshine duration over South Africa. The Hadley cell diagnostics could further be used as a proxy to climate change impact studies. The conclusions found in this study will therefore contribute to a better understanding

of the generation of energy, not only in South Africa, but also to southern Africa.

2 Project research question

In its Integrated Resource Plan (IRP) 2010, the South African government has identified a number of renewable energy options to inform the country's energy mix on the 2030 horizon and beyond. One of these options is solar energy, which depends on the ability of incoming short wave radiation to penetrate through the atmosphere to the ground, where solar energy conversion technologies are located. One of the major phenomena that influence solar power generation is large scale cloud formation. As the former might be impacted by climate change (Crook et al., 2011), increasing GHGs might present opportunities or threats to South Africa's renewable energy industry since this would influence the country's ability to generate electricity from the solar energy resource.

Large scale cloud formation requires two things to occur; the large scale ascent of atmospheric processes and enough moisture content for adiabatic cooling to lead to condensation. A review of such thermodynamical processes can be found in many well-known text books such as Wallace and Hobbs (2006). Over South Africa, this large scale ascent is informed by the subtropical branch of the Hadley cell, and so climate change induced changes in this branch might have a knock-on effect that eventually ends up enhancing or threatening solar power generation as depicted schematically in Figure 1. A detailed analysis over South Africa of this causal knock-on effect is dependent on the ability to properly diagnose Hadley cell motions over the country. The necessity of such diagnostics is clearly indicated by the zonal gradient of rainfall during the summer and the dominance of the winter high pressure system over the country (van Heerden and Taljaard, 1998).

The unavailability of local Hadley cell diagnostics have prevented a detailed dynamical analysis of GHGs concentrations on changes in the subtropical branch of this cell over South Africa, and its subsequent impacts on large scale cloud formation and solar generation. This begs the broad (as in indicated by the large curved arrow above the boxes in Figure 1) research question that can be stated as follows: Can a causal effect of changes in the subtropical branch of the Hadley cell on cloud formation and solar power generation be established over South Africa?

3 Objectives of the Research

This study investigates the effect of the Hadley cell expansion to cloud cover in South Africa and the resulting implications on energy generation in South Africa. Therefore the overall objective of this study is to establish a causal chain reaction that begins with climate induced changes on the Hadley cell upstream and ends with solar power generation downstream (Figure 1). The specific objectives are:

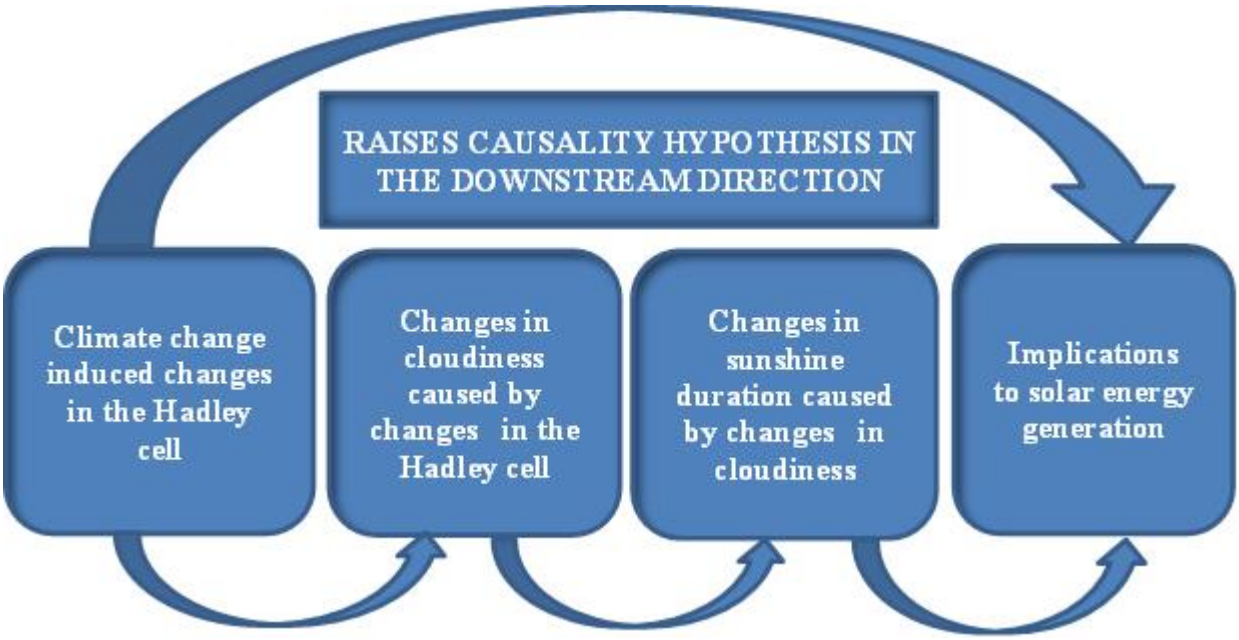

Figure 1: Schematic diagram showing the causal knock on effect that begins with climate change induced changes in the Hadley circulation up stream and ends with solar power generation downstream.

- To form an integrated climatology of the Hadley cell, cloudiness and sunshine duration and associated trends over South Africa;
- To establish the influence and associated causality of observed changes in the subtropical branch of the Hadley cell on trends in cloudiness over South Africa;
- To establish the influence of climate induced changes on the Hadley cell on sunshine duration over South Africa; and
- To determine the implications of the changes in the Hadley cell caused by climate change on energy generation over South Africa.

These objectives and related research questions are addressed in chapters 2, 3, 4 and 5 in the form of published,accepted and submitted peer reviewed journal papers. The period for the study spans 1980-2014 for objectives 2-3 and 1980-2099 for objective 4.

4 Thesis outline

Six chapters are transcribed within this thesis. Chapter 1, as already outlined, gives a background on the Hadley cell and its possible link to cloud cover and sunshine duration. The main objectives of this study are also outlined in Chapter 1. Chapter 2 lays the foundation of the study, by producing local Hadley cell diagnostic over South Africa, using the method of Schwendike et al., (2014). These diagnostics are further used throughout the study to meet different objectives as outlined in Chapter 1. The psi-vector method of Keyser et al. (1989) is used to partition the irrotational part of the three dimensional flow into a pair of orthogonal two-dimensional circulations. This analysis leads to a vertical flow field that can be decomposed into longitudinal and latitudinal parts, which in turn are used to define two zonally varying vertical fluxes that can be used to define the local Hadley and local Walker circulations, respectively. The partitioning of the vertical flow field in the zonal and meridional planes is made possible by the psi-vector that is obtained via a non-homogenous Poisson's partial differential equation. Given vertical motion (omega) obtained from reanalysis data, the Poisson's equation is solved using FORTRAN 77 subroutines of Swarztrauber (1974) as in D'Abreton and Tyson (1995). This method is applied to Era-Interim reanalysis datasets to produce a time series of local Hadley cell. An integrated climatology of the Hadley cell, cloud cover and sunshine duration is then formed over South Africa. Linear trends of these annual time series are calculated per season and the two-sided t-test is used to ascertain statistical significance, following Kruger (2007).

Chapter 3 introduces the concept of Granger causality to establish the causality between the Hadley cell and cloud cover. This method is also used in Chapter 4. To test the relationship between the Hadley cell and cloud cover, the Granger causality test (Granger, 1969) is employed as a three steps procedure. Firstly the suitability of the time series of both cloud cover and Hadley cell is tested for stationarity. The non-stationarity in the data is excluded by detrending the non-stationery variables using the backwards differences (Granger, 1969). Secondly, the model which makes the best fit to the time series is chosen, by using (BIC and AIC) information criteria. Thirdly, the simple two-variable model autoregressive process of finite order is used. The model uses past and current cloud cover and the Hadley cell values to forecast both variables. Using the bivariate model, two hypotheses are defined to test the causality of the cloud cover to Hadley cell. The first hypothesis normally called the Null hypothesis states no causal impact of cloud cover to the Hadley cell and the second hypothesis opposes the first one by implying the past cloud cover data are used to predict the strength of the Hadley cell. The first hypothesis is rejected in order to prove the causality of cloud cover to the Hadley cell, if not then there is no causality between cloud cover to the Hadley cell. Similarly the causality of the Hadley cell to cloud cover is also tested.

In Chapter 4, the causality between the Hadley cell and sunshine duration is tested using the Granger causality explained in Chapter 3. The Hadley cell diagnostics used were calculated in Chapter 2. In Chapter 5, the implications caused by the Hadley cell in energy security over South Africa are investigated. The Long-range Energy Alternatives Planning system (LEAP) is used to explore such. The LEAP system is developed by the Stockholm Environment Institute, Boston (SEI-B). The LEAP is used to investigate the role of the Hadley cell to energy generation. The LEAP includes an environmental database namely the Technology and Environmental Database (TED), which has been developed jointly by SEI-B, and the United Nations

Environment Programme (UNEP) (SEI, 2008). TED provides information describing the technical characteristics, costs, and environmental impacts of different energy technologies. As such, TED allows for the tracking of pollution resulting from each stage of the fuel chain. The demand and supply-side energy flows are analysed from the initial point of primary energy and secondary energy production, transformation, losses in transmission, and distribution to the end-users (SEI, 1995). The LEAP is used to assess the current energy patterns and for simulating alternative energy futures along with GHG emissions under a range of user-defined.

The summary and general conclusions are presented in Chapter 6. Given that all figures and tables are specific to the papers sent to Journals for publication, a list is not included in the contents section. Furthermore, a specific reference list specific to each paper and constructed according to each journal requirements is added at the end each paper (Chapters 2-5). The reference list for the first and last chapters is provided at the end of Chapter 6.

Chapter 2
Integrated Climatology of the Hadley cell, cloud cover and sunshine duration over South Africa
Preface

This chapter consists of published paper and is cited as follows:

Mahlobo DD, Ndarana T, Grab S and Engelbrecht F, 2018: Integrated Climatology of the Hadley cell, cloud cover and sunshine duration over South Africa, International Journal of Climatology. 39. 1805-1821.

This study produces local asymmetric diagnostics of the Hadley cell over South Africa. Using these diagnostics a combined climatology of the Hadley cell, cloud cover and sunshine duration is established over South Africa. Furthermore a combined trends analysis of the three variables is also established over South Africa. The paper addresses objective 1 of the study, while it lays foundations for objectives 2 to 4.

An integrated climatology and trends of the subtropical Hadley cell, sunshine duration and cloud cover over South Africa

ABSTRACT: This study uses two methods to diagnose the local Hadley circulation; first the zonally averaged mass streamfunction, and second the stream function vector method. The two methods have been applied to the ERA-Interim reanalysis data for the period 1980-2015 to calculate both the climatology and trends of the Hadley cell. Both diagnostics advocate downwards massflux being dominant over the subtropics, particularly over South Africa, yet the strength of Hadley cell is seasonal. Contrasts have been found between linear trends of the two diagnostics. Zonally symmetric diagnostics indicate strengthening of the Hadley cell, particularly in the subtropics of the Southern Hemisphere in winter and weakening in summer. The zonally asymmetric results indicate maximum strengthening of the Hadley cell over South Africa to be in spring and weakening in summer. Furthermore, maximum decrease in cloud cover and increase in sunshine duration over South Africa is in spring, implying more opportunities for solar energy generation.

Keywords: Hadley circulation, streamfunction, massflux, total cloud cover, sunshine duration

1.INTRODUCTION

The Hadley cell may be defined as a large-scale meridional circulation regime that is caused by differential heating at the earth's surface (e.g., Wallace and Hobbs, 2006). Unlike the Ferrell

cell polewards of it, it is a thermally direct circulation that is characterized by ascending and descending branches in the tropical and subtropical regions, respectively. The convergence of warm air in the equatorial trough leads to uplift and polewards divergence in the upper troposphere and subsidence in the subtropics within the cell (under the influence of the Coriolis effect). The Hadley cell spans the tropical–subtropical belt in each hemisphere (Ceppi and Hartmann, 2013) and is the most prominent single circulation feature of the atmospheric circulation (Kang and Lu, 2012). The meridional extent of the Hadley cell characterizes the climates of the tropical and subtropical regions. On average, the air in the subsiding subtropical branch of the Hadley cell is dry and warm, which suppresses convective cloud formation.

As a consequence, the climates of subtropical land regions are largely arid to semi-arid, particularly on the west coast side of continents. The Hadley cell has been demonstrated to play an integral role in the context of anthropogenic-induced climate change and associated changes in the atmospheric circulation. Several studies have shown that the Hadley cell has progressively been widening (e.g., Johanson and Fu, 2009). Seidel and Randel (2007) demonstrated that increased frequency of higher subtropical tropopause heights and widening of the subtropical dry zones may have detrimental effects to precipitation and moisture budget in these regions. These changes have largely been attributed to increases in the concentrations of greenhouse gases (GHGs) in the atmosphere (Lu et al., 2007). During the austral summer months, ozone depletion has also played a role in augmenting the effects of GHGs (Polvani et al., 2011). It is expected that as GHG concentrations continue to increase into the future under various mitigation scenarios (Solomon et al., 2007), the changes discussed above will persist. During the summer months, future widening will depend on the prevailing GHG scenario that actually materialize, with an opposing effect induced by ozone recovery (Polvani et al., 2011). For the strongly mitigated GHG scenario—Representative Concentration Pathway (RCP) 2.6-ozone re-

covery will overwhelm the impact of GHG's and widening will be reversed. With the RCP 8.5 (low mitigation) scenario, the effect of the GHGs will overwhelm that of ozone depletion, resulting in a continued widening of the Hadley cell (Johanson and Fu, 2009).
In addition to this meridional expansion, some studies have suggested that the descending branch is strengthening (e.g., Engelbrecht et al., 2009; Engelbrecht et al., 2011) and will continue to do so in future under low mitigation. This has been postulated as a key reason for the projected decrease in rainfall over southern Africa under low mitigation scenarios (Engelbrecht et al., 2009). Indeed, a widening and potential strengthening of the Hadley cell could lead to decreasing cloud cover and increasing sunshine or solar radiation over the subtropical land regions.

Clouds play an integral role in the earth's atmosphere and they involve a wide range of space and timescales (Bergman and Salby, 1997). They interact strongly with long wave and short wave radiation, which affects the distribution of surface and atmospheric heating. This in turn modulates atmospheric motions (Bergman and Salby, 1997). Through their characteristics and movement, clouds can also be seen as indicators of atmospheric motion as well as contributors to atmospheric and oceanic energetics (Warren et al., 1986). For this reason, the effects of cloud cover should not be separated from atmospheric circulation changes, as indicated above through potential changes in the Hadley cell. Cloud processes, including their interaction with atmospheric dynamics as well as their influence on the surface, must be understood clearly in order to understand climate regimes and circulation systems.

Solar radiation and sunshine duration at the earth's surface are impacted by cloud cover and could thus also be affected by changes in the Hadley circulation. The available solar energy at the earth's surface is determined by surface net solar radiation and is a renewable energy

resource (Kaggwa et al., 2011). The spatial and temporal distribution of solar radiation at the earth's surface under contemporary climate change is thus important to understand in order to assess climate change impacts on circulation and to understand impacts on the solar potential for renewable energy generation (e.g., Ruiz-Arias et al., 2011). According to Power and Mills (2004), South Africa has high climatological insolation values, receiving about 24 GWhm^{-2} per annum of solar radiation (Bugaje, 2006).

The topography of South Africa plays an important role in cloud cover and sunshine duration distribution (see Figure 1). The nine provinces of South Africa, Western Cape (WC), Eastern Cape (EC), Northern Cape (EC), North West (NW), Gauteng (GAU), Mpumalanga (MPU) and Limpopo are also shown in Figure 1. The western interior of South Africa receives more than 80% of possible annual sunshine. The eastern parts of South Africa receive a smaller percentage (50–60%) of possible annual sunshine due to greater cloud cover. The highest mean total radiation occurs during summer in the least cloudy western parts of the country (Tyson and Preston-Whyte, 2000; Kruger and Esterhuyse, 2005). Trends in cloud cover, solar radiation and sunshine duration for various regions have been documented in a number of studies (e.g., Liepert, 2002; Groisman et al., 2004; Wang and Key, 2005). A recent study (Singh and Kruger, 2017) on sunshine duration trends using point observations from 22 sunshine recording stations across South Africa identified a general decreasing trend for all seasons. However, the decrease was most prominently observed for the summer season. Over most parts of South Africa, Warren et al. (2007) found a decreasing trend in annual mean daily cloud cover. Kruger (2007) examined cloud cover trends over South Africa for the period 1960–2005 and found a decrease in both low and total cloud cover over much of the country. The extent of increasing cloud cover trends is greatest in spring and summer over the southern parts of South Africa.

The abundance in solar radiation and sunshine over South Africa is due to the fact that the country is located in the subtropical belt, exactly where the Hadley cell descending branch is located. However, it should be noted that solar radiation reaching the surface has a strong longitudinal gradient, which exists in relation to the longitudinal cloud cover (Loeb and Schuster, 2008), rainfall and sunshine duration. Against this background, it is important to determine how anthropogenic climate change may impact on the regional circulation, cloud cover and thus rainfall and solar potential in South Africa. Whereas most studies of future climate change over southern Africa have focused on changes in the regional circulation and rainfall, the implications of changing cloud cover remains to be explored from a renewable energy perspective. Changes in the Hadley cell circulation would be key to understanding and anticipating the potential for such changes to occur. However, such a dynamic understanding and climatology of the Hadley circulation is missing for South Africa. Both zonally symmetric diagnosis, especially using the mass weighted stream function (Holton and Hakim, 2012), and zonally asymmetric (Schwendike et al., 2014; 2015) diagnosis, have focused more on the global scale.

However, first, an analysis of the Hadley cell, cloud cover and sunshine duration has not been undertaken to establish some form of relationship between the three variables using both zonally symmetric and zonally asymmetric diagnostics. Second, there has not been any regional study focussing on the Hadley cell in South Africa. Hence, this study aims to address this research gap by using the zonally symmetric diagnostics of the Hadley circulation to establish the climatology of zonally averaged Hadley cell, cloud cover and sunshine duration over subtropical regions of the Southern Hemisphere (SH). Furthermore, zonally asymmetric diagnostics will be used to construct the climatology as well as trends for the Hadley cell, cloud cover and sunshine duration.

2. DATA AND METHODS

2.1 Data

This study covers a 35-year period spanning from 1980 to 2015. Data for this study are based on the European Centre for Medium-Range Weather Forecasts (ECMWF) Interim Reanalysis (ERA-Interim). The ERA-Interim data set has been previously used by Nguyen et al. (2013), among other seven reanalysis data sets to diagnose the Hadley cell. All reanalysis data sets were in agreement with the climatology and variability of the Hadley cell. Hence, due to its fine resolution, we use the ERA-Interim data set for our analysis. The data are on a horizontal resolution of $0.75^{\circ} \times 0.75^{\circ}$ on 37 pressure levels (Dee et al., 2011). This horizontal resolution is considered sufficient to properly diagnose the dynamics of the descending branch of the Hadley circulation over South Africa. The vertical velocity at 500 hPa (which is the level that approximates maximum upwards vertical motion; Lu et al., 2007), meridional velocity from 1,000 to 10 hPa levels, total cloud cover and sunshine duration were used to construct climatologies and linear trends of the Hadley cell, total cloud cover and sunshine duration. Additional data to analyse the climatology and trends of cloud cover and sunshine hours, was obtained from the South African Weather Service (SAWS).

Only stations with continuous data for the period 1980-2015 were used in the analysis, and these made up a total of 24 stations with cloud cover and 17 stations with sunshine hours. SAWS cloud cover and sunshine hours observations are made in accordance with World Meteorological Organisation (WMO) standards. Cloud cover trends over South Africa for the period 1960 to 2005 were constructed by Kruger (2007) using observational data from SAWS. In this study, an update of cloud cover trends is presented using both ERA-Interim and SAWS observations.

2.2 Methods

2.2.1 Zonally averaged mass streamfunction

To quantify changes of the Hadley cell, we use the zonally symmetric diagnosis, which have been used in a number of studies (e.g., Johanson and Fu, 2009; Polvani et al., 2011; Nguyen et al., 2013). The Hadley circulation is described as a large-scale meridional overturning of a rotating atmosphere and is characterized by maximum heating at the surface close to the equator. The strength and structure of the Hadley cell can be quantified using the zonally averaged stream function, given by the motivation outlined in Appendix A. The resulting stream function expression that will be used is given by (Polvani et al., 2011),

$$\psi(\phi, p) = \frac{2\pi a \cos\phi}{g} \int_{p}^{p_s} \overline{v} dp', (Polvani et al., 2011) \tag{1}$$

where ϕ is latitude, p pressure, $\overline{v}$ the zonal mean meridional wind, a the radius of the earth and g the gravitational acceleration.

We note that ψ describes the meridional circulation in general (i.e. both direct and indirect cells). To distinguish between these cells, Holton and Hakim (2012) show that

$$\psi \propto -\frac{\partial \overline{J}}{\partial y} + \frac{\partial^2}{\partial^2 y}(\overline{v'T'}) + \frac{\partial^2}{\partial y \partial z}(\overline{u'v'}) + \frac{\partial}{\partial z}(\text{zonal drag force}) \tag{2}$$

where y and z represent the northwards and upwards directions, respectively, u', v' and T' are the perturbations of the eastwards component of the wind, northwards component of wind as well as the temperature, respectively. This decomposition of ψ demonstrated that diabatic heating ($\overline{J}$), large-scale eddy processes viz large-scale eddy heat fluxes ($\overline{v'T'}$) and momentum fluxes ($\overline{u'v'}$), and friction play a role in determining which aspect of ψ applies to which aspect of the meridional circulation (the Hadley circulation, the Ferrel cell or the polar cells).

A positive meridional temperature gradient occurs in the SH, implying that the aspect of ψ in Eq. (2) associated with diabatic heating, will thus be negative there. The first term is associated with the thermally direct circulation. This means that $\psi < 0$ represents the Hadley cell in the SH.

To define the strength of the Hadley, we use the maximum value of meridional mass stream function averaged between 900 and 200hPa (Nguyen et al., 2013), but take the possible expansion of the cell by dividing values by the difference in latitude (i.e. $\psi_{max}/(\phi_{max} - \phi_{edge})$, where ϕ_{max} and ϕ_{edge} are the latitudes where ψ is maximum and at the edge of the cell. This edge is defined first by determining the maximum meridional mass streamfunction at 500hPa, and the edges are then determined by taking the first latitude poleward of the maximum at which $\psi = 0$ (Lu et al., 2007).

2.2.2 Diagnostics for the local Hadley circulation

Schwendike et al. (2014) showed that it is possible to decompose Equation (A1) in such a way that continuity is satisfied independently in both the zonal and meridional direction, using a variation of the vector method (Keyser et al., 1989). The continuity equations in the zonal and meridional directions are, respectively, given by

$$\frac{1}{a}\frac{\partial u}{\partial \lambda} + \frac{\partial}{\partial p}(\omega_\lambda \cos\phi) = 0 \tag{3a}$$

and

$$\frac{1}{a}\frac{\partial}{\partial \phi}(v \cos\phi) + \frac{\partial}{\partial p}(\omega_\phi \cos\phi) = 0 \tag{3b}$$

where $\omega = \omega_\lambda + \omega_\phi$, is the sum of the vertical motion, partitioned into zonal and meridional directions, as indicated by the subscripts λ and ϕ, respectively. Note that an outline of the

derivation of this partitioning of (A1) is given in the Appendix B.

Equations (3a and b) operate on orthogonal vertical zonal and meridional planes, respectively. In particular, (v, ω_ϕ) represents the overturning circulation on the vertical meridional plane, which when confined to the tropics and subtropics uniquely diagnoses the Hadley circulation. Following Schwendike et al. (2014), the upward vertical flux of mass in this circulation is represented by $m_\phi = -(\omega_\phi \cos \phi) g^{-1}$, where g is the gravitational acceleration.

Given the vertical motion ω obtained from the ERA-Interim dataset, we calculate the potential function μ by solving the Poisson' equation (B3) using the HWSSSP subroutine of the National Centre for Atmospheric Research (NCAR) Software Library (Swarztrauber, 1974), which is written in FORTRAN 77, as in D'Abreton and Tyson (1995). From the resulting μ field, the ψ vector stream function components are calculated using (A7) from which the vertical massflux m_ϕ is then calculated. Linear trends of the Hadley diagnostics, sunshine hours and total cloud cover from the Era-Interim for the four seasons were constructed. The Student t- test was used to test trends for statistical significance at the 95% level.

3. RESULTS AND DISCUSSION

3.1 Climatology of zonally symmetric diagnostics: Streamfunction, sunshine duration and total cloud cover

Several previous studies (e.g., Johanson and Fu, 2009; Polvani et al., 2011; Kang and Lu, 2012; Nguyen et al., 2013) have addressed the variability and changes in the Hadley circulation; here we consider possible implications of these changes to cloud cover and sunshine hours. While it is difficult to make conclusions of a regional nature from zonally averaged diagnostics, they

serve as a prelude to the zonally asymmetric discussion; we therefore consider these issues from the former first.

Fig. 2 shows the seasonal variations of the ψ in 10^9 kg.s^{-1}. The negative values indicate anticlockwise motion, with the contours south of the central axis (represented by the thick red contour) which goes through the maximum value of ψ showing areas of subsidence south of it, according to (A4). Similarly, the negative values of ψ north of the central axis represent regions of ascent. As the region of interest is southern Africa, we therefore consider these variables between 50°S and 5°N.

A strong seasonal dependence, as well as intensity of the circulation, is evident (Figure 2 and Table 1). Subsidence over austral subtropics is noted during all seasons, which is weakest during December–February (DJF) (Figure 2a) but strongest from June to August (JJA) (Figure 2b). The strength of subsidence during the solstice seasons appear to be comparable, which suggests that these are transition seasons between the DJF minimum and JJA maximum strengths. The variations in strength are indicated by the meridional gradient, as implied by Equation (A4). Tighter (higher) gradients induce stronger flow. The ascending branch of the circulation exhibits exactly the same behaviour. A similar argument about the meridional flow can be made based on differences in the vertical gradients of Equation (A3). Again, these gradients reach minimum and maximum values during DJF and JJA, respectively (Table 1). The intensity of the Hadley circulation reaches minimum (i.e. -8.97 $\times$ 10^6 kg s^{-1} km^{-1}) and maximum (i.e. -38.5 $\times$ 10^6 kg s^{-1} km^{-1}) values during DJF and JJA, respectively.

There are significant seasonal variations in the position of the Hadley circulation (Figure 2). During austral winter, the circulation appears to migrate northwards. This migration is clearly

evident in Table 1 (column 3), where the edge is at its southern (northern) most position during DJF (JJA) at 36°S (28°S).The Asian summer monsoons and displacement of the ITCZ are the main contributors of the meridional shift of the circulation. In fact there is a strong link between the migration of the Hadley cell edges of the Hadley cell and the ITCZ (Kang and Lu, 2012).

The seasonal variations of cloud cover as a percentage of total sky, and sunshine hours are represented as a dashed line in Figures 3 and 4, for DJF and JJA, respectively. The seasonal variability of total cloud cover is broadly consistent with that of the Hadley circulation (compare Figures 2, 3a and 4a for the corresponding seasons). Where there is descending motion in the subtropical regions, less total cloud is found, compared to regions where rising motion of air is found. This is not unexpected, of course, because tropical air is expected to be moist and warm, while the descending branch in the subtropics is characterized by air that is dry as it adiabatically warms. The subtropical dry zones migrate northwards from DJF to JJA, which is consistent with the variability of rainfall over South Africa (Tyson and Preston-Whyte, 2000). This part of the SH receives most of its rainfall during the summer months, when the Hadley circulation is at its weakest.

3.2 Trends in streamfunction, total cloud cover and sunshine duration

Linear trends of the zonally averaged Hadley cell at 500 hPa level for DJF and JJA for the period 1980–2015 are shown in Figure 2, the Hadley cell intensity trends are also shown in Table 1. The positive Hadley cell intensity index indicates an increase in upwards mass streamfunction (downwards mass streamfunction) over the tropics (subtropics) and vice versa. A decrease in the upwards mass streamfunction is evident over areas of positive meridional mass streamfunction and subsequently a decrease in the downwards mass streamfunction over the SH subtropical

zones in DJF. The general decrease in downwards motion in the subtropical Hadley cell is evidenced by the Hadley cell intensity index of $9.76x10^4$.

The maximum rate of increase in downwards motion is found in JJA and the Hadley cell index is $-5.46x10^4$. The linear trends of the meridional mass streamfunction also indicate a polewards shift of the Hadley cell (i.e., the Hadley cell edges are located further polewards than in the climatology and this is consistent with previous studies) (Johanson and Fu, 2009). The southwards expansion and intensification of the cell, which also manifests as an increase in the subtropical dry zones (Seidel and Randel, 2007), is evident in all seasons except for DJF.

Lu et al. (2007) found that the expansion of the Hadley cell is positively correlated with an increase in greenhouse gases (GHGs), while Garfinkel et al. (2015) attribute the expansion of the Hadley cell to GHGs, stratospheric ozone depletion, tropospheric ozone and SSTs. Stratospheric ozone depletion is the more dominant driver of tropospheric changes such as the expansion of the Hadley circulation and the polewards shift of the eddy-driven jet (Polvani et al., 2011). The increase in subtropical zones could mean the spatial extent of limited cloud development and more sunshine hours has also increased, as is consistently found in this study. This is in agreement with Tselioudis et al. (2016), who further pointed out that the expansion of the Hadley cell is linked to the polewards shift of mid-latitude clouds. This polewards shift enables more sunlight to reach the surface and hence leads to surface radiative warming.

The linear trends of total cloud cover and sunshine duration over the descending branch of the Hadley cell are shown in Figures 3 and 4 for DJF and JJA, respectively. An increase in total cloud cover is evident from the equator to latitude 20°S in JJA and a decrease from latitude 20°S to further southwards, but but in DJF (Figure 3a) a decrease is evident from the equator

to about 7°S and from 24°S to further southwards. The rate of increase (tropics) and decrease (subtropics) is more in JJA and less in DJF. This is consistent with the Hadley cell intensification in JJA and weakening in DJF. Similar to the meridional mass stream function and zonally averaged cloud cover trends, linear trends in zonally averaged sunshine duration are also seasonal. A decrease in sunshine duration from the equator to the subtropics (around latitude 29°S) is evident in DJF (Figure 3b); however, in JJA (Figure 4b) a decrease in sunshine duration is evident from the equator to latitude 19°S, thereafter an increase is evident for all lower latitudes. A clear correspondence between trends over the different latitudes compares well with results from Singh and Kruger (2017), for example, positive trend in sunshine duration south of 30°S but turning negative northwards in DJF and negative trends south of 30°S in JJA.

The combined trend analysis between the zonally averaged Hadley, total cloud cover and sunshine hours over the subtropics, is broadly consistent. In JJA the descending motion resulting from the negative gradient of the stream function is consistent with a decrease in total cloud cover and an increase in sunshine hours over the descending branch of the Hadley. Over the tropics (SH), an increase in upwards vertical motion (positive meridional mass stream function), increase in total cloud cover and decrease in sunshine hours is mostly evident in JJA.

In summary, the subtropical branch of the Hadley cell has intensified and expanded southwards in JJA (with negative values of the meridional stream function becoming more negative), which is consistent with other studies (Engelbrecht et al., 2011). Also in JJA, total cloud cover has decreased and sunshine duration has increased over the subtropics of the SH and both have shifted polewards. A quantitative correlation of the Hadley intensity, total cloud cover, as well as the sunshine duration over the subtropics of the SH, has also been performed for all seasons (Table 2). Only weak correlations are established for all the seasons. It is likely that zonal

averaging may have compromised the correlation between the zonally averaged mass stream function and zonally averaged cloud cover and sunshine duration.

These results are further perpetuated when examining regional changes of the Hadley, in particular over South Africa, which in some way contributes to the intensification and expansion of the subtropical Hadley. Since these diagnoses were based on zonally averaged data, some of the regional features that may contribute to the expansion may be missed. A possible way of investigating regional changes is through zonally asymmetric methods.

3.3 Climatology of zonally asymmetric diagnosis

The local Hadley cell over South Africa, as defined by the meridional massflux at 500 hPa, is characterized by the general decent of vertical motion in all seasons (Figure 5a,d), which is typical of subtropical weather. Consequently, the subtropics are characterized by semi-permanent anticyclones which are caused by large-scale subsidence on the descending branch of the Hadley cell. These anticyclones are a large contributing factor to the weather of South Africa (Tyson and Preston-Whyte, 2000), such as when they ridge and bring moisture over the eastern parts of the country. The mean vertical motion over South Africa is downwards, however the strength of this motion is seasonal and vertical motion occurs at times, as the number of anticyclones decreases (Tyson and Preston-Whyte, 2000). When upwards vertical motion occurs, it is confined to where weather systems such as cut-off lows (COLs; e.g., Engelbrecht and Landman, 2014) and tropical-temperate troughs (TTTs; e.g., Hart et al., 2010) occur and elsewhere subsidence dominates (Tyson and Preston-Whyte, 2000). This is shown by the grey dots over the interior of the country, south of the northern thick contour in Figure 5. The southern and western parts of the country experiences maximum subsidence and this is consistent with ridging Atlantic

anticylones (Tyson and Preston-Whyte, 2000).

The weaker Hadley circulation over the country that is evident in DJF (Figure 5a) and September–November (SON; Figure 5d) may also be linked to the frequency of anticyclones. In DJF the number of anticyclones decreases and the circulation over South Africa is dominated by a weak heat low that is joined by a trough across the Northern Cape to a tropical low north of Botswana (Tyson and Preston-Whyte, 2000). The centre of the low is fashioned in an east–west direction along the southern branch of the ITCZ in the Congo Air Boundary and seldom southwards towards Namibia and Botswana. East of the trough or low, upwards vertical motion exists (Tyson and Preston-Whyte, 2000), resulting in the reduction of the Hadley cell subsidence over the summer rainfall region. This is advocated by the low values of subsidence over interior of South Africa. Lowest values are confined to the far northern parts of Limpopo Province, far northern parts of North West Province and further southwards to Free State Province. Warming of the surface in the austral summer also plays a role in the seasonal strength of the subtropical Hadley cell. Land surface warming affects the meridional temperature gradients that weaken subsidence during summer months (Cook, 2003). It is also warming of the surface that causes convection at the surface, leading to thunderstorm development (Tyson and Preston-Whyte, 2000). Vertical ascent due to thunderstorms and other weather systems which are prevalent over South Africa during summer suppress the descending motion of the Hadley cell, making it weaker.

In JJA, maximum subsidence is evident throughout the country with higher values of negative massflux confined to the summer rainfall region of South Africa and less negative massflux values over the all year rainfall region (Figure 5c). Surprisingly, the south western parts of South Africa also show highest values of the subsidence. The downwards massflux over the

Western Cape should be lower because this is a winter rainfall region (as also shown by the upwards vertical motion there). The austral winter experiences the maximum frequency of anticyclones (Tyson and Preston-Whyte, 2000). These anticyclones are more intense during this season. They migrate northwards and are located over the interior of South Africa replacing the surface trough. Simultaneously, the upper-level westerlies widen and the upper tropical easterlies are displaced northwards, resulting in maximum subsidence over South Africa. This leads to subsidence throughout the country, confirming the descent in JJA, with exceptions of the South Western Cape (as noted above) and southern parts where weather is dominated by frontal systems (Tyson and Preston-Whyte, 2000). The subsidence is greatly linked to high atmospheric stability and subsidence inversion. The surface inversions suppress convection and dispersion of pollutants. These inversions restrict the extent of meridional temperature gradients due to surface cooling in winter, leading to more subsidence and thus a stronger subsidence in the Hadley circulation.

As was the case with the zonally averaged diagnostics, the solstice seasons exhibit transitional behaviour of the Hadley circulation, in both strength and movement. This and the discussion above shows that the zonally varying Hadley circulation migrates northwards from DJF to JJA. However, the contradiction is that the descending motion appears to be stronger during summer in this case, south of the African continent. This highlights the importance of using locally varying diagnostics as these enable local meteorology to be taken into consideration.

The seasonal climatology of total cloud cover is shown in Figure 6. Correlation greater than 0.5 is established only in DJF but found only north of South Africa from latitude 22°S northwards. Weak correlation (between 0 and 0.5) is also found north of South Africa in DJF and SON, and no correlation was established in South Africa. One noticeable feature about the cor-

relation is that although weak, it is only found in JJA over the central interior of South Africa, exactly where the Hadley cell and the subsequent subsidence are dominant. This could mean that cloud cover over South Africa, does not entirely depend on the Hadley cell but depends more on weather producing systems that dominate the country, and particularly in summer.

The climatology of cloud cover and sunshine duration informed by the ECMWF data is represented in contours and the bold values represent each SAWS station used in the analyses and the climatology of cloud cover for that particular station (Figures 6 and 7). Although there are some inconsistencies spatially, cloud cover from both the SAWS station data and ECMWF data indicate high cloud cover values over the eastern parts of South Africa; these values decrease as one moves westwards. South African coasts also receive less sunshine and more cloud cover; however, over the west coast, less cloud cover can be attributed to the persistent radiation fog that occurs over this region (Kruger and Esterhuyse, 2005).

Although all seasons follow the above overview of sunshine duration and cloud cover, there are significant seasonal variations. The western parts appear to have more or less consistent sunshine and cloud cover in all seasons, whereas the eastern parts possess more variations in terms of sunshine duration and cloud cover in the four seasons. This may be due to different circulations that occur over southern Africa. These circulation types are linked to cloud bands that define widespread cloud cover over South Africa. In DJF maximum cloud cover is experienced over most of South Africa but to a larger extent over the eastern parts of the country (Figure 6a). This could be attributed to major cloud bands over South Africa. Major cloud bands account for most of South Africa's annual rainfall; they occur together with TTTs and are frequent in South Africa during austral summer (Tyson and Preston-Whyte, 2000). From March to May (MAM) and September to November SON (Figure 6b, d), relatively lower values of cloud cover are

evident over South Africa; the eastern parts exhibit higher values and the western parts indicate lower cloud cover values.

The frequency of major and truncated cloud bands is still high during transitional seasons. These bands define cloud cover over the north-western interior and southwards to the south eastern coasts during these seasons. Other cloud bands that define widespread cloud cover during the transitional seasons are the west coast and frontal bands, which result from an increase in frequency of westerly and easterly troughs over southern Africa. West coast troughs occur in conjunction with active tropical convergence and are linked with west coast bands leading to widespread cloud cover over the central interior to the south western parts (Tyson and Preston-Whyte, 2000). The east coast troughs are associated with frontal brands and account for cloud cover over south eastern parts of South Africa (Tyson and Preston-Whyte, 2000). Because of the maximum subsidence that prevails over South Africa in JJA, least cloud cover is experienced and confined to the south western parts of the country (Figure 6c). Frontal activity is the main reason for cloud cover over the southern and south western parts of South Africa. The amount of sunshine duration exhibited at a location can be directly linked to cloud cover over the particular area, that is, areas of high sunshine duration coincide with areas of low cloud cover. This is quantified by strong negative correlations between the two (not shown), but also when comparing Figures 6 and 7. The abundance of sunshine as well as low values of cloud cover over South Africa is clearly evident in all seasons and seasonal variability is noticeable (Figure 7). In all seasons, the western interior of South Africa has the highest amount of sunshine duration and lowest cloud cover values. The eastern parts receive the least sunshine and highest amounts of cloud cover as shown in Kruger and Esterhuyse (2005) and this is consistent with the rainfall climatology (Tyson and Preston-Whyte, 2000). The effect of orography (Figure 1) is also evident over the higher lying areas, especially over Mpumalanga Province where high

cloud cover and least sunshine are received.

3.4 Trends in massflux, sunshine duration and total cloud cover

Linear trends of massflux are displayed in Figure 8. During DJF, a statistically significant decrease in downwards massflux is observed over the central and north eastern parts of South Africa. Simultaneously, an increase in downwards massflux is established over the southern parts of South Africa (Figure 8a). In MAM (Figure 8b), a minimum decrease in downwards massflux fashioned in a northwest to southeast directed band is evident over South Africa. This could indicate an increase in TTTs and the cloud bands that are associated with them. A tendency towards an increase in the downwards massflux is evident over the western, southern and north-eastern parts of the country. In JJA (Figure 8c), an increase in downwards massflux is dominant over South Africa. However, there are some places over the interior showing a slight decrease in downwards massflux.

For JJA the increase in downwards massflux implies a strengthening of the Hadley over the country and could be as a result of an increase in the formation of midlevel-highs enhancing subsidence over the country (Engelbrecht et al., 2009). The maximum and statistically significant increase in downwards massflux for most of South Africa is in SON (Figure 8d). It is only over Lesotho and some parts of northern KZN, where there is tendency towards a slight decrease in downwards massflux in SON.

The ECMWF and the SAWS station data broadly indicate positive trends in total cloud cover during DJF and MAM (although there are stations showing an increasing trend) (see Figure 9a,b). In JJA, both observations show an increasing trend over the central interior and

western parts of the country (Figure 9c). Over the far eastern parts of South Africa, a decreasing trend is established from both data sets (Figure 9c). In SON, a decreasing trend dominates, based on both SAWS station data as well as the ECMWF data. The difference between the two data sets is evident over the south western parts in all seasons; SAWS station data advocate a decreasing trend while the ECMWF shows an increasing trend along that region.

Linear trends of sunshine duration are shown in Figure 10. Both ECMWF and SAWS observations broadly show statistically significant negative trends in sunshine duration for almost the entire country during DJF and MAM (Figure 10a, b). In JJA, the entire subcontinent records a decreasing trend of sunshine duration, with the exception of four SAWS stations that indicate an increasing trend (Figure 10c). Positive trends are evident during SON (Figure 10d) from both the ECMWF and SAWS observations. This is consistent with findings by Singh and Kruger (2017), which, although using point observations from weather stations across South Africa, use a similar period and found a general decrease in sunshine duration trends, mostly in DJF and MAM, while a maximum increase is recorded in SON. Trends between cloud cover and sunshine duration are largely consistent, with some areas of disagreement. Positive total cloud cover trends during DJF are found exactly where the negative sunshine duration trends are, except perhaps along coastal regions (Figure 10a).

In JJA, decreased cloud cover over the eastern regions and increased cloud cover over western regions is consistent with sunshine duration, which shows a tendency to decrease over western parts (although the spatial extent is relatively larger than the increase in total cloud cover) and increase over the eastern parts of South Africa (Figure 10c). Maximum decrease in cloud cover and maximum increase in sunshine duration is in SON (Figures 9d and 10d); this could imply that more opportunities for solar energy exist in SON. Changes in the Hadley circulation

are in broad agreement with changes in total cloud cover and sunshine duration. Because the Hadley circulation is a fundamental process in the general circulation, we hypothesize here on the basis of these results that cloud cover and sunshine duration changes respond to changes in circulation.

4. CONCLUSIONS

This paper presents a combined climatology and trend analysis of the descending branch of the Hadley cell, cloud cover and sunshine duration over the subtropics and further over South Africa using zonally symmetric and asymmetric diagnostics, respectively. Although there is some form of consistency between the two diagnostics, a contrast has also been established. A weaker and more polewards Hadley is found in DJF, while a stronger and more equatorwards Hadley occurs in JJA. Consistently, the subtropical dry zones in the SH are located further southwards in DJF and further northwards in JJA. Associations between the Hadley cell, cloud cover and sunshine duration has been established from both diagnostics. Minimum total cloud cover, maximum sunshine duration, and the Hadley cell edges are located polewards in DJF, and equatorwards in JJA. Both diagnostics show maximum weakening of the Hadley in DJF. The maximum intensification of the subtropical Hadley, according to the zonally symmetric diagnostics is in JJA; however, the zonally asymmetric diagnostics indicate maximum intensification of the Hadley over South Africa to be in SON. The maximum intensification in SON coincides with a maximum decrease in cloud cover and increase in sunshine over South Africa.

Finally, apart from observing links between the Hadley cell, cloud cover and sunshine duration from the combined climatology and trends; the relationship between the Hadley cell and cloud cover was tested quantitatively using correlation coefficients. Results from the correlation

coefficients suggest that cloud cover does not depend entirely on the Hadley cell. This is quite evident from the zonally asymmetric analysis, e.g. in DJF correlation was not established for almost the entire southern African region and mainly because cloud cover depends on weather systems that prevail over the country in summer. In JJA, cloudlessness over the interior of South Africa is informed by the Hadley cell and this could be the result of the correlation between the Hadley cell and cloud cover (although weak) over the interior of South Africa in JJA. It is evident from this study that the combined analysis of the Hadley cell, cloud cover and sunshine duration may be obtained from both zonally symmetric and asymmetric analysis. However, using the zonally asymmetric diagnosis, it was established that different weather systems (e.g., TTTs and COLs) have a crucial role in this complex interplay. Thus, the next step will be to investigate the link between the Hadley cell and different climate systems that account for weather in southern Africa.

Acknowledgements

This work was financially supported by the National Research Foundation (NRF) Grant number 102215.The authors are grateful to Dr Andries Kruger for his valuable input prior the submission of this manuscript. Special thanks also go to the two anonymous reviewers for their contribution to improve the manuscript.

APPENDIX A: DERIVATION OF THE ZONALLY SYMMETRY HADLEY CELL USING THE ZONALLY AVERAGED MASS-STREAM FUNCTION

The strength and structure of the Hadley cell can be quantified using the zonally averaged streamfunction, given by the following motivation:

In the isobaric vertical coordinate system, the spherical version of the continuity equation is given by

$$\frac{1}{a\cos\phi}\frac{\partial u}{\partial \lambda} + \frac{1}{a\cos\phi}\frac{\partial}{\partial \phi}(v\cos\phi) + \frac{\partial \omega}{\partial p} = 0 \tag{A0}$$

where u and v are the zonal meridional components of the divergent ageostrophic flow, respectively, ω the vertical component of the velocity, a is the radius of the earth, λ is the longitude and ϕ is the latitude. The zonally averaged (A0) reduces to its two dimensional version, given by

$$\frac{1}{a}\frac{\partial \overline{v}}{\partial \phi} + \frac{\partial \overline{\omega}}{\partial p} = 0 \tag{A1}$$

The overbar in A1 represent zonally averaged fields. Equation (2) represents non-divergent two dimensional flow on the meridional plane, and so it can be represented in terms of a streamfunction (ψ), so that the zonally averaged meridional and vertical components of the wind fields may written as

$$\overline{v} = \frac{g}{2\pi a\cos\phi}\frac{\partial \psi}{\partial p} \tag{A2}$$

and

$$\overline{\omega} = -\frac{g}{2\pi a^2\cos\phi}\frac{\partial \psi}{\partial \phi} \tag{A3}$$

Because both components in A2 and A3 satisfy the continuity equation described in A1, either one of them can be used to solve for the streamfunction ψ by integrating the vertical and meridional directions, respectively. However, most studies (e.g. Polvani et al., 2011) make use of the

expression involving $\overline{v}$ because the meridional velocity is more directly and more accurately observed than $\overline{\omega}$.

APPENDIX B: DERIVATION OF THE ZONALLY ASYMMETRIC HADLEY CELL USING A VARIATION OF THE STREAM FUNCTION VECTOR METHOD

In this section we follow Schwendike et al. (2014) to outline the approach they took to partition the isobaric continuity equation (see Equation (A1)). On each isobaric surface, the divergent, irrotational flow in Equation (A1) may be written in terms of a velocity potential χ, such that

$$u = \frac{1}{a\cos\phi}\frac{\partial\chi}{\partial\lambda} \text{ and } v = \frac{1}{a\cos\phi}\frac{\partial}{\partial\phi}(\chi\cos\phi) \tag{B1}$$

since $\nabla \times \nabla\chi = 0$. Let

$$\chi \equiv \frac{\partial\mu}{\partial p} \tag{B2}$$

where μ is a potential function, and then combine this with A0 to produce a Poison's equation in μ, i.e.

$$\frac{1}{a^2\cos^2\phi}\frac{\partial^2\mu}{\partial\lambda^2} + \frac{1}{a^2\cos\phi}\frac{\partial}{\partial\phi}\left(\sin\phi\frac{\partial\mu}{\partial\partial\phi}\right) = -\omega, \tag{B3}$$

which is solved numerically, given suitable boundary conditions as discussed in subsection 2.2.2.

Now define a vector stream function $\overrightarrow{\psi}$ (here the over arrow indicates that this quantity is a vector), such that

$$\psi_\lambda = -\frac{1}{a\cos\phi}\frac{\partial\mu}{\partial\lambda} \text{ and } \psi_\phi = -\frac{1}{a}\frac{\partial\mu}{\partial\phi} \tag{B4}$$

and taking the divergence of $\overrightarrow{\psi}$ and using (B3), we obtain

$$\frac{1}{a\cos\phi}\frac{\partial\psi_\lambda}{\partial\lambda}+\frac{1}{a\cos\phi}\frac{\partial}{\partial\phi}(\psi_\phi\cos\phi)=\omega \tag{B5}$$

Clearly, from (B5), vertical motion ω is partitioned into two orthogonal directions so that

$$\omega_\lambda\cos\phi=\frac{1}{a}\frac{\partial\psi_\lambda}{\partial\lambda} \tag{B6}$$

$$\omega_\phi\cos\phi=\frac{1}{a}\frac{\partial}{\partial\phi}(\psi_\phi\cos\phi) \tag{B7}$$

with $\omega=\omega_\lambda+\omega_\phi$.

It follows then from (B1) and (B2) that the zonal component of the ageostrophic flow may be written in terms of zonal component of the ψ vector:

$$u=\frac{1}{a\cos\phi}\frac{\partial}{\partial\lambda}\left(\frac{\partial\mu}{\partial p}\right)=\frac{\partial}{\partial p}\left(\frac{1}{a\cos\phi}\frac{\partial\mu}{\partial\lambda}\right)=-\frac{\partial\psi_\lambda}{\partial p} \tag{B8}$$

Similarly, the meridional component of the ageostrophic flow may be written in terms of meridional component of the ψ vector as follows

$$v=-\frac{\partial\psi_\phi}{\partial p} \tag{B9}$$

Using (B6) and (B8) and the fact that partial derivatives are interchangeable, we have

$$\frac{1}{a}\frac{\partial u}{\partial\lambda}+\frac{\partial}{\partial p}(\omega_\lambda\cos\phi)=0 \tag{B10}$$

and similarly

$$\frac{1}{a}\frac{\partial}{\partial\phi}(v\cos\phi)+\frac{\partial}{\partial p}(\omega_\phi\cos\phi)=0 \tag{B11}$$

REFERENCES

Bergman, J.W. and Salby, M.L. (1997) The role of cloud diurnal variations in the time mean energy budget. Journal of Climate, 10, 1114–1124.

Bugaje, I.M. (2006) Renewable energy for sustainable development in Africa: a review. Renewable and Sustainable Energy Reviews, 10, 603–612.

Ceppi, P. and Hartmann, D.L. (2013) On the speed of the eddy-driven jet and the width of the Hadley cell in the Southern Hemisphere. Journal of Climate, 26, 3450–3465.

Cook, K.H. (2003) Role of continents in driving the Hadley cells. Journal of Atmospheric Sciences, 60, 957–976.

D'Abreton, P.C. and Tyson, P.D. (1995) Divergent and non-divergent water vapour transport over southern Africa during wet and dry conditions. Meteorology and Atmospheric Physics, 55, 47–59.

Dee, D.P., Uppala, S.M., Simmo, A.J., Berrisford, P., Poli, P., Kobayashi, S., Andrae, U., Balmaseda, M.A., Balsamo, G., Bauer, P., Bechtold, P., Beljaars, A.C.M., van de Berg, L., Bidlot, J., Bormann, N., Delsol, C., Dragani, R., Fuentes, M., Geer, A.J., Haimberger, L., Healy, S.B., Hersbach, H.,Hólm, E.V., Isaksen, L., Kållberg, P., Köhler, M., Matricardi, M., McNally, A.P., Monge-Sanz, B.M., Morcrette, J.-J., Park, B.-K., Peubey, C., de Rosnay,P., Tavolato, C., Thépaut, J.-N. and Vitart, F. (2011) The ERA-Interimreanalysis: configuration and performance of the data assimilation system.Quarterly Journal of the Royal Meteorological Society, 37, 553–597.

Engelbrecht, C.J. and Landman, W.A. (2014) Interannual rainfall variability over the Cape South Coast of South Africa linked to cut-off low associated rainfall. In: 30th Annual Conference of South African Society for AtmosphericSciences (SASAS), Potchefstroom, South Africa.

Engelbrecht, F.A., McGregor, J.L. and Engelbrecht, C.J. (2009) Dynamics of the conformal-cubic atmospheric model projected climate-change signal over southern Africa. International Journal of Climatology, 29, 1013–1033.

Engelbrecht, F.A., Landman, W.A., Engelbrecht, C.J., Landman, S., Bopape, M.M., Roux, B., McGregor, J.L. and Thatcher, M. (2011) Multi-scale climate modelling over southern Africa using a variable-resolution global model. Water SA, 37, 647–658.

Garfinkel, C.I., Waugh, D.W. and Polvani, L.M. (2015) Recent Hadley cell expansion: the role of internal atmospheric variability in reconciling modelled and observed trends. Geophysics Research Letter, 42(24), 824–831.

Groisman, P.Y., Knight, R.W., Karl, T.R., Easterling, D.R., Sun, B. and Lawrimore, J.H. (2004) Contemporary changes of the hydrological cycle over the contiguous United States: trends derived from in situ observations. Journal of Hydrometeorology, 5, 64–85.

Hart, N.C.G., Reason, C.J.C. and Fauchereau, N. (2010) Tropical extratropical interactions over southern Africa: three cases of heavy summer season rainfall. Monthly Weather Review, 138, 2608–2623.

Holton, J.R. and Hakim, G.J. (2012) An Introduction to Dynamic Meteorology. Burlington, USA: Academic Press.

Johanson, C.M. and Fu, Q. (2009) Hadley cell widening: model simulations versus observations. Journal of Climate, 22, 2713–2725.

Kaggwa, M., Mutanga, S. and Simelane, T. (2011) Factors determining the affordability of renewable energy. A note for South Africa. Johannesburg, South Africa: AISA Policy Brief 65.

Kang, S.M. and Lu, J. (2012) Expansion of the Hadley cell under global warming: winter versus summer. Journal of Climate, 25, 8387–8393.

Keyser, D., Schmidt, B.D. and Duffy, D.G. (1989) A technique for representing three dimensional vertical circulations in baroclinic disturbances. Monthly Weather Review, 117, 2463–2494.

Kruger, A. (2007) Trends in cloud cover from 1960 to 2005 over South Africa. Water SA, 33, 603–608.

Kruger, A. and Esterhuyse, D. (2005) Climate of South Africa: Sunshine and Cloudiness, Vol. 35. Pretoria, South Africa: South African Weather Service.

Liepert, B.G. (2002) Observed reductions of surface solar radiation at sites in the United States and worldwide from 1961 to 1990. Geophysics Research Letter, 29(10), 1421.

Loeb, N.G. and Schuster, G.L. (2008) An observational study of the relationship between cloud, aerosol and meteorology in broken low-level cloud conditions. Journal of Geophysical research, 113, D14214.

Lu, J., Vecchi, G.A. and Reichler, T. (2007) Expansion of the Hadley cell under global warming. Geophysics Research Letter, 34, L06805.

Nguyen, H., Evans, A., Lucas, C., Smith, I. and Timbal, B. (2013) The Hadley circulation in reanalyses: climatology, variability, and change. Journal of Climate, 26, 3357–3376.

Polvani, L.M., Waugh, D.W., Correa, G.J.P. and Son, S.-W. (2011) Stratospheric ozone depletion:The main driver of the twentieth century atmospheric circulation changes in the Southern Hemisphere. Journal of Climate, 24, 795–812.

Power, H.C. and Mills, D.M. (2004) Trends in solar radiation over South Africa and Namibia during the period 1957–1997. AGU Spring Meeting Abstracts.

Ruiz-Arias, J.A., Pozo-Vázquez, D., Lara-Fanego, V., Santos-Alamillos, F.J. and Tovar-Pescador, J. (2011) A high-resolution topographic correction method for clear-sky solar irradiance derived with a numerical weather prediction model. Journal of Applied Meteorology and Climatology, 50, 2460–2472.

Schwendike, J., Govekar, P., Reeder, M.J., Wardle, R., Berry, G.J. and Jakob, C. (2014) Local partitioning of the overturning circulation in the Tropics and the connection to the Hadley and Walker circulations. Journal of Geophysical Research, 119, 1322–1339.

Schwendike, J., Berry, G.J., Reeder, M.J., Jakob, C., Govekar, P. and Wardle, R. (2015) Trends in the local Hadley and local Walker circulations. Journal of Geophysical Research, 120, 7599–7618.

Seidel, D.J. and Randel, W.J. (2007) Recent widening of the tropical belt: evidence from tropopause observations. Journal of Geophysical Research, 112, D020113.

Singh, J. and Kruger, A. (2017) Is the summer season losing potential for solar

energy applications in South Africa. Journal of Energy in Southern Africa, 28, 52–60.

Solomon, S., Qin, D., Manning, M., Chen, Z., Marquis, M., Averyt, K.B., Tignor, M. and Miller, H.L. (2007) Summary for policymakers. In: Climate Change 2007: Synthesis Report. Contribution of Working Group I, II and III to the Fourth Assessment Report of the Intergovernmental Panel on Climate Change. Cambridge and New York, NY: Cambridge University Press.

Swarztrauber, P.N. (1974) The direct solution of the discrete Poisson equation on the surface of a sphere. Journal of Computational Physics, 15, 46–54.

Tselioudis, G., Lipat, B.R., Konsta, D., Grise, K.M. and Polvani, L.M. (2016) Midlatitude cloud shifts, their primary link to the Hadley cell, and their diverse radiative effects. Geophysics Research Letter, 43(9), 4594–4601.

Tyson, P.D. and Preston-Whyte, R.A. (2000). The Weather and Climate of Southern Africa. second ed. Oxford University Press.

Wallace, J.M.and Hobbs, P.V. (2006). Atmospheric science: an introductory survey. Academic press.

Wang, X., Key, J.R. (2005). Arctic surface, cloud, and radiation properties based on the AVHRR Polar Pathfinder dataset. Part I: Spatial and temporal characteristics. Journal of Climate, 18, 2558-2574.

Warren G, Hahn J, London J, ChervinM, Jenne L. (1986). Global distribution of total cloud cover and cloud type amounts over land. NCAR Technical Note NCAR/TN-273+STR.

Warren, S.G., Eastman, R.M. and Hahn, C.J. (2007). A Survey of changes in cloud cover and cloud types over land from surface observations, 1971–96. Journal of Climate, 24, 795–812.

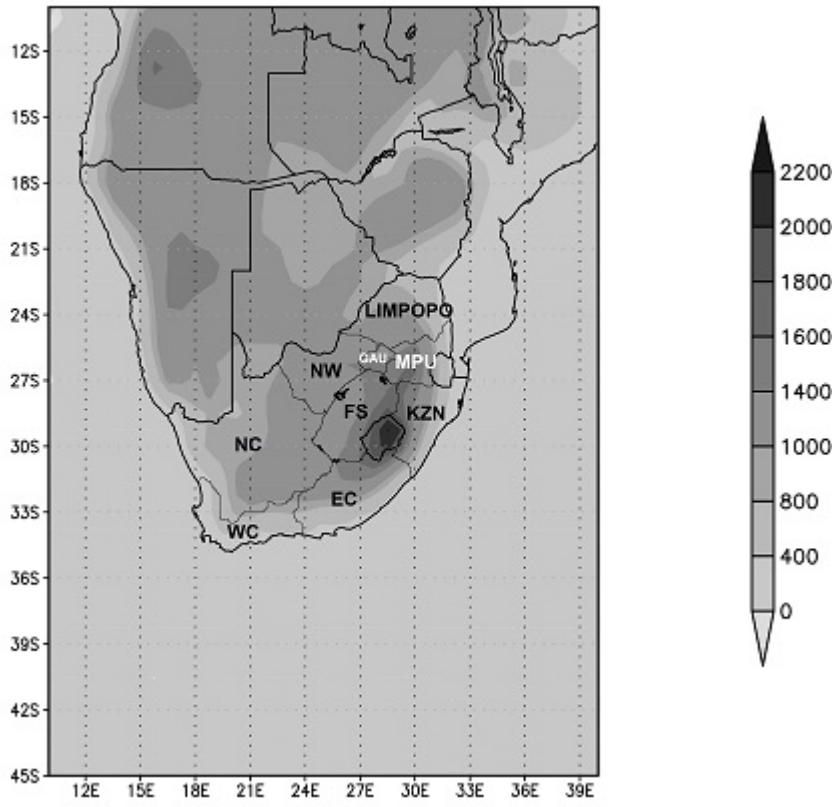

FIGURE 1 The provinces and topography of South Africa (altitude in meters above mean sea level)

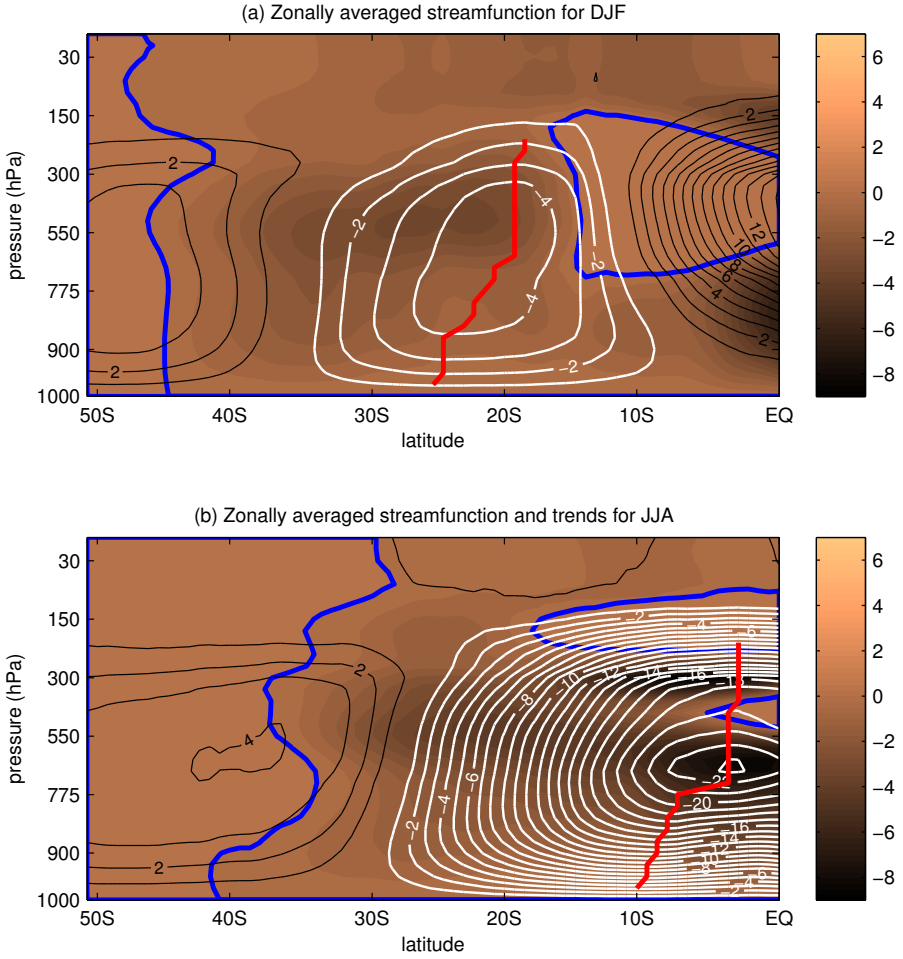

Climatology of zonally averaged negative (thin black contours) and positive (thin white contours) streamfunction and associated trends (shaded) for (a) DJF and (b) JJA. The thick blue contours represent regions where the zonally averaged streamfunction is zero and the thick red contours represent regions where the trends turn from negative (lighter shade) to positive (darker shade). The contour intervals for the stream function is 1×10^9kg s^{-1} [Colour figure can be viewed at wileyonlinelibrary.com]

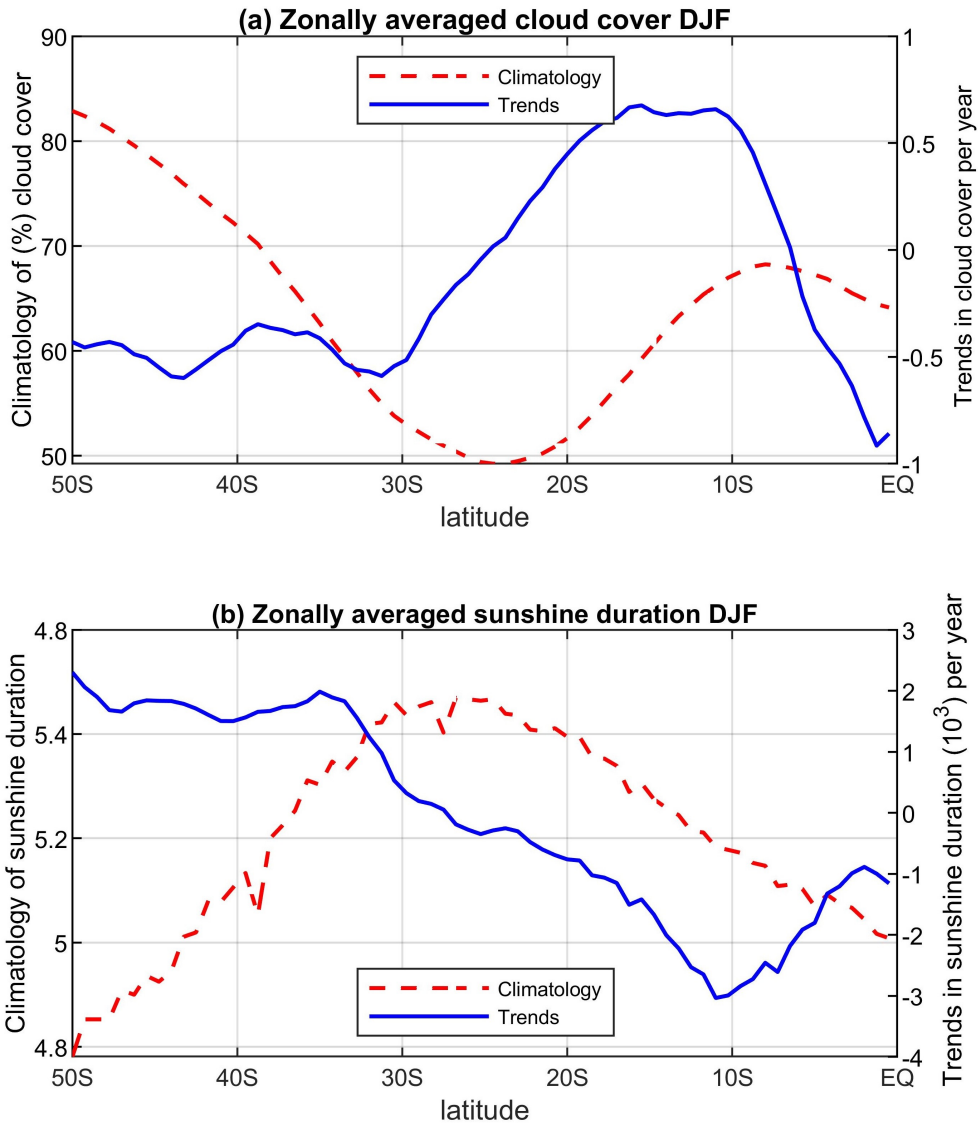

FIGURE 3 (a) The climatology (dashed line) and trends (solid line) of zonally averaged cloud cover for DJF. (b) Same as (a) but for zonally averaged sunshine duration (hours) [Colour figure can be viewed at wileyonlinelibrary.com]

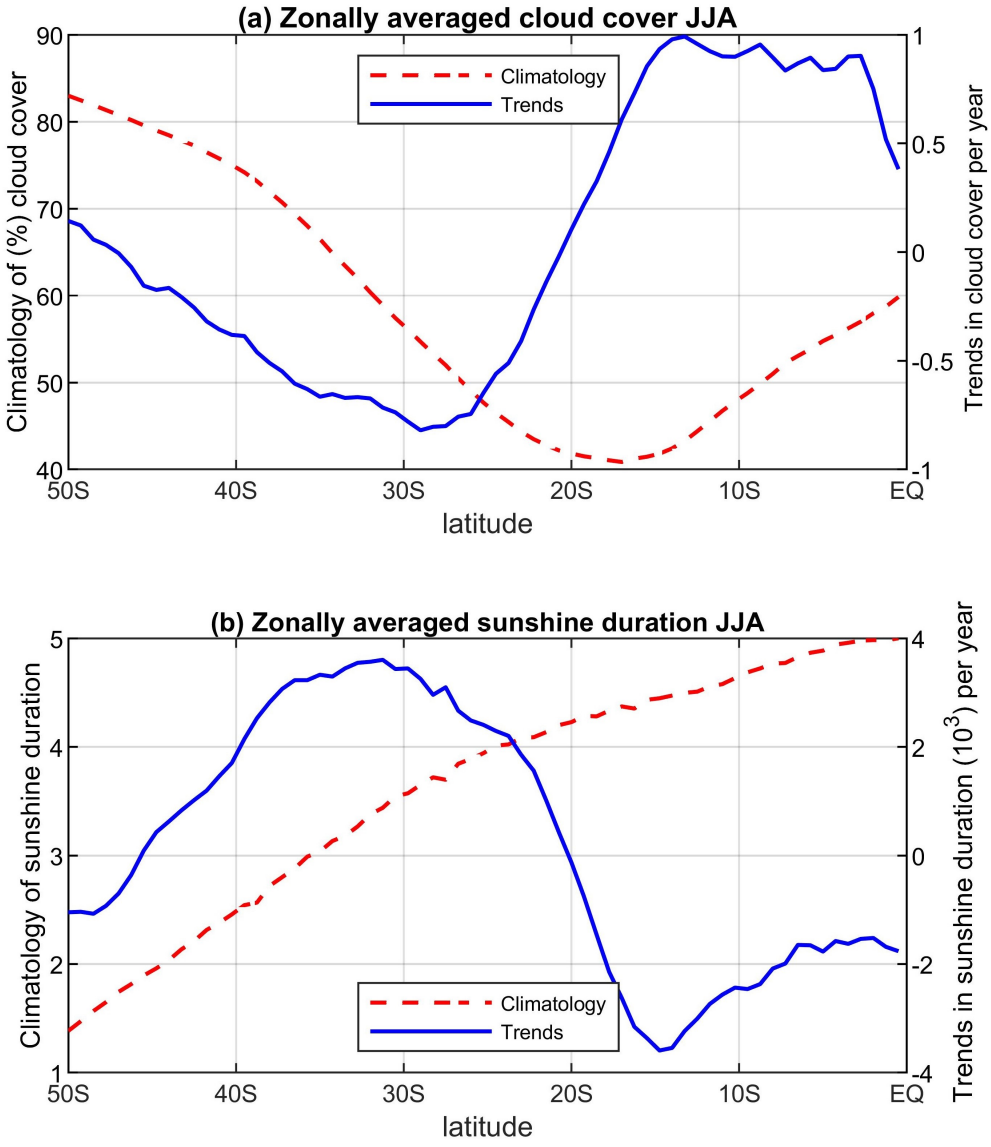

FIGURE 4 (a) The climatology (dashed line) and trends (solid line) of zonally averaged cloud cover for JJA. (b) Same as (a) but for zonally averaged sunshine duration (hour) [Colour figure can be viewed at wileyonlinelibrary.com]

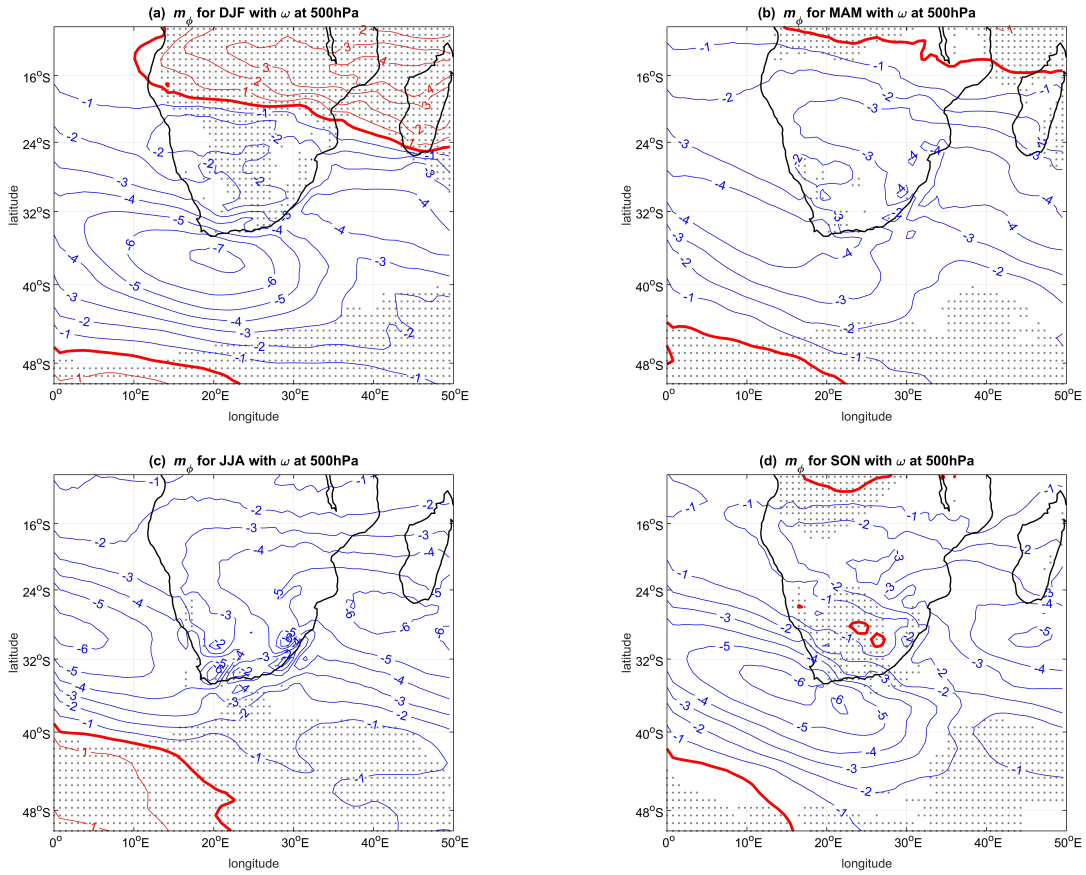

FIGURE 5. Seasonal mean of the massflux (m_ϕ) and the units are kgm^{-2}s^{-1} and vertical velocity (ω) in Pa s^{-1} for (a) DJF, (b) MAM, (c) JJA and (d) SON. Values of the massflux are represented by thin contours.The thick contours represent regions where the massflux is zero. The contours are plotted in 10^3 kgm^{-2}s^{-1} intervals. Regions of upward vertical velocity is represented using the grey dots and where there are no grey dots then there is downward motion there (i.e. $\omega > 0$).[Colour figure can be viewed at wileyonlinelibrary.com]

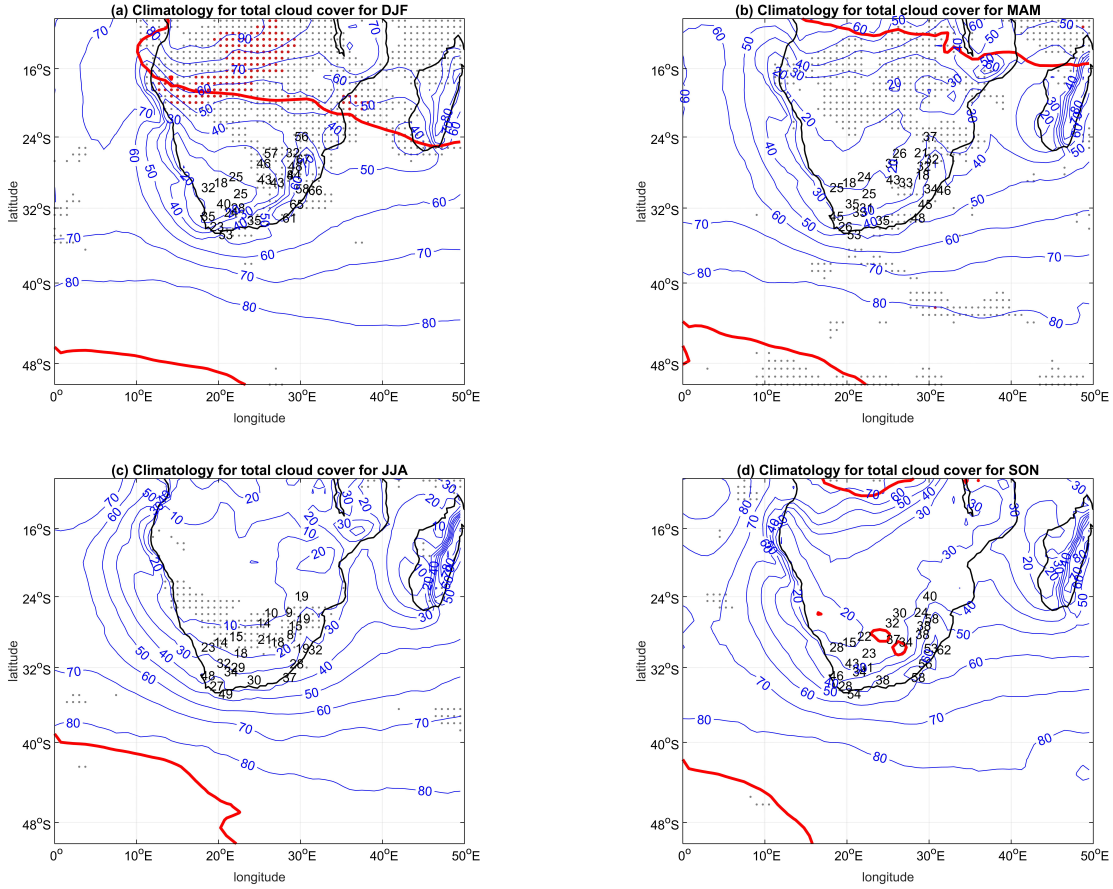

FIGURE 6 Total cloud area fraction shown as a percentage for (a) DJF, (b) MAM, (c) JJA and (d) SON is presented as thin contours (from the ERA-Interim) and the values in black (for each SAWS station observation used in the analyses). Regions where the massflux is zero are presented as thick contours. Correlations between total cloud cover and massflux of Figure 5 are represented as dots. Only positive correlations are shown, grey dots are correlations between zero and 0.5 and where there are no dots, cloud cover and massflux are negatively correlated [Colour figure can be viewed at wileyonlinelibrary.com]

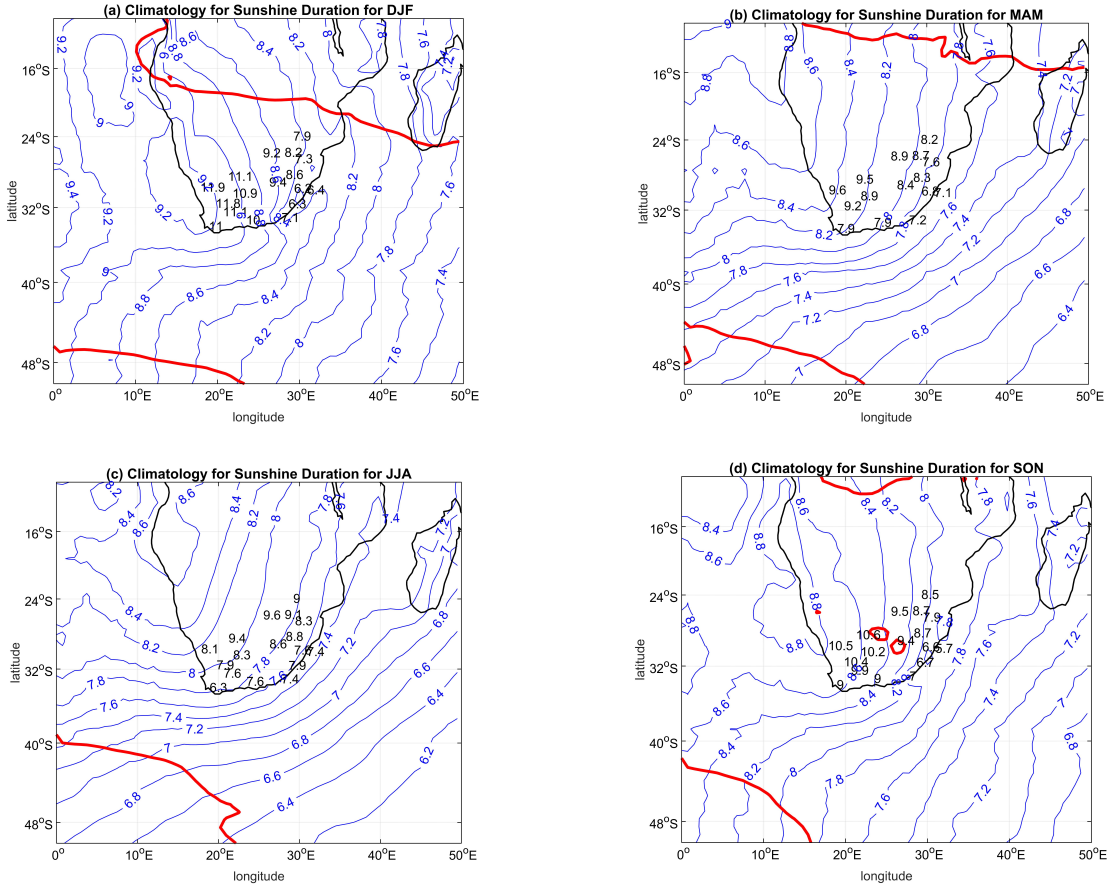

FIGURE 7 Sunshine duration (in hours) represented by the thin contours (ERA-Interim) and the values in black (SAWS observations). Regions where the massflux is zero (thick contours) for (a) DJF, (b) MAM, (c) JJA and (d) SON [Colour figure can be viewed at wileyonlinelibrary.com]

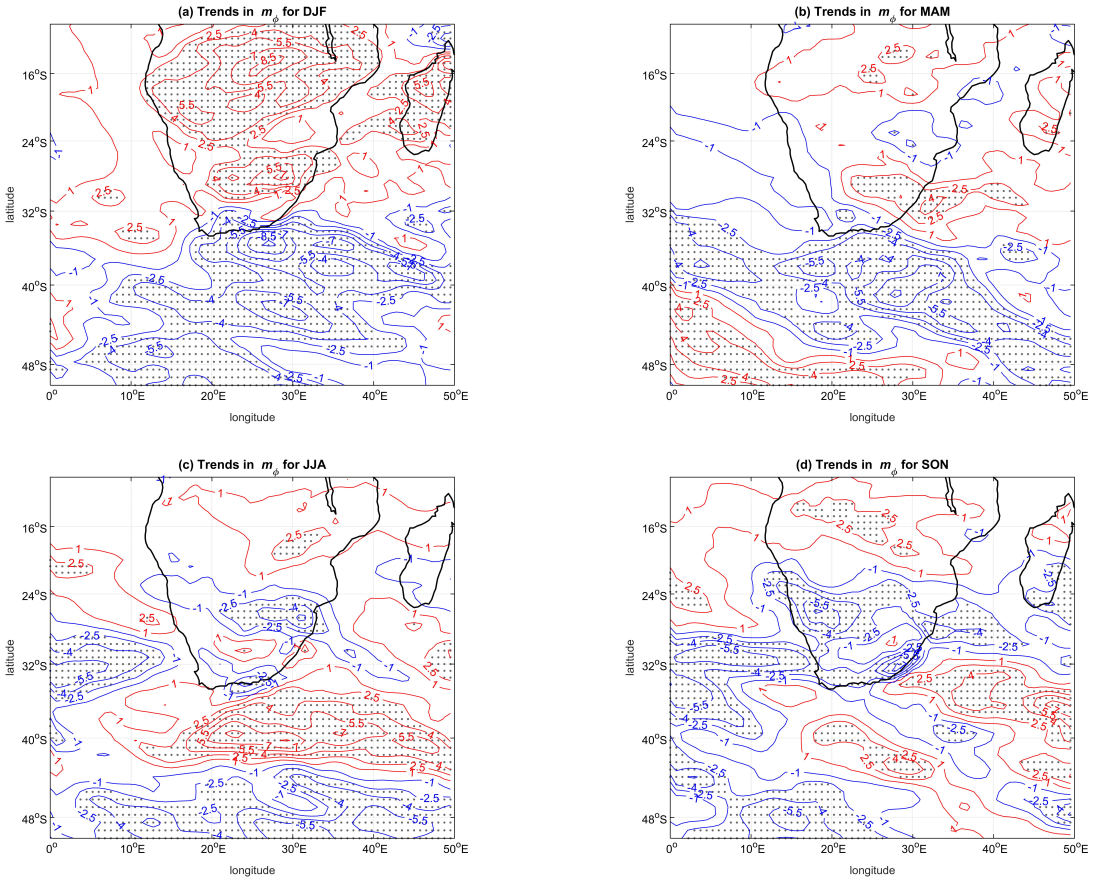

FIGURE 8 Trends in massflux (kgm^{-2} s^{-1} year $^{-1}$) for (a) DJF, (b) MAM, (c) JJA and (d) SON. The contours represent positive and negative trends. The dotted regions represent 95% statistical significance greater than 0.5 [Colour figure can be viewed at wileyonlinelibrary.com]

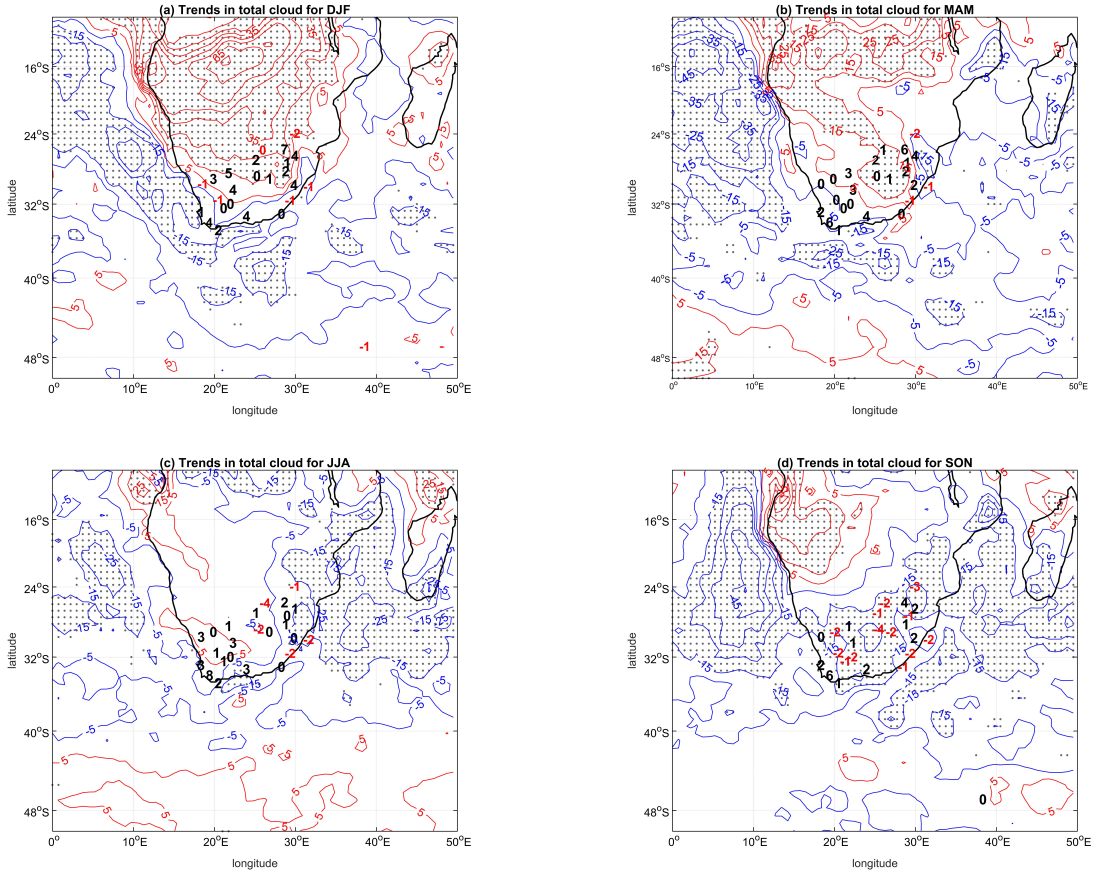

FIGURE 9. Same as in Figure 8 but for total cloud cover. Bold values represent trends for the SAWS station observation are represented as black values (positive trends) and red values (negative trends) [Colour figure can be viewed at wileyonlinelibrary.com]

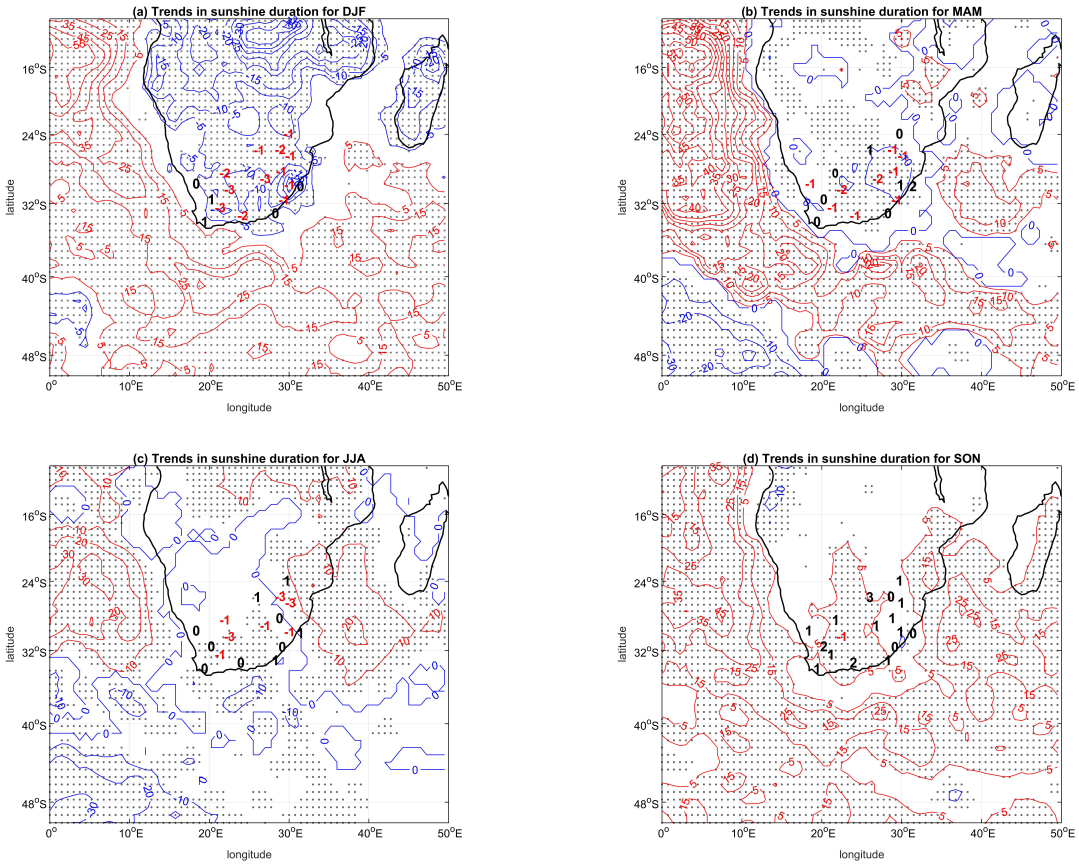

FIGURE 10 Same as in Figure 9 but for sunshine duration. Trends for the SAWS station observations are represented as red values (positive trends) and black values (negative trends) [Colour figure can be viewed at wileyonlinelibrary.com]

Table 1: The Hadley Cell Intensity climatology (10^6 kg.s^{-1}km^{-1}), trends (10^4 kg.s^{-1}km^{-1}) and the climatology for the Hadley Cell edge(degrees of latitude) for DJF, MAM, JJA and SON.

	Hadley cell intensity climatology	Hadley cell intensity trends	Hadley cell edge 0 latitude
DJF	-8.97	-9.6	-36
MAM	-20.1	4.85	-33
JJA	-38.5	5.46	-28
SON	-21.2	0.02	-30

Table 2: Correlation coefficients between the Hadley Cell Intensity (HCI), zonally averaged total cloud cover (TCC) and zonally averaged sunshine duration (SunD) for DJF, MAM, JJA and SON.

	Correlation HCI and TCC	Correlation HCI and SunD	Correlation SunD and TCC
DJF	-0.4	0.27	-0.8
MAM	-0.15	0.03	-0.73
JJA	-0.29	0.19	-0.79
SON	-0.35	0.23	-0.75

Chapter 3
Granger causality of the local Hadley cell and large-scale cloud cover over South Africa
Preface

This chapter consists of a journal paper accepted by the South African Journal of Science.

This study addresses objective 2 of the thesis. The concept of Granger causality is introduced. Furthermore using the Granger causality, the causality between the Hadley cell and cloud cover over South Africa is established. It was also established that there is Granger causality from cloud cover to Hadley cell, but this is a case of false causality in bivariate systems caused by the exclusion of a third variable in the analysis. Further analysis has shown that vertical velocity is the main variable that could have led to the causality of cloud cover to the Hadley cell.

Granger causality of the local Hadley cell and large scale cloud cover over South Africa

ABSTRACT: This study demonstrates that Hadley cell dynamics could be used as a proxy to determine cloud cover and thus solar energy potential over South Africa. Granger causality is used to investigate causal interactions between the Hadley cell and cloud cover for the period 1980-2015. Causal links were established from the Hadley cell to cloud cover. Areas of strong causality are found over the north-western parts of South Africa. Moreover, weak causality from cloud cover to the Hadley cell does exist, with vertical velocity being the main variable responsible for this causality, which hence indirectly links cloud cover to Hadley cell causality.

Significance of the main findings: Hadley cell may be used to identify regions of limited cloud cover over South Africa. The Hadley cell may further be used as a proxy for climate in the generation of solar energy over South Africa.

Keywords: Hadley circulation, streamfunction, massflux, total cloud cover, sunshine duration

1. INTRODUCTION

The South African government has identified a number of renewable energy options to inform the country‘s energy mix on the 2030 horizon and beyond.[1] One of these options is solar energy, which depends on the ability of incoming short wave radiation to penetrate through the atmosphere to the ground, where solar energy conversion technologies are located. The abundance in solar radiation and sunshine over South Africa is due to the fact that the country is located

in the subtropical belt, exactly where the Hadley cell descending branch is located. Solar radiation reaching the surface has a strong longitudinal gradient, which exists in relation to the longitudinal cloud cover rainfall and sunshine duration.[2] Interactions between the Hadley cell and cloud cover is therefore key to understanding and anticipating the potential of solar power as a renewable energy source for South Africa.

The Hadley circulation is a key component of the global circulation and accounts for ascending motion in the tropics and descending air in the subtropics. Weather and climate in both the tropics and subtropics are thus strongly influenced by the Hadley circulation.[3] Southern Africa with its location in the subtropics is on the average under the influence of the descending branch of the Hadley cell.[3] This is the main reason why southern Africa is in general a relatively dry and warm region, in fact, much of southern Africa is semi-arid.[4] Winters are dry with clear skies given the dominance of the subtropical high-pressure belt (the surface manifestation of the descending branch of the Hadley cell) during these months.[5] It is only the most southern parts of the southern Africa, namely the south-western Cape and Cape south coast of South Africa, that receives substantial amounts of rainfall during winter.[3] During wet summers the non-divergent part of the Hadley circulation causes a southwards shift in the Indian Ocean cyclonic cell, resulting in surplus water vapour transport across southern Africa from the north.[6] During the dry summers the spatial extent of the tropical western Indian Ocean anticyclone decreases, thereby leading to the reduction of water vapour transport from the south-east, whilst the descending branch of the Hadley cell strengthens over southern Africa.[7] Both the long-term climate and inter-annual climate variability over southern Africa are thus strongly controlled by Hadley cell circulation dynamics, with pronounced implications for the region's agriculture, water security and biodiversity. Moreover, Hadley cell dynamics have also been linked to variations in sunshine duration across southern Africa, which may be important within the context of a growing

renewable energy sector in the region.[8]

The meridional shift of the Hadley cell is linked with the seasonal migration of the Inter-Tropical Convergence Zone (ITCZ).[9] Tropical disturbances occur in summer over southern Africa as the Inter-Tropical Convergence Zone (ITCZ) propagates southwards to approximately 17 °C.[3] The behaviour of cloud bands is seasonal and they contribute to the seasonal rainfall of southern Africa .[10] Cloud bands and are associated with most of the late summer rainfall over the region link the ITCZ to the north [3] with a westerly-wave to the south. These tropical-extratropical cloud bands are defined as a regions of elongated cloudiness, that start in the tropics and extends south-eastwards into the mid-latitudes.[6] The cloud bands export moisture and heat from the tropics to the middle latitudes, through which the deep Hadley cell overturning is replaced during periods of weakened ITCZ activity.[11] These cloud bands can also be linked with midtropospheric cutoff low tracks.[12] The Hadley cell overturning is associated with convective intensity over southern Africa, anticyclonic ridging and moist air inflows from the Indian Ocean.[9]

Climate change over southern Africa may be anticipated to be closely linked to changes in the dynamics of the regional Hadley cell. In fact, The mean positions of storm tracks, high and low pressure systems, jet streams and associated precipitation patterns are all projected to change in response to the expansion of the Hadley cell in a warmer world.[5] Over southern Africa, the strengthening and expanding subtropical high-pressure belt is under climate change projected to contribute to the southward displacement (or blocking) of frontal systems bringing rainfall over southern Africa.[13] Moreover, a general strengthening of the descending branch of the Hadley cell in summer has been postulated as a key reason why the southern Africa is projected to become generally drier under global warming.[3,13]

Large scale cloudiness over South Africa is linked to the dynamics of the Hadley circulation over the country.[8] Whether changes in cloudiness are directly caused by changes in the Hadley circulation or whether cloudiness may impact on the Hadley via feedback processes, remains to be rigorously investigated. To address this, causality between changes in the Hadley cell and cloud cover need to be established. Thus, the aim of this study is to use Granger causality,[14] to investigate causal links between the Hadley cell and large scale cloud cover over South Africa.

2. DATA AND METHODS

2.1 Data

The study covers the period 1980 to 2015. Data used in this study were extracted from the European Centre for Medium-Range Weather Forecasts (ECMWF) Interim Reanalysis (ERA-Interim).[15] The ERA-Interim has a fine resolution and is sufficient enough to provide appropriate diagnostics of the Hadley circulation over South Africa. Meridional velocity from 1000 to 10 hPa was used to calculate the zonally averaged mass stream function (see Appendix 1). The zonally asymmetric Hadley cell time series was calculated using the massflux,[16] as outlined in Appendix 2. The vertical velocity at 500hPa (which is the level of maximum upward vertical motion) was used to calculate the Hadley cell diagnostics (see Appendix 2). Data are on a horizontal resolution of $0.75^{\circ} \times 0.75^{\circ}$ on 37 pressure levels[15,17]. Total cloud cover (cloud cover due to low, middle and high clouds) was also extracted from the ERA-Interim data set. To account for both short- and long-term effects of the Hadley cell on total cloud cover and vice versa, daily time-steps were used. The total cloud cover data for the area 18°-34°S and 15°-34°E was divided into low and high cloudiness years. The high cloudiness years for DJF are 1982,1983,1991,1997, 2001, 2004, 2007, 2010, 2011, 2012, 2013, 2014 and the low cloudiness

years are 1986, 1987, 1990, 1992, 1993, 1995, 2004. In JJA the high cloudiness years are 1982, 1985, 1991, 1993, 1998, 2002, 2004, 2005, 2007, 2009, 2010, 2012, 2013, 2014 and the low cloudiness years are 1980, 1984, 1986, 1987, 1988, 1990, 1992, 1994, 1995, 1996, 1997, 1999, 2000, 2006, 2008, 2009.

2.2 Methods

Several studies have used linear and lag correlation statistics to help establish the links between time series in climate science.[18,19] However, it is a challenge to identify the direction of causality from such methods. Causality studies between climate variables have also been undertaken through Bayesian network [20.21],and Granger causality.[22−25] The two frameworks were compared to each other using biological data, from which it was established that the Bayesian network performs better for shorter temporal data sets, while for longer data sets, Granger causality seems to perform better.[26] One remarkable feature of Granger causality is that it has a decomposition property, which is not present in the Bayesian network inference.[26] This feature enables one to establish the best frequency at which causality may be established between two time series. Thus, Granger causality seems to be the best method for testing the direction and strength of causality between two time series. We therefore introduce the notion of Granger causality, to establish the causal relationships between the Hadley cell and cloud cover.

Granger causality can be defined as variable Y granger causing variable X, if X can be predicted better by using the past values of Y, more than the past values of X itself. This definition, when applied to the study, means that the cloud cover has a Granger causal relationship to the Hadley cell, if past values of cloud cover could be used to help predict the Hadley cell. Granger causality analysis tests for both the presence and direction of causality.[27] Granger causality

was initially designed and mainly applied to econometrix data, yet several studies have applied Granger causality to the atmospheric sciences.[21−24] The main challenge in employing Granger causality to climate data is the fact that climate systems are highly nonlinear.[14] Studies have employed nonlinear Granger causality to overcome such challenges.[28] However, it has been shown that using average data (e.g. seasonal averages) can produce near-linear relationships between climate variables,[25] and hence reasonable estimates of causal links can be obtained from a linear model.

Granger causality studies using climate data include a causality study investigating Southern and Northern Hemisphere temperatures,[29] and a Granger causality study between the North Atlantic Oscillation (NAO) and Atlantic SST at a seasonal scale.[22] Although most climate studies make use of a bivariate system when investigating causality between two variables,[22,24,28] bivariate systems have problems of spurious causality and of non-causality due to omission of a relevant variable.[24] These problems can be solved by introducing an auxiliary third variable in the analysis.[24,30] An alternative method for shorter time series is cross validation.[28] Other techniques used to test a direct Granger causality of Y on X include Ex Conditional Granger causality[31] and Partial Granger causality.[32] However, studies have not yet employed Granger causality to the Hadley cell and cloud cover. We thus test this using a four-step procedure. The procedure includes unit root testing and differencing, selecting the appropriate model for the time series data, and testing for Granger causality.

2.2.1 Unit Root Testing

The fundamental issue in testing for causality between variables is to use a suitable time series that is stationary or does not contain unit roots. Stationarity in a time series is defined as one

with a statistical process (mean or standard deviation) that does not change over time, whereas a non stationary time series may lead to false causality results.[33] The most common way of testing for stationarity is through the Augmented Dickey Fuller Test (ADF). The ADF test uses estimates from an augmented autoregression as follows:

$$\Delta y_{t=1}^{n} = \beta_1 + \alpha y_{t-1} + \gamma \Sigma \delta y_{t-1} + \varepsilon_t \tag{1}$$

where y_t represents all variables (in the natural logarithmic form) at time t, Δ is the first difference operator. β_1 is a constant, α and γ are model parameters where ($\alpha = [\alpha_1, ..., \alpha_p]$ and $\gamma = [\gamma_1, ..., \gamma_n]$) , ε_t is the noise residual in the regression and n is the optimal lag length on the dependent variable. The test for a unit root is conducted on the coefficient of y_{t-1} in the regression model. The null and alternative hypotheses are represented by (H_0) and (H_1) respectively. The null hypothesis states that data need to be differenced to make it stationary, while the alternative hypothesis states that data are stationary and do not need to be differenced. To check for the existence of a unit root in variable y_t we use: $H_0; = 0$ versus $H_1 :< 0$.. The coefficient should be significantly different from zero (less than zero) for the hypothesis that y contains a unit root to be rejected. Rejection of the null hypothesis indicates stationarity in the series.

2.2.2 Differencing

Granger causality test is ideal for stationary time series; however if any of the time series in question is not stationery or if there is a root, then the series should be temporally differenced. For a variable y depending on another variable x, i.e. $y = f(x)$, for a set of n points on an equispaced grid, the first f'_t at i=1 ,.....n, the backward difference will be given by:

$$\Delta y_t \equiv y_{t-1} - y_t \tag{2}$$

2.2.3 Model Selection

Vector auto-regressions (VAR) are often used in climate science to estimate the maximum lags used for testing data for Granger causality.[34−36] The Akaike information criteria (AIC) and the Bayesian information criteria (BIC) are used to find the optimal maximum lag. For this study daily time steps were used to construct the massflux and cloud cover time series for both DJF and JJA, a lag length of one and two represents the previous day and two previous days respectively and so on.[37] The two information criteria mentioned above follow a general form, which consists of the log-likelihood estimates as well as the penalty functions for the parameters in the model. Model estimates with the least information criteria is the best fitting model. The general information criteria are given as:

$$IC(p) = \ln|\Sigma^l| + C_T\frac{p}{T} \tag{3}$$

Where Σ^l is an approximation of the residual covariance matrix associated with the fitted VAR(p) model, C_T is a deterministic penalty term, T denotes the number of observations used for estimation and p denotes the lag order. The definition of the penalty term C_T differs with the choice of information criteria used i.e.: for AIC,

$$C_T = 2k^2, \tag{4}$$

and for BIC,

$$C_T = k^2, \tag{5}$$

where k is the number of equations in the VAR model.

2.2.4 Granger Causality

The presence and direction of Granger causality between each grid point of the Hadley cell and cloud cover is tested by means of vector auto-regressions (VAR), indicated by Equations (6)

and (7):

$$X_t = \alpha_1 + \Sigma_{i-1}^{S} \beta_i X_{t-i} + \Sigma_{i-1}^{S} \gamma_{1i} Y_{t-i} + e_{1t}, \tag{6}$$

$$Y_t = \alpha_2 + \Sigma_{i-1}^{S} \beta_{2i} X_{t-i} + \Sigma_{i-1}^{S} \gamma_{2i} Y_{t-i} + e_{2t}, \tag{7}$$

where α , β , and γ are regression coefficients, e's are error terms, and s is the lag length, which is determined by using AIC and the BIC (equation 3). The structural VAR consisting of present values of the Hadley cell and cloud cover as functions of the lagged values of the dependent variables, and the present and lagged values of the independent variables, is the basis for the derivation of equations (6) and (7). Structural VAR is based on the fact that for each season, present values of both the Hadley cell and cloud cover do not only depend on present values of the other variable, but also on the history of the other variable. The direction of causal order is thus determined by estimating the restricted forms of equations (6) or (7), and by eliminating the causal variable. For example, to determine whether the Hadley cell Granger causes cloud cover, we estimate a restricted form of equation (6) in which cloud cover is eliminated. The restricted version of equation (6) is thus:

$$X_t = \alpha_1^{'} + \Sigma_{i-1}^{S} \beta_{1i}^{'} X_{t-i} + e_{1t}, \tag{8}$$

Conversely, it can also be determined whether the Hadley cell can be Granger caused by cloud cover. This is possible by estimating a restricted version of equation (7), where the lagged values of the Hadley cell are omitted. We further test whether the restricted model is statically significantly different from the unrestricted model, as per the following procedure:

$$\omega = \frac{\left(\frac{RSS_T - RSS_u}{S}\right)}{\left(\frac{RSS_u}{T-k}\right)}, \tag{9}$$

Here, RSS is the sum of the residuals squared; the subscripts r and u refer to the restricted and unrestricted versions of equations (6) or (7), respectively; T is the number of observations; k

is the number of regressors in the unrestricted version of the equation; and s is the number of coefficients restricted to zero in equation (8). The test statistic can be evaluated against an F distribution with s and T-k degrees of freedom in the numerator and denominator respectively, in order to evaluate the null hypothesis that the cloud cover does not Granger cause the Hadley cell. In this study, equations (6) and (7) are used to analyse links between the Hadley cell and total cloud cover for each season (DJF and JJA) separately. The restrictive assumption is then constructed, such that the coefficients vary with the lag lengths and seasons. Equations (6) and (7) are then modified to cater for each season. Since daily time steps were used to construct time series for both DJF and JJA, a lag length of one thus indicates the previous day, a lag length of two implies two previous days, and so on. It is recognized that the detection of Granger causality does not necessarily imply a physical causal mechanism between the two fields. Conclusions about the presence and direction of causality depend on the validity of the statistical models. Challenges on using Granger causality between two variables is that Granger causal implication estimates may be biased by the omission of relevant variables (e.g. vertical motion due to weather systems may contribute to total cloud cover, and its omission may have bearing on the Granger causal statistic) that are in fact the causal variables. Notwithstanding such limitations, the causality test is more reliable than lagged correlation statistics because the latter only shows the interaction between two variables, but may not indicate the presence and direction of causality.

3. RESULTS AND DISCUSSION

3.1 Climatology of the Hadley cell and total cloud cover

The Hadley cell is usually defined in terms of the zonally averaged stream function.[5,11] The zonally averaged stream function (defined in Appendix 1) is displayed in Figure 1, together with the vertical cross section of the divergent circulation in the meridional plane displayed by means of

wind vectors. The clockwise direction of the mass stream function is indicated by blue shades; similarly the anticlockwise direction is illustrated by red shades of the stream function. The Hadley circulation consists of two branches, an ascending branch equatorward and a descending branch poleward. On the descending branch of the Hadley cell, the wind vectors advocate downward motion. Similarly, vertical ascent is evident on the ascending branch of the Hadley cell. The seasonal strength of the Hadley circulation is also evident from the stream function as well as the divergent circulation. In DJF, the Hadley circulation is positioned more southwards; its descending branch is weak and has a wider gradient (Fig.1a). In JJA, the Hadley cell is positioned more northwards; it is more pronounced and stronger, as indicated by the tight gradient of the stream function (Fig.1b). This meridional migration of the Hadley cell also displays intra-seasonal variability as demonstrated by composite anomalies of the mass stream function for low and high cloudiness years during DJF (Fig. 2a and Fig. 2b) and JJA (Fig.2c and Fig. 2d).

For the low cloudiness years, the mass stream function anomalies have reversed sign compared to the climatological mass stream function shown in Figure 1a and 1b. This means that for low cloudiness years during DJF (Fig. 2a) (eg. low DJF: 1986, 1987,1990,1992,1993,1995, 2004 and high DJF:1982,1983,1991,1997, 2001, 2004, 2007, 2010, 2011, 2012, 2013, 2014) and JJA (Fig. 2c) (low JJA: 1980, 1984, 1986, 1987, 1988, 1990, 1992, 1994, 1995, 1996, 1997, 1999, 2000, 2006, 2008, 2009 and high JJA: 1982, 1985, 1991, 1993, 1998, 2002, 2004, 2005, 2007, 2009, 2010, 2012, 2013, 2014), the Hadley cell is positioned towards the equator and its width is narrower than in climatology.[38] The equatorward displacement of the Hadley cell is linked to subsidence over the subtropical regions of the Southern Hemisphere. In high cloudiness years for both DJF (Fig. 2b) and JJA (Fig. 2d), the mass stream function anomalies have the same sign as the climatological mass stream function.[38] In both seasons the statistical significance covers a wider area for the high cloudiness years compared to the low cloudiness

years. This implies that the Hadley cell extends more polewards than normal, enhancing cloud formation over the Southern Hemisphere subtropics. While the zonally averaged stream function gives a general overview of the Hadley cell, it is easy to miss regional features of the Hadley circulation due to zonal averaging. Therefore, to examine the behaviour of the Hadley cell over South Africa, a zonally asymmetric diagnostic of the Hadley cell is necessary.

The zonally asymmetric Hadley cell is represented by the meridional massflux at 500hPa, as indicated in the Appendix 2. The climatology of the zonally asymmetric Hadley cell and total cloud cover for DJF is provided in Figures (3) and (4) respectively. For both the DJF and JJA seasons (Fig. 3 and Fig. 4), the downward massflux is dominant over the country, as indicated by negative massflux values. Simultaneously, lower cloud amount is evident throughout the country. Both massflux and cloud cover are indicative of the subtropical weather. Vertical velocity plays an integral role in both the Hadley cell and total cloud cover. Negative vertical velocity in the pressure coordinate system is associated with vertical uplift and cloud formation, whereas positive vertical velocity values are linked subsidence and limited cloud development.

Negative vertical velocity is evident in DJF (Fig. 3 and Fig. 4), but very close to zero, which means that even if there is some vertical uplift, it is less since the mean vertical motion over South Africa is downward. The eastern escarpment also indicates negative values of vertical velocity. High negative vertical velocity values are confined to areas of positive massflux over the northern parts of the subcontinent. However, over South Africa, negative velocity is confined to the western interior of South Africa and the eastern escarpment. These areas are characterized by the downward massflux (Fig. 3) and relatively higher values of cloud cover (Fig. 4), which means the downward massflux is not responsible for the negative vertical velocity, but is rather the effect of weather systems that dominate over interior regions of South Africa during sum-

mer months, while uplift is due to orography (over the eastern escarpment) that contributes to negative vertical velocity and cloud cover.

In JJA, a semi-permanent high pressure system dominates the country, resulting in a strong negative massflux (Fig. 5), as well as limited cloud development over the country (Fig. 6). Subsidence due to the Hadley cell could be the main cause for the lack of upward vertical motion (negative vertical velocity), and could mean that limited cloud development results from a lack of upward vertical motion. These results demonstrate that vertical velocity plays a crucial role in the causality between Hadley cell and cloud cover. Therefore effect of vertical velocity should thus be kept in mind when interpreting causality between the Hadley cell and cloud cover.

3.1.1 Stationarity

Based on the results of the ADF test (Table 1), the unit root hypothesis could not be rejected for both time series, however, when the backward difference was performed for both time series, the unit hypothesis was rejected. This suggests that both Hadley cell and total cloud cover are not stationary and might be considered stationary at the first differenced level. After attaining stationarity of the time series, the best model was further investigated by identifying the maximum lags that could be used in the VAR model. Most climate studies have used a lag length of 4, as the optimal length for causality analysis. In this study, we have an optimal lag length established by using the AIC and BIC for DJF and JJA. Results from the two information criterion tests favoured lag 2, as the maximum lag for fitting the VAR model (Fig. 7a and 7b). This means that the previous two days are very critical for predicting cloud cover when using the Hadley as the predictor, and vice versa.

3.2 Correlations

A number of studies make use of linear and lag correlations to study associations between two time series in climate science (e.g. Wu et al., 2015; Mosedale et al., 2006).[19,24] Linear correlation represents the correlation of variables within the same time period, while lagged correlation means there's a temporal (could be daily, monthly etc) lag in the correlation of the variables. In this study daily lagged correlations between the Hadley cell and total cloud cover for DJF and JJA are averaged over South Africa (Fig. 7c and Fig. 7d) and used to measure the strength and direction of the lag relationship between the cloud cover and Hadley cells. In the first week (1 to 7 days), relatively higher correlations (0.56 and for DJF; 0.39 to 0.516 for JJA) were established. This is followed by a substantial decrease in lag lengths. The decrease in lagged correlation from the second week onwards could mean that longer timescales (e.g. weeks to months) might have detrimental effects in the prediction of total cloud cover using the Hadley cell. In the first week, the second day (day 2) gave the highest correlation (0.56 and 0.516) for both DJF and JJA.

To determine zonal gradients of temporal correlations for different lag lengths between the Hadley cell and total cloud cover for DJF and JJA, a zonally asymmetric analysis for lag lengths of 1 to 4 days was performed, as informed by Figures 3-6. Positive correlations for lag lengths of 1 to 2 days over South Africa are recorded for the north-western parts of South Africa and Namibia in DJF (Figs. 3a, 3b, 4a and 4b). The north-western parts of South Africa are the most arid in the country, and mostly dominated by the Hadley cell. The eastern parts of South Africa also show positive correlations for lag lengths of 1 to 2 days. No strong correlation is established over the southern interior of South Africa in DJF, which is attributed to the fact that cloud

cover over these areas is caused by weather systems that are prevalent over South Africa, rather than the Hadley cell. Lag lengths of 2 days followed by a lag length of 1 day has a stronger positive correlation than for lag lengths of 3 and 4 days, as indicated in Fig. 3c, Fig. 3d, Fig. 4c and Fig. 4d.

In JJA, a positive correlation between the Hadley cell and cloud cover for lag lengths of 1 and 2 days has been established over the interior of South Africa, as shown in Fig. 5a and Fig. 5b. This is attributed to the fact that a high pressure system is dominant over the interior of South Africa in JJA.[3] Enhanced subsidence ahead of subtropical high due to isentropic flow leads to limited cloud development over these areas. Subsidence leading to limited cloud development is hence expected over these areas. A strong positive correlation between the Hadley cell and cloud cover is recorded over the Atlantic Ocean, west of South Africa. From the 4 lag lengths investigated, the lag length of one showed the strongest correlation. No discernible correlation is established over South Africa for lag lengths of 3 to 4 days (Fig. 5c, Fig. 5d, Fig.6c and Fig. 6d).

3.3 Granger Causality

To determine whether variability in cloud cover is caused by the Hadley cell, the bivariate model indicated in equations (6) and (7) was used. The F statistic and critical values of the bivariate model were established at each grid point. The presence of Granger causality is denoted by values of the F statistic being greater than the critical value, and conversely, values of the F statistics less than the critical value show the absence of Granger causality. The strength of Granger causality from the Hadley cell to total cloud cover (denoted as HC-CC) and total cloud cover to the Hadley (denoted as CC-HC) is indicated in Figures 8 and 9 for DJF and JJA respec-

tively. The presence of Granger causality is established from the HC-CC interaction over South Africa. In DJF, the western and north-western regions show higher values of HC-CC causality. However, maximum causality is located over the far north-eastern parts of the subcontinent between latitudes 15 ° to 10.5°S.

The presence CC-HC Granger causality has also been established over South Africa, but is limited to only the eastern parts of the country, while the western and south-eastern parts are absent of causality. Some places over Mozambique and Zimbabwe indicate very weak CC-HC causality. In JJA, the HC-CC causality is stronger than the CC-HC causality, and the maximum causality values are situated over the northern interior of South Africa. No causality has been established over the south-western parts of South Africa. One notable feature is that the HC-CC maximum causality has moved further northwards in JJA, than in DJF, and this could be linked with the northwards migration of the ITCZ during austral winter. Although the CC-HC causality is weak over most parts of South Africa, especially in JJA, the south-western parts advocate an absence of Granger causality.

As previously mentioned [22,24,28] the main challenge with Granger causality in a bivariate model is the exclusions of other variables that may affect the causing variable, thus leading to false causality of the variables being testing. This could mean that although weak, the CC-HC causality may be false due to the omission of a third variable that is affecting the causality result. For example, cloud cover is a function of vertical velocity, which in turn may affect the Hadley cell. The effect of vertical velocity due to other weather systems has indirect impact in the causality of both the Hadley cell and cloud cover. Secondly, the structure of the CC-HC causality in DJF is oriented in a north-westerly to south-easterly direction, resembling the structure of tropical temperature troughs (TTT's). This could mean that the vertical velocity

due to TTT's, which are a summer phenomenon over southern Africa,[39] is responsible for the causality from the cloud cover to the Hadley cell. This leads to CC-HC false causality. In JJA, the HC-CC causality is stronger than the CC-HC causality. The HC-CC stronger causality is greater over the interior and northwards of South Africa. This could be attributed to the fact that the Hadley cell informs limited cloud development over the subtropics and during JJA (Fig. 9a). The far northern and south-western parts of South Africa show relatively weaker HC-CC causality. Cloud cover over the south-western parts is greater because of frontal systems, and not entirely due to the Hadley cell, and hence produces weaker causality.

To illustrate the effect of vertical velocity causality on both the Hadley cell and cloud cover, Granger causality was analysed between vertical velocity and cloud cover (Fig. 10). The omega to cloud cover interaction is denoted as OMEGA-CC. Causality is established for both DJF and JJA. In DJF, the OMEGA-CC causality is located predominantly over the eastern to western escarpment of South Africa (Fig. 10a), which means that vertical velocity due to topography (orographic uplift) is the main cause of cloud cover along the escarpment regions of South Africa. The western and adjacent oceanic regions show maximum OMEGA-CC causality. Strong OMEGA-CC causality is also evident between Mozambique and Zimbabwe. In JJA, most of the South African interior shows very weak OMEGA-CC causality, however the northern and north-western parts of South Africa show strong OMEGA-CC causality (Fig. 10b). Figure 11 depicts Granger causality of vertical velocity to the Hadley cell and we identify this as OMEGA-HC. The OMEGA-HC causality is further southwards and weaker in DJF and further northwards and stronger in JJA, which may be linked with the northwards-southwards seasonal migration of the ITCZ. In DJF, OMEGA-HC causality is strong over the summer region of South Africa and stronger along the south-eastern parts. In JJA, strong OMEGA-HC causality is located over the interior of South Africa where the subtropical high pressure cell is

located. The south-western parts of South Africa show an absence of OMEGA-HC causality for both DJF and JJA, which may be attributed to weather over the south-western parts being Mediterranean in nature, and mostly owing to southerly frontal systems, rather than the Hadley cell.

4. CONCLUSIONS

Our study uses Granger causality time series modelling to quantitatively diagnose the influence of the seasonal Hadley cell on cloud cover and vice versa. Bivariate vector autoregressive time series models for the period 1980 to 2015 were fitted to the seasonal Hadley cell and total cloud cover. According to the AIC and BIC statistics, the optimum lag used in the Hadley cell-cloud cover bivariate model was two days. The highest correlation coefficient of the lag correlations from averaged data was also two days. The lag correlations calculated from each grid point indicates lag lengths of one to two days for strongest correlation. The strength of these correlations is seasonally dependent and advocates linkage between the meridional shift of the Hadley cell and the seasonal migration of the Inter-Tropical Convergence Zone (ITCZ).[11] The meridional shift of the Hadley cell is seasonal but with intra-seasonal variability as informed by the seasonal climatology of the mass stream function as well as from composite anomalies of the mass stream function during high and low cloudiness years. The lag correlation between the Hadley cell and cloud cover is stronger in DJF than in JJA. This may be owing to the synoptic systems (e.g tropical temperate troughs and westerly waves) leading to cloud formation, dominating in the DJF period. Such systems have life spans of one to several days.[39,40] It should also be noted that typically two days before the development of tropical temperate troughs over South Africa, there is a migration of easterly moisture from Botswana to the subtropical region of South Africa, which is an example of the strong two day lag correlation in DJF.[40]

This paper further establishes that the Hadley cell can Granger cause cloud cover for both DJF and JJA. This causality is associated mostly with limited cloud development. For example, causality is found over the interior of South Africa, where the subtropical high pressure cell dominates. In DJF, the western parts of South Africa experience limited cloud development, and this is mostly where causality is established. Weak causality from cloud cover to the Hadley cell has also been established. This is a typical case of spurious causality in bivariate systems caused by the exclusion of a third variable in the Granger causality analysis. Further analysis has shown that vertical velocity is the main variable that could have led to the causality of cloud cover to the Hadley cell. Finally, although we have shown that Granger causality is a useful tool in establishing causality from the Hadley cell to cloud cover, to obtain the best outputs, the scientific background of the variables being analysed should be well understood before correct interpretations of the causality results can be made.

Formally establishing the causality of anomalously strong regional Hadley cell circulation in terms of limited cloud development over southern Africa is of profound importance within the context of future climate change over the region. Southern Africa has been assessed to be likely to become generally drier under low mitigation climate change futures. [13,41,39,42,43] The underlying circulation changes in the model projections of climate change that led to this assessment have in fact been shown to include the frequent occurrence of mid-level anti-cyclones and subsidence [13,41] over the region, which implies a strengthening of the descending branch of the Hadley cell. Enhanced limited cloud development over southern Africa in a warming world, in response to changes in the regional Hadley cell, may thus be an important driving factor driving the relatively high rate of observed and projected temperature increases over southern Africa.[44] Enhanced limited cloud development may further enhance southern Africa's solar po-

tential within the context of a growing renewable energy sector, but will be largely detrimental to agriculture and may further compromise water security in the region.

Acknowledgements

This work was financially supported by the National Research Foundation (NRF) Grant number 102215. The authors are grateful to Mr. Chang-Hyan Park for his valuable input prior to the submission of this manuscript. The anonymous reviewers are also acknowledged for their input in improving the manuscript.

Appendix 1: Zonally averaged mass stream function

The zonally averaged mass stream function is given by:

$$\psi(\phi, p) = \frac{2\pi a \cos\phi}{g} \int_{p}^{p_s} \overline{v} dp' \tag{A0}$$

, (Polvani et al., 2011)

where ϕ is latitude, p pressure, $\overline{v}$ the zonal mean meridional wind, a the radius of the earth and g the gravitational acceleration.

Appendix 2: Zonally asymmetric diagnostics of the Hadley cell

In the isobaric vertical coordinate system, the spherical version of the continuity equation is given by:

$$\frac{1}{a\cos\phi}\frac{\partial u}{\partial \lambda} + \frac{1}{a\cos\phi}\frac{\partial}{\partial \phi}(v\cos\phi) + \frac{\partial \omega}{\partial p} = 0 \tag{A1}$$

where u and v are the zonal meridional components of the divergent ageostrophic flow, respectively, ω the vertical component of the velocity, a is the radius of the Earth, λ is the longitude and ϕ is the latitude. In this section we partition the isobaric continuity equation (see A1). On each isobaric surface, the divergent, irrotational flow in Equation (A1) may be written in terms of a velocity potential χ, such that

$$u = \frac{1}{a \cos\phi}\frac{\partial \chi}{\partial \lambda} \ ) \tag{A2}$$

$$v = \frac{1}{a \cos\phi}\frac{\partial}{\partial \phi}(\chi \cos\phi) \tag{A3}$$

since $\nabla \times \nabla\chi = 0$. Let

$$\chi \equiv \frac{\partial \mu}{\partial p} \tag{A4}$$

where μ is a potential function, and then combine this with A1 to produce a Poison's equation in μ, i.e.

$$\frac{1}{a^2 \cos^2\phi}\frac{\partial^2 \mu}{\partial \lambda^2} + \frac{1}{a^2 \cos\phi}\frac{\partial}{\partial \phi}\left(\sin\phi \frac{\partial \mu}{\partial \partial \phi}\right) = -\omega, \tag{A5}$$

which is solved numerically, given suitable boundary conditions as discussed in Subsection 2.2.2.

Now define a vector stream function $\overrightarrow{\psi}$ (here the over arrow indicates that this quantity is a vector), such that

$$\psi_\lambda = -\frac{1}{a \cos\phi}\frac{\partial \mu}{\partial \lambda} \ \text{ and } \ \psi_\phi = -\frac{1}{a}\frac{\partial \mu}{\partial \phi} \tag{A6}$$

and taking the divergence of $\overrightarrow{\psi}$ and using (A5), we obtain

$$\frac{1}{a \cos\phi}\frac{\partial \psi_\lambda}{\partial \lambda} + \frac{1}{a \cos\phi}\frac{\partial}{\partial \phi}(\psi_\phi \cos\phi) = \omega \tag{A7}$$

Clearly, from (A7), vertical motion ω is partitioned into two orthogonal directions so that

$$\omega_\lambda \cos\phi = \frac{1}{a}\frac{\partial \psi_\lambda}{\partial \lambda} \tag{A8}$$

$$\omega_\phi \cos\phi = \frac{1}{a}\frac{\partial}{\partial \phi}(\psi_\phi \cos\phi) \tag{A9}$$

with $\omega = \omega_\lambda + \omega_\phi$.

It follows then from (A2) , (A3)and (A4) that the zonal component of the ageostrophic flow may be written in terms of zonal component of the ψ vector:

$$u = \frac{1}{a\cos\phi}\frac{\partial}{\partial \lambda}\left(\frac{\partial \mu}{\partial p}\right) = \frac{\partial}{\partial p}\left(\frac{1}{a\cos\phi}\frac{\partial \mu}{\partial \lambda}\right) = -\frac{\partial \psi_\lambda}{\partial p} \tag{A10}$$

Similarly, the meridional component of the ageostrophic flow may be written in terms of meridional component of the ψ vector as follows

$$v = -\frac{\partial \psi_\phi}{\partial p} \tag{A11}$$

Using (A8) and (A10) and the fact that partial derivatives are interchangeable, we have

$$\frac{1}{a}\frac{\partial u}{\partial \lambda} + \frac{\partial}{\partial p}(\omega_\lambda \cos\phi) = 0 \tag{A12}$$

and similarly

$$\frac{1}{a}\frac{\partial}{\partial \phi}(v\cos\phi) + \frac{\partial}{\partial p}(\omega_\phi \cos\phi) = 0 \tag{A13}$$

REFERENCES

1. Department of Energy (DoE), 2013. Integrated Resource Plan For Electricity (IRP) 2010-2030. Update Report 2013.
2. Loeb NG, Schuster GL. An observational study of the relationship between cloud, aerosol and meteorology in broken low-level cloud conditions, J. Geophys. Res. 2008; 113,D14214,doi:10.1029/2007JD009763
3. Tyson PD, Preston-Whyte RA. The weather and climate of Southern Africa, 2nd edn. Cape Town. Oxford University Press. 2000.
4. Engelbrecht CJ, Engelbrecht FA. Shifts in Köppen-Geiger climate zones over southern Africa in relation to key global temperature goals. Theor. Appl. Climatol. 2016; 123: 247- 261. https://doi.org/10.1007/s00704-014-1354-1
5. Seidel DJ, Fu Q, Randel WJ, Reichler TJ. Widening of the tropical belt in a changing climate. Nat. Geosci. 2008; 1: 21-24. https://doi.org/10.1038/ngeo.2007.38
6. d'Abreton PC, Lindesay JA. Water vapour transport over southern Africa during wet and dry early and late summer months. Int. J. Climatol. 1993; 13: 151-170. https://doi.org/10.1002/joc.3370130203
7. Tennant WJ, Reason CJC. Associations between the Global Energy Cycle and Regional Rainfall in South Africa and Southwest Australia. J. Clim. 2005; 18:3032-3047. https://doi.org/10.1175/JCLI3464.1
8. Mahlobo DD, Ndarana T, Grab S, Engelbreht F. Integrated climatology and trends in the subtropical Hadley cell, sunshine duration and cloud cover over South Africa. Int. J. Climatol. 2018; 39.1805-1821. https://doi.org/10.1002/joc.5917
9. Manabe S, Holloway JL. The seasonal variation of the hydrological cycle as

simulated by a global model of the atmosphere. J. Geophys. Res. 1975; 80: 1617-1649. https://doi.org/10.1029/JC080i012p01617.

10. Hart N, Reason CJC, Fauchereau N (2012) Cloud bands over southern Africa: seasonality, contribution to rainfall variability and modulation by the MJO. Clim. Dyn. 2012. 41: 1199–1212. doi:10.1007/s00382-012-1589-4

11. Kang SM, Lu J. Expansion of the Hadley cell under global warming: Winter versus summer. J. Clim. 2012; 25: 8387-8393. https://doi.org/10.1175/JCLI-D-12-00323.1

12. Hart N, Reason CJC, Fauchereau N (2013) Building a tropical extratropical cloud band metbot. Mon. Wea. Rev. 140: 4005– 4016. doi:10.1175/MWR-D-12-00127.1

13. Engelbrecht FA, McGregor JL, Engelbrecht CJ. Dynamics of the conformal-cubic atmospheric model projected climate-change signal over southern Africa. Int. J. Climatol . 2009; 29: 1013-1033.

14. Granger CWJ. Investigating causal relations by econometric models and cross spectral methods. Econometrica.1969 ;37: 424-438. https://doi.org/10.2307/1912791.

15. Dee DP, Uppala SM, Simmo AJ, Berrisford P, Poli P, Kobayashi S, et al. The ERA-Interim reanalysis: Configuration and performance of the data assimilation system. Q. J. Royal Meteorol. Soc. 2011; 37: 553-597. https://doi.org/10.1002/qj.828.

16. Schwendike J, Govekar P, Reeder MJ, Wardle R, Berry GJ, Jakob C. Local Partitioning of the overturning circulation in the tropics and the connection to the Hadley and Walker circulations J. Geophys. Res. 2014; 119: 1322-1339. https://doi.org/10.1002/2013JD020742.

17. Nguyen H, Evans A, Lucas C, Smith I, Timbal B. The Hadley circulation in

reanalyses: Climatology, variability, and change. J. Clim. 2013; 26: 3357-3376. https://doi.org/10.1175/JCLI-D-12-00224.1.

18. Nemani R, Keeling CD, Hashimoto H, Jolly WM, Piper SC, Tucker CJ, et al. Running SW. Climate driven increases in global terrestrial net primary production from 1982 to 1999. Science. 2003; 300:1560-1563. https://doi.org/10.1126/science.1082750.

19. Wu D, Zhao X, Liang S, Zhou T, Huang K, Tang B, et al. Time-lag effects of global vegetation responses to climate change. Glob. Change Biol. 2015; 21: 3520-3531. https://doi.org/10.1111/gcb.12945

20. Abramson B, Brown J, Edwards W, Murphy M, Winkler R. A bayesian system for forecasting severe weather. Int. J. Forecast.1996; 12: 57-71. https://doi.org/10.1016/0169-2070(95)00664-8.

21. Cofino A, Cano R, Sordo C, Gutierrez JM. Bayesian networks for probabilistic weather prediction. In Proceedings of the 15th European Conference on Artifical Intelligence: IOS Press; 2002. 695-700.

22. Wang W, Anderson BT, Kaufmann RK, Myneni RB. The relation between the North Atlantic Oscillation and SSTs in the North Atlantic Basin. J. Clim. 2004; 17: 4752-4759. https://doi.org/10.1175/JCLI-3186.1

23. Elsner JB. Evidence in support of the climate change Atlantic hurricane hypothesis. Geophys. Res. Lett. 2006; 33. https://doi.org/10.1029/2006GL026869.

24. Mosedale TJ, Stephenson DB, Collins M, Mills TC. Granger causality of coupled climate processes: Ocean feedback on the North Atlantic Oscillation. J. Clim. 2006; 19: 1182 -1194. https://doi.org/10.1175/JCLI3653.1

25. Attanasio A, Pasini A, Triacca U. Granger causality analyses for climatic attribution. Atmos. Clim. Sci. 2013; 3: 515-522. https://doi.org/10.4236/acs.2013.34054

26. Zou C, Feng J. Granger causality vs. dynamic bayesian network inference: a comparative study. BMC Bioinformatics. 2009; 10: 122. https://doi.org/10.1186/1471-2105-10-122.

27. Diks C, Mudelsee M. Redundancies in the Earth's climatological time series. Phys. Lett. 2000; 275: 407-414. https://doi.org/10.1016/S0375-9601(00)00613-7

28. Papagiannopoulou C, Miralles DG, Decubber S, Demuzere M, Verhoest NEC, Dorigo WA,et al. A non-linear Granger-causality framework to investigate climate–vegetation dynamics. Geosci. Model Dev. 2017; 10: 1945-1960. https://doi.org/10.5194/gmd-10-1945-2017

29. Kaufmann RK ,Stern DI. Evidence for human influence on climate from hemispheric temperature relations. Nature.1997; 388: 39-44. https://doi.org/10.1038/40332

30. Geweke J. Measurement of linear dependence and feedback between multiple time series. J. Am. Stat. Assoc.1982; 77: 304-313. https://doi.org/10.2307/2287238

31. Barnett L, Seth AK . The MVGC multivariate Granger causality toolbox: a new approach to Granger-causal inference. J. Neurosci. Methods. 2014; 223: 50-68. https://doi.org /10.1016/j.jneumeth.2013.10.018

32. Guo S, Seth AK, Kendrick KM, Zhoud C, Feng J. Partial Granger causality—eliminating exogenous inputs and latent variables. 2008; 172: 79-93. https://doi.org/10.1016/j.jneumeth.2008.04.011

33. Sims CA, Stock JH, Watson MW. Inference in linear time series models with some unit roots. Econometrica.1990; 58: 113 -144. https://doi.org/10.2307/2938337

34. Triacca U. On the use of Granger causality to investigate the human influence on climate. Theor. Appl. Climatol. 2001;69:137-138. https://doi.org/10.1007/s007040170019

35. Attanasio A, Pasini A, Triacca U. A contribution to attribution of recent global warming by out-of-sample Granger causality analysis. Atmos. Sci. Lett. 2012; 13: 67-72. https://doi.org/10.1002/asl.365

36. Pasini A, Triacca U, Attanasio A. Evidence of recent causal decoupling between solar radiation and global temperature. Environ. Res. Lett. 2012; 7. https://doi.org/10.1088/1748-9326-7-3-034020

37. He W. Model selection for cointegrated relationships in small sample. MSc. dissertation. Port Elizaberth: Nelson Mandela Metropolitan University; 2008.

38. Guo Y-Pe, LI J-Ping. Impact of ENSO events on the interannual variability of Hadley circulation extents in boreal winter. Adv. Clim. Change Res. 2016; 7: 46-53. https://dx.doi.org/10.1016/j.accre.201605.001

39. Hart NCG, Reason CJC, Fauchereau N. Tropical extratropical interactions over southern Africa: Three cases of heavy summer season rainfall. Mon. Wea. Rev. 2010; 138: 2608-2623. https://doi.org/10.1175/2010MWR3070.1

40. Singleton AT, Reason CJC. Variability in the characteristics of cut-off low pressure systems over subtropical southern Africa. Int. J. Climatol. 2007; 27: 295 -310. https://doi.org/ 10.1002/joc.1399.

41. Christensen JH, Hewitson B, Busuioc A, Chen A, Gao X,Held I, Jones R, et al. Regional climate projections. In: Climate Change 2007: The Physical Science Basis. Contribution of Working Group I to the Fourth Assessment Report of the Intergovernmental Panel on Climate Change [Solomon S, Qin D, Manning M, Chen Z, Marquis M, Averyt KB, et al. (eds.)]. 2007.Cambridge University

Press, Cambridge.

42. Niang I, Ruppel OC, Abdrabo MA, Essel A, Lennard C , Padgham J , et al. Africa. In: Climate Change 2014: Impacts, Adaptation, and Vulnerability. Part B: Regional Aspects. Contribution of Working Group II to the Fifth Assessment Report of the Intergovernmental Panel on Climate Change [Barros VR, Field CB, Dokken DJ, Mastrandrea MD, Mach KJ, Bilir TE, et al.(eds.)]. 2014.Cambridge University Press, Cambridge.

43. Hoegh-Guldberg O, Jacob D, Taylor M, Bindi M, Brown S, Camilloni I, et al. Chapter 3: Impacts of 1.5°C global warming on natural and human systems. In: Global Warming of 1.5 °×C an IPCC special report on the impacts of global warming of 1.5 °×C above pre-industrial levels and related global greenhouse gas emission pathways, in the context of strengthening the global response to the threat of climate change. Intergovernmental Panel on Climate Change. 2018.

44. Engelbrecht F, Adegoke J, Bopape M, Naidoo M, Garland R, Thatcher M, et al. Projections of rapidly rising surface temperatures over Africa under low mitigation. Environ. Res. Lett .2015;10, https://doi.orgi:10.1088/1748-9326/10/8/085004.

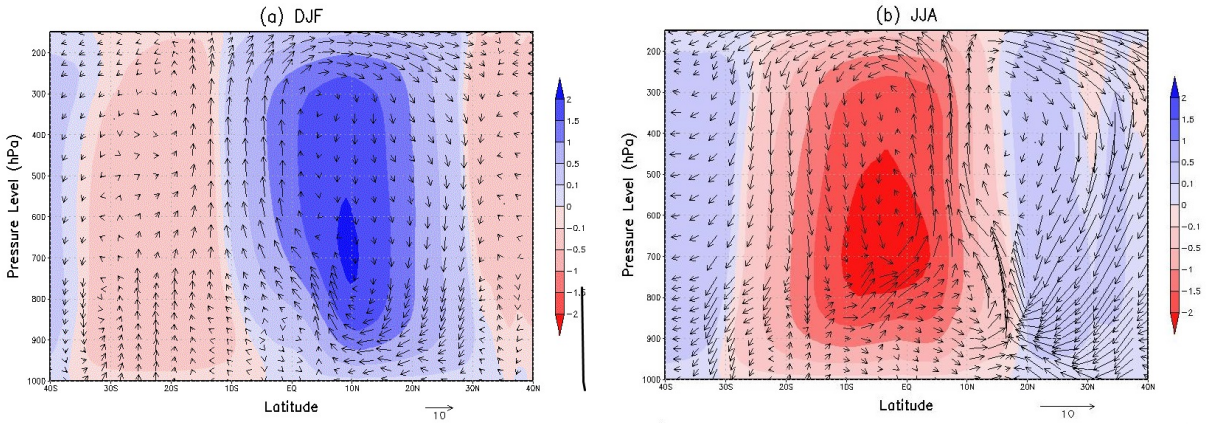

Fig. 1. Climatology of zonally averaged stream function with clockwise direction (red shades) and anticlockwise direction (blue shades) and divergent circulation on a meridional plane (wind vectors) for (a) DJF and (b) JJA. The contour intervals for the stream function are 10^{11}.

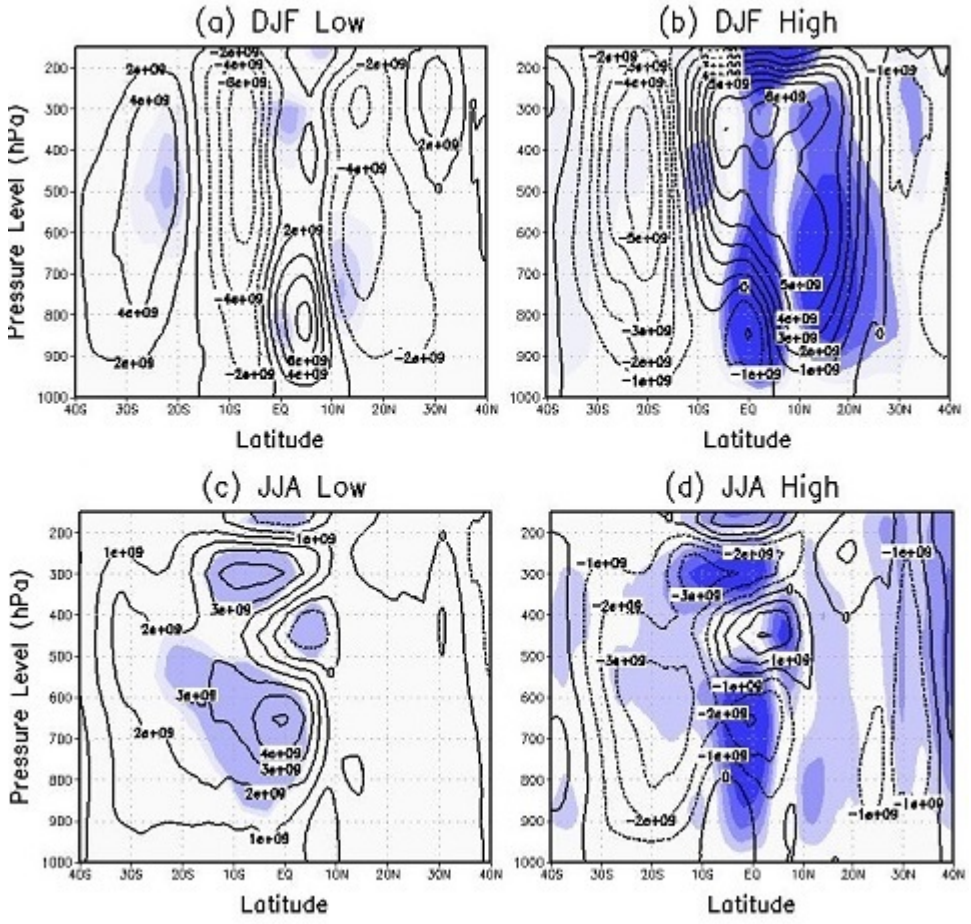

Fig. 2. The mass stream function composite anomalies (contour plot) and statistical significance (blue shaded plot) for low cloudiness period for (a) DJF, (c) (JJA) and high cloudiness period for (b) DJF and (c) JJA.

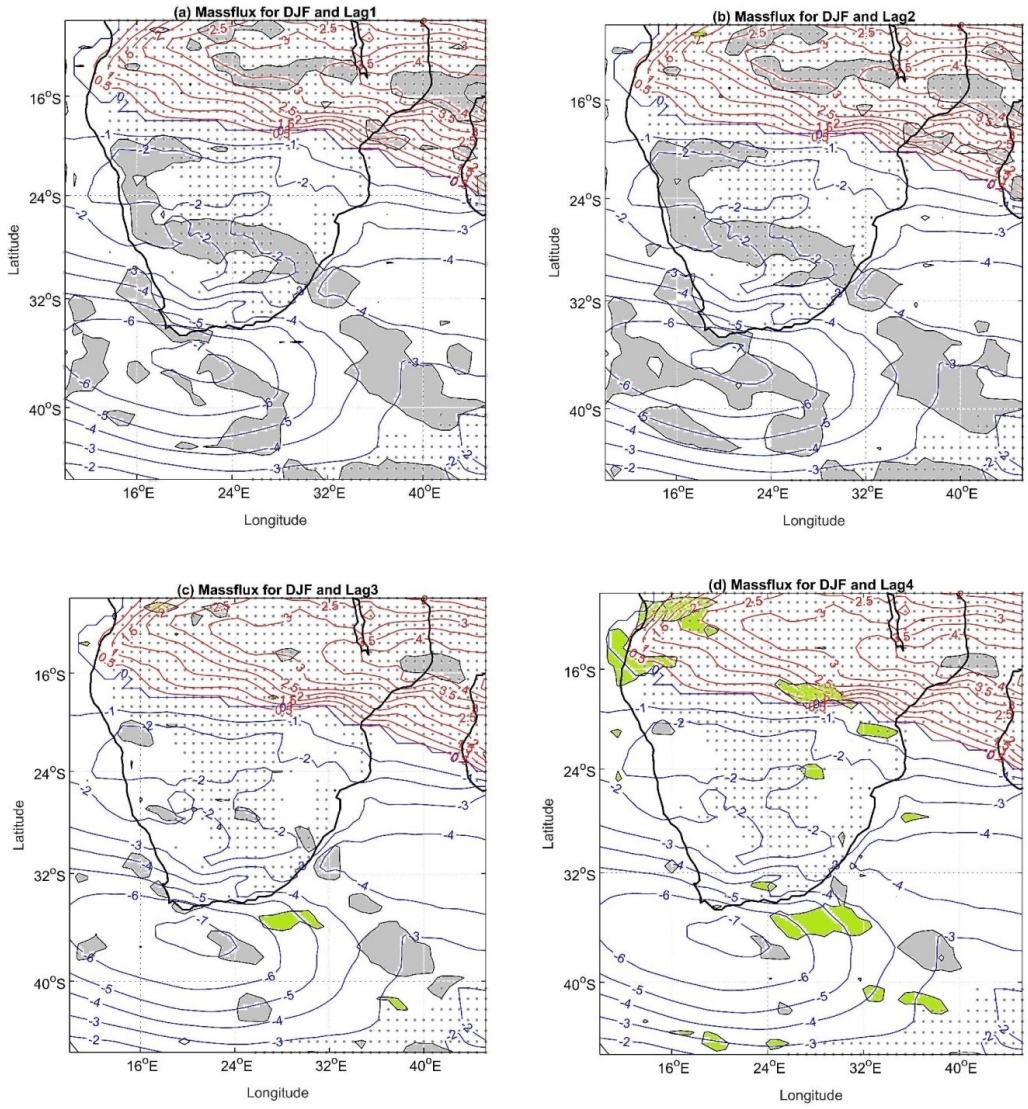

Fig. 3. Seasonal mean of the massflux (m_ϕ) and the units are kgm^{-2}s^{-1} in DJF. The contours are plotted in 10^3 kgm^{-2}s^{-1} intervals. (a) Correlation Coefficients for the Hadley and total cloud cover in DJF for (a) Lag 1, (b) Lag 2, (c) Lag 3 and (d) Lag 4. Grey shading denotes correlation coefficients greater than 3 and green shading indicates correlation coefficients less than -3. Regions of upward vertical velocity is represented using the grey dots and where there are no grey dots then there is downward motion there (i.e. $\omega > 0$).

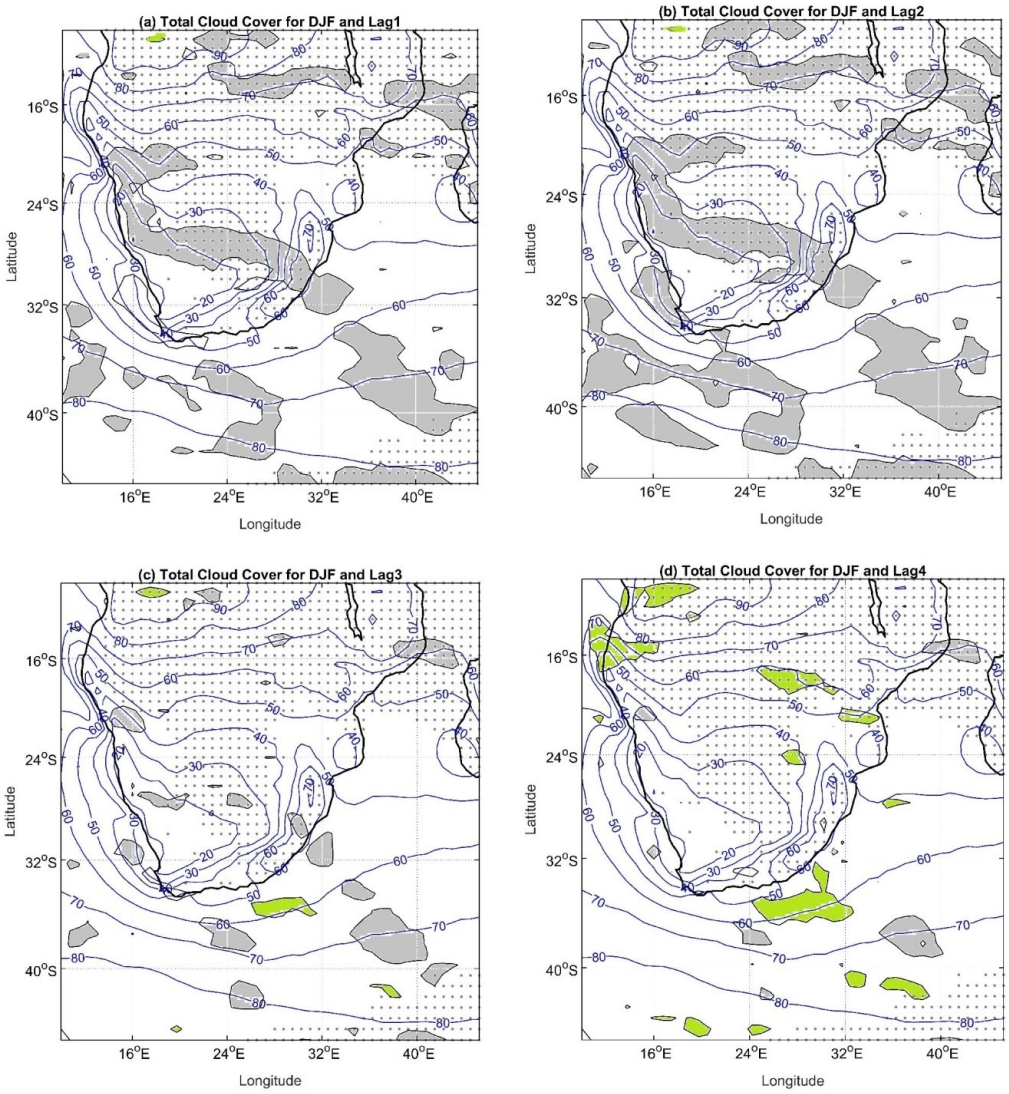

Fig. 4. Total cloud cover area fraction (a-d) presented as percentage (contours) in DJF. Correlation Coefficients for the Hadley and total cloud cover in DJF for (a) Lag 1, (b) Lag 2, (c) Lag 3 and (d) Lag 4. Grey shading denotes correlation coefficients greater than 3 and green shading indicates correlation coefficients less than -3. Regions of upward vertical velocity is represented using the grey dots and where there are no grey dots then there is downward motion there (i.e. $\omega > 0$)

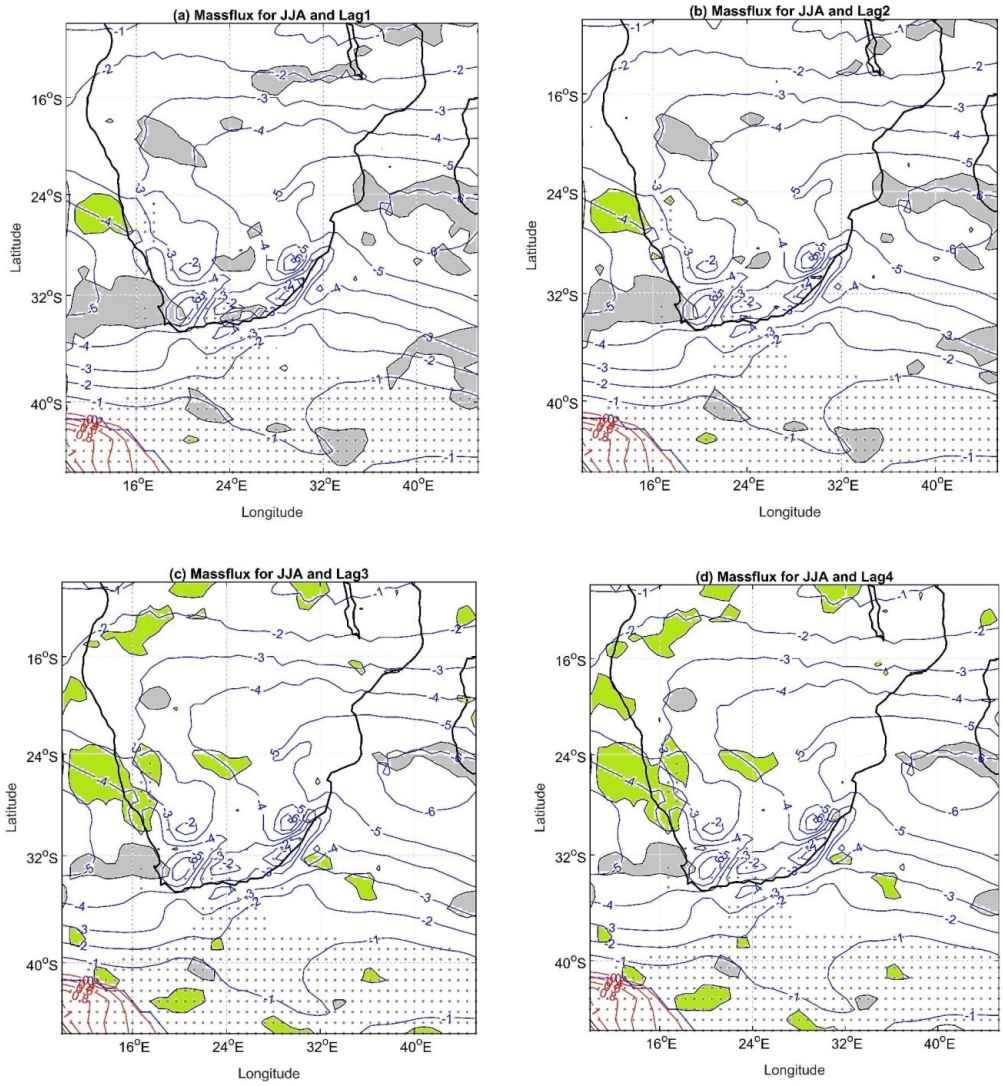

FIGURE 5. Seasonal mean of the massflux (m_ϕ) and the units are kgm^{-2}s^{-1} in JJA. The contours are plotted in 10^3 kgm^{-2}s^{-1} intervals. (a) Correlation Coefficients for the Hadley and total cloud cover in JJA for (a) Lag 1, (b) Lag 2, (c) Lag 3 and (d) Lag 4. Grey shading denotes correlation coefficients greater than 3 and green shading indicates correlation coefficients less than -3. Regions of upward vertical velocity is represented using the grey dots and where there are no grey dots then there is downward motion there (i.e. $\omega > 0$).

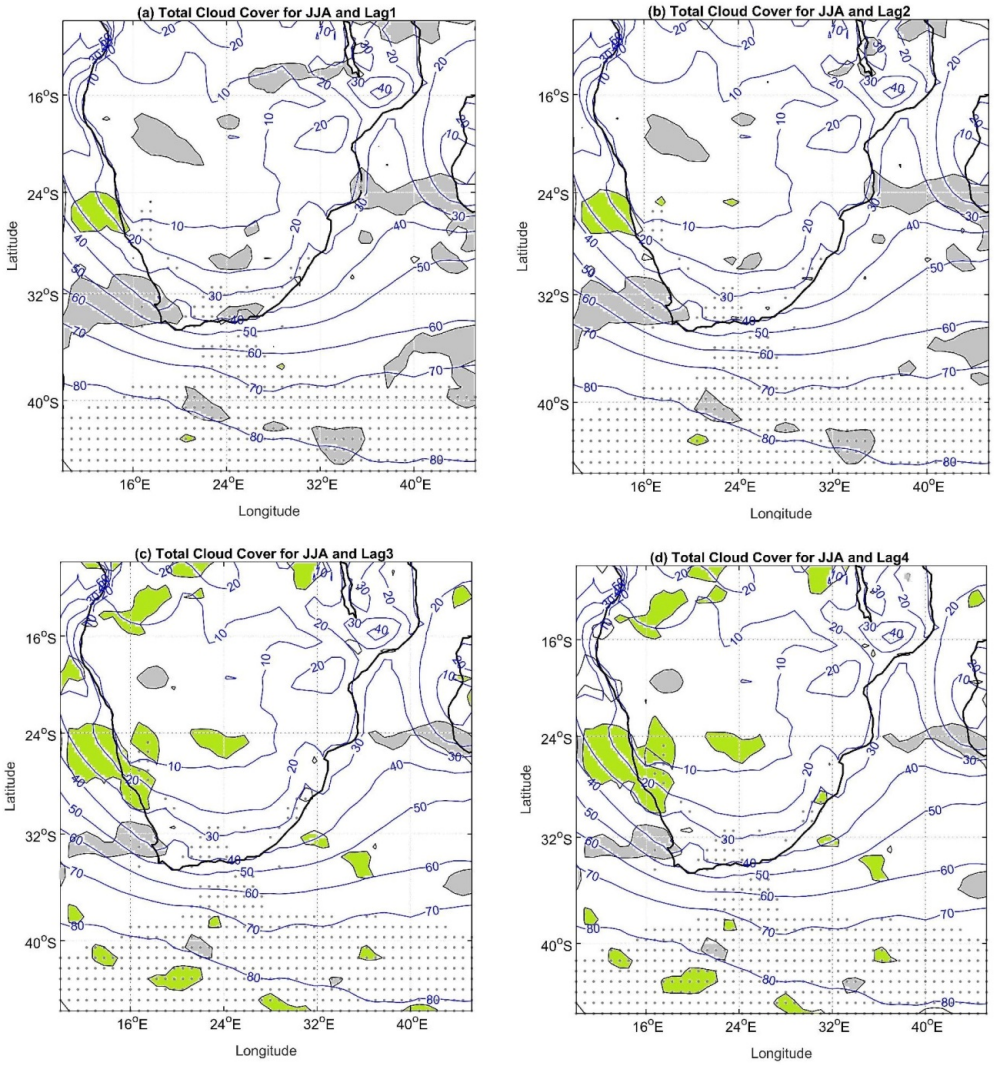

Fig. 6. Total cloud cover area fraction (a -d) presented as percentage (contours) in JJA. Correlation Coefficients for the Hadley and total cloud cover in JJA for (a) Lag 1, (b) Lag 2, (c) Lag 3 and (d) Lag 4. Grey shading denotes correlation coefficients greater than 3 and green shading indicates correlation coefficients less than -3. Regions of upward vertical velocity (ω) in Pas^{-1} are represented using grey dots. Where there are no grey dots, there is downward motion (i.e. $\omega > 0$]

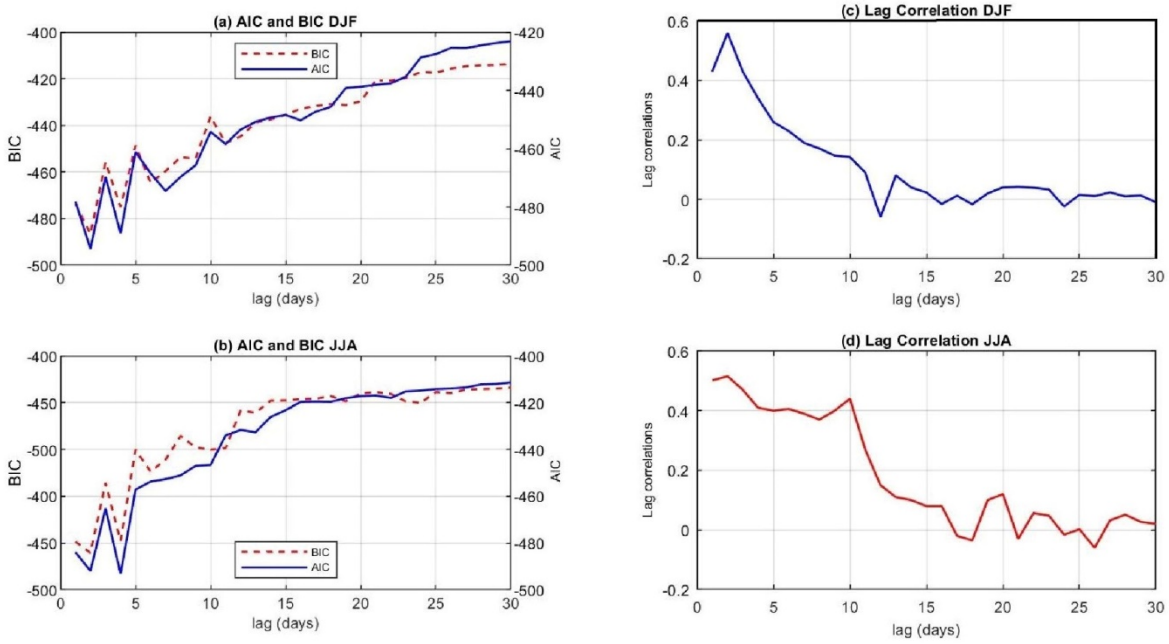

Fig. 7. The AIC (blue solid line) and BIC (red dashed line) values for (a) DJF and (b) JJA, lag correlations for (c) DJF and (d) JJA.

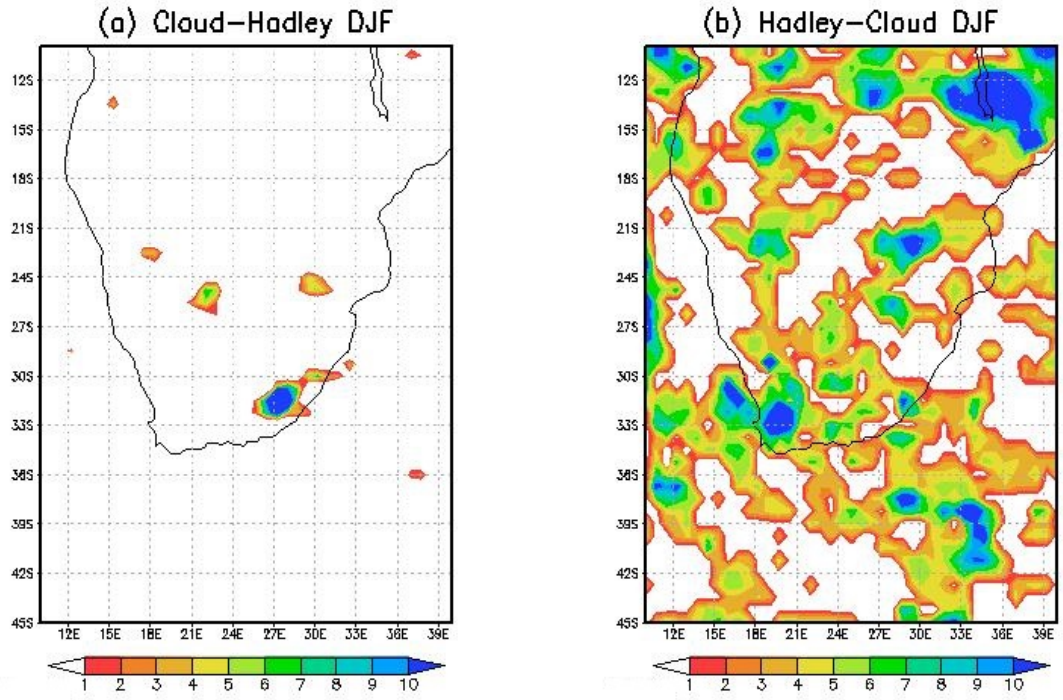

Fig. 8. (a) Granger causality of total cloud cover to the Hadley cell; (b) Hadley cell to total cloud cover in DJF.

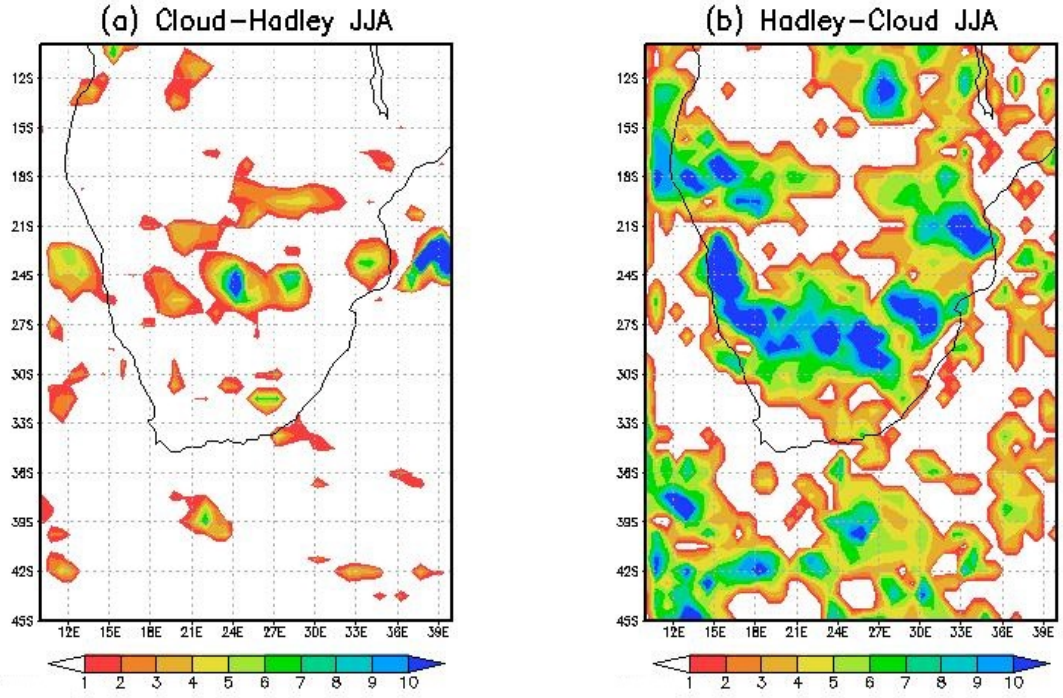

Fig. 9. (a) Granger causality of total cloud cover to the Hadley cell; (b) Hadley cell to total cloud cover in JJA.

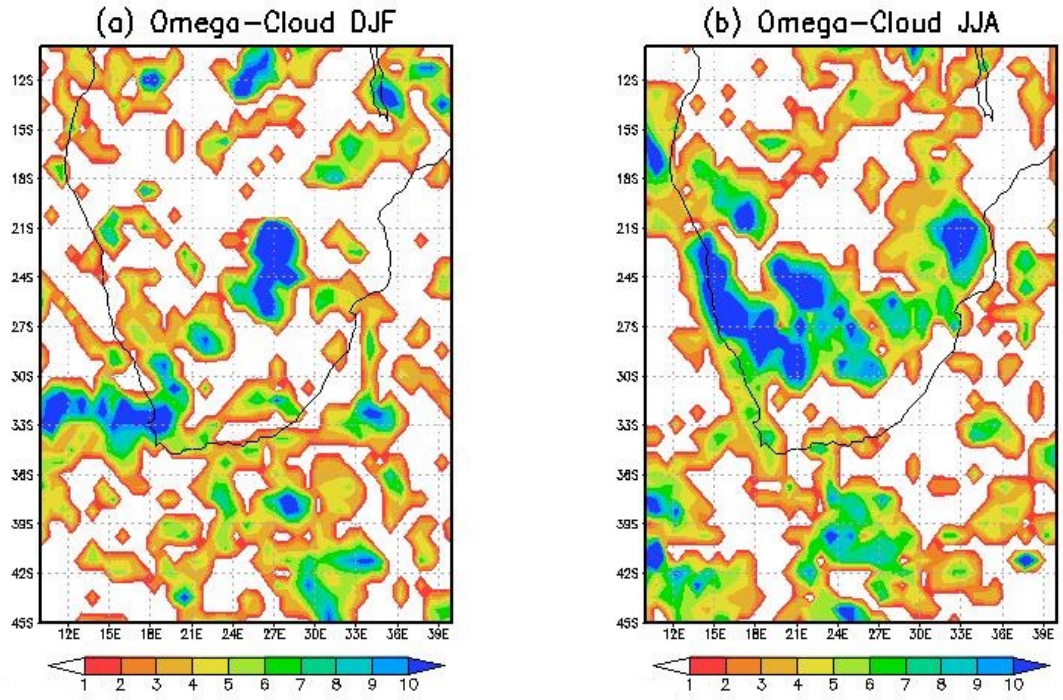

Fig. 10. Granger causality of omega to cloud cover in (a) DJF, (b) JJA.

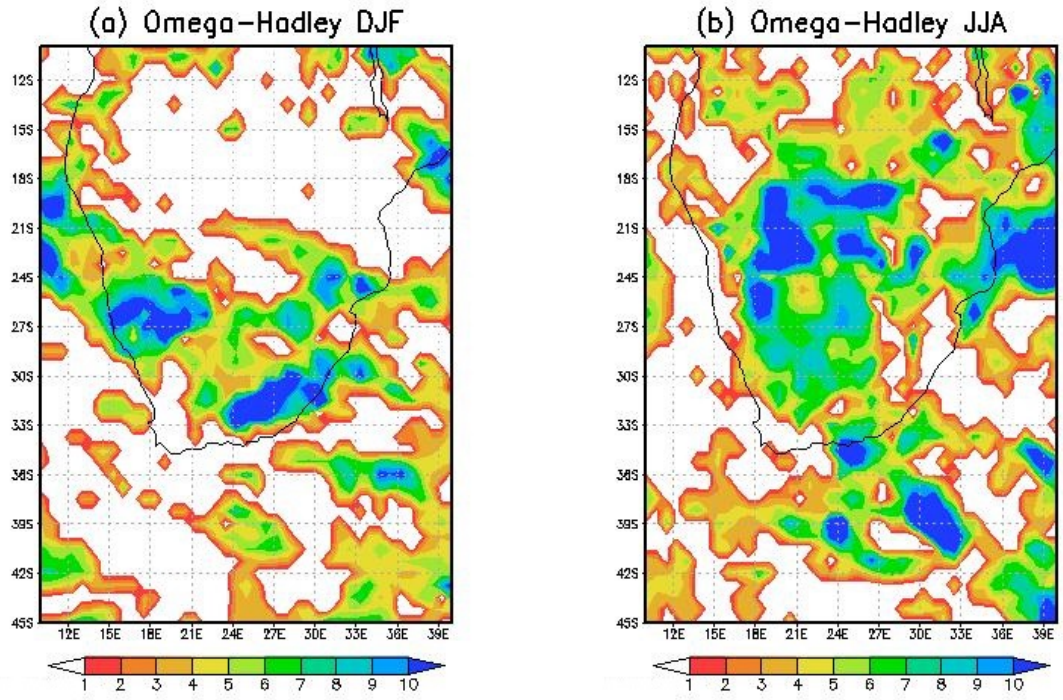

Fig. 11. Granger causality of omega to the Hadley cell in (a) DJF (b) JJA.

Table 1: The Dickey Fuller Test for Hadley cell, Cloud cover, first differenced Hadley cell and cloud cover.

Time Series	DF Value	P Value	Decision
HC	0	0.1	Do not reject
TCC	0	0.1	Do not reject
HC'	-5.327	0.0001	Reject
TCC'	-4.865	0.0001	Reject

Chapter 4
Granger causality of the local Hadley cell and sunshine duration over South Africa Preface

This chapter consists of a paper submitted to the Journal of Energy in southern Africa

This study addresses objective 3 of the thesis. Granger causality time series modelling approach, introduced in Chapter 3, is employed to analyse the influence of sunshine duration on the Hadley cell. Bivariate vector autoregressive time series models for the period 1980-2015 were fitted to sunshine duration and the Hadley cell. Granger Causality from the Hadley cell to sunshine duration was established for both summer and winter over South Africa; however, there is no discernable Granger causality from sunshine duration to the Hadley cell for both seasons.

Granger causality of the Hadley cell and Sunshine Duration over South Africa

ABSTRACT: This study uses Granger Causality to determine the causal interactions between sunshine duration and the Hadley cell. Bivariate autoregressive time series models were fitted to sunshine duration and the Hadley cell data sets covering the period 1980-2015. Granger causality has been established between the Hadley cell to sunshine duration and no discernable causality from sunshine duration to the Hadley cell was established.

Keywords: Hadley circulation, Granger causality, bivariate model, sunshine duration

1. INTRODUCTION

Solar power may play an increasingly important role in contributing to the South African energy mix as the technology becomes more affordable (IRENA, 2017) and in response to South Africa's ambitious climate change mitigation targets (DEA, 2018). South Africa has a landmass of 1.2 million km^2, much of which is semi-arid and which receives about 24 GWhrm^{-2} per annum of solar radiation (Bugaje, 2006) and is rated as one of the highest in the world (Edkins et al., 2010).

Maximum solar radiation values in South Africa and subsequently highest solar resource potential is in the Northern Cape. It is also over the Northern Cape De Aar where the largest solar plant in the Southern hemisphere as well as the Middle East is located (CBN, 2016). The solar plant is made up of 700 000 solar panels and make use of photovoltaic (PV) and constitutes an installed capacity of 175 MW (megawatt) (CBN, 2016). Apart from this massive solar

plant, a solar park comprising of different solar plants including PV, concentrated photovoltaic (CPV) and concentrated solar plants (CSP) was established over Upington area in the Northern Cape (Zawilska, 2012). By 2016 the installed capacity of the solar park was 1000 MW, however with the addition of more solar power plants the installed capacity is expected to be 2GW by 2020 (Zawilska, 2012). Due to climate change solar plants in the North West province are envisaged to increase going forward into the future. Furthermore, it has been shown in climate change simulations that the rainfall over South Africa is likely to decrease (Engelbrecht et al., 2009); this implies the reduction of cloud cover over the western half of South Africa. This therefore changes the solar radiation climatology of South Africa and results in the increase of solar potential for solar energy generation. Given this likely increase in solar power generation in South Africa, it is important to understand how climate variability and change impact on the solar potential of the region, particularly within the context of South Africa being located in the subtropics where it is under the influence of the regional Hadley cell.

Links between the Hadley cell and solar radiation have been documented in a number of studies (e.g. Trenberth and Stepaniak, 2003; Hoskins, 1996; Herwiejer et al., 2005). Chen et al. (2002) found that decadal trends in tropical mean radiative fluxes are linked to the strength of the Hadley circulation by showing strong temporal correlations between the observed radiative fluxes and a number of indicators of the circulation strength. According to Trenberth and Stepaniak (2003), clear skies in the subsiding branch in the subtropics mean that solar radiation is abundant at the surface. In fact, the subtropics are characterized by relatively high outgoing long-wave radiation and low reflected short-wave radiation (Clement and Soden, 2005), and this is caused by dynamically induced drying in the subtropics in the subsiding branch of the Hadley cell (Herwiejer et al., 2005). According to Merlis et al. (2013), the impact on insolation by the Hadley cell is stronger in summer than in winter, mainly due to the thermodynamic

and energetic changes being close to the angular-momentum conserving limit in summer. High insolation during summer leads to increased massflux and this affects the annual-mean Hadley circulation (Merlis et al., 2013).

Solar radiation that reaches the surface has a strong longitudinal gradient, as does sunshine duration given that sunshine duration can be used to estimate solar radiation (Falayi et al., 2008). Over South Africa, this longitudinal gradient is due to topography, prevailing weather systems, rain bearing winds, influence of ocean currents, these result in less solar radiation in the eastern parts and more in the western parts. Because South Africa is located on the subtropical belt, exactly where the Hadley cell descending branch is located, the country receives abundant sunshine (Kruger and Esterhuyse, 2005). Links between the Hadley cell and sunshine duration have already been established for this region (Mahlobo et al., 2018). For instance, areas of strong subtropical Hadley cell induced subsidence over South Africa coincide with areas of high sunshine duration (Mahlobo et al., 2018). Whether these links are causal to each other is yet to be formally established. The current study thus aims to establish whether a causal relationship exists between sunshine duration and the Hadley cell over South Africa.

2. DATA AND METHODS

2.1 Data

Sunshine duration and vertical velocity data at 500hPa were obtained from the European Centre for Medium-Range Weather Forecasts (ECMWF) Interim Reanalysis (ERA-Interim). Observational sunshine duration data was obtained from the South African Weather Service (SAWS). The period for the study spans from 1980 through 2015. The vertical velocity at 500hPa was used to calculate the massflux, which was then used to represent the asymmetric Hadley cell

circulation. The full derivation of the massflux is shown by Schwendike et al. (2014) and reviewed by Mahlobo et al. (2018). The horizontal resolution of the data used is $0.75^{\circ} \times 0.75^{\circ}$ and data is available on 37 pressure levels (Dee et al., 2011). This horizontal resolution is considered sufficient to diagnose the dynamics of the descending branch of the Hadley cell over South Africa.

2.2 Methods

Granger causality (Granger, 1969) is used to investigate causality between sunshine duration and the Hadley cell. It is defined as variable Y granger causing variable X if X can be predicted better by using the past values of Y, more than the past values of X itself. This definition, when applied to the study, means that the Hadley cell has a Granger causal relationship to sunshine duration, if past values of sunshine duration could be used together with past values of the Hadley cell to help predict the Hadley cell. Four steps are used to employ the Granger causality procedure and these include unit root testing and differencing, the selection of the appropriate model for the time series data, and testing for granger causality. The widely used Augmented Dickey Fuller (ADF) test (Dickey and Fuller, 1981) is used to test for stationarity.

The ADF is defined as follows:

$$\Delta y_{t=1}^{n} = \beta_1 + \alpha y_{t-1} + \gamma \Sigma \delta y_{t-1} + \varepsilon_t, \tag{1}$$

where y_t represents all variables (in the natural logarithmic form) at time t, Δ is the first difference operator. 1 is a constant, n is the optimum number of lags on the dependent variable. The test for a unit root is conducted on the coefficient of y_{t-1} in the regression model. The null and alternative hypothesis for the existence of unit root in variable y_t is: $H_0; = 0$ versus $H_1 :< 0$.

The coefficient should be significantly different from zero (less than zero) for the hypothesis that y contains a unit root to be rejected. Rejection of the null hypothesis indicates stationarity in the series. Should the time series be not stationery, then temporal differencing of the time series is employed.For a variable y depending on another variable x (i.e. y = f(x)), and for a set of n points on an equi-spaced grid, the first derivative with respect to time t, f't at i = 1 ,.....n, the backward difference will be given by:

given by:

$$\Delta y_t \equiv y_{t-1} - y_t, \tag{2}$$

In climate sciences, Vector Auto regression (VAR) is mostly used to estimate the maximum lags to be used for testing data on granger causality (Attanasio, 2012; Triacca, 2001). This study uses two criteria; the Akaike Information Criteria (AIC) and the Bayesian Information Criteria (BIC) to find the optimum maximum lag. The two information criteria mentioned above follow a general form which consists of the log-likelihood estimates as well as penalty functions for parameters in the model (He, 2008). The best fitting model estimates is the one with the least information criteria. The general information criteria are given as:

$$IC(p) = \ln |\Sigma^l| + C_T \frac{p}{T}, \tag{3}$$

Where Σ^l is an approximation of the residual covariance matrix associated with the fitted VAR(p) model, C_T is a deterministic penalty term, T denotes the number of observations used for estimation and p denotes the lag order. The definition of the penalty term C_T differs with the choice of information criteria used i.e.: for AIC,

$$C_T = 2k^2, \tag{4}$$

and for BIC,

$$C_T = k^2, \tag{5}$$

where k is the number of equations in the VAR model. The presence and direction of Granger causality for each grid point between sunshine and the Hadley Cell is then tested by means of a VAR and is given by the following equations:

$$X_t = \alpha_1 + \Sigma_{i-1}^{S} \beta_i X_{t-i} + \Sigma_{i-1}^{S} \gamma_{1i} Y_{t-i} + e_{1t}, \tag{6}$$

$$Y_t = \alpha_2 + \Sigma_{i-1}^{S} \beta_{2i} X_{t-i} + \Sigma_{i-1}^{S} \gamma_{2i} Y_{t-i} + e_{2t}, \tag{7}$$

where α , β , and γ are regression coefficients, e's are error terms, and s is the lag length, which is determined by using AIC and the BIC (equation 3). The structural VAR is based on the fact that for each season, the present values of both variables do not only depend on the present values of the other variable, but also on the history of the other variable. The direction of causal order is thus determined by estimating the restricted forms of equations (6) or (7), and by eliminating the causal variable. For example, to determine whether the Hadley cell Granger causes sunshine duration, we estimate a restricted form of equation (6) in which sunshine duration is eliminated. The restricted version of equation (6) is thus

$$X_t = \alpha_1^{'} + \Sigma_{i-1}^{S} \beta_{1i}^{'} X_{t-i} + e_{1t}, \tag{8}$$

We further test whether the restricted model is statically significantly different from the unrestricted model, as per the following procedure:

$$\omega = \frac{(\frac{RSS_T - RSS_u}{S})}{(\frac{RSS_u}{T-k})}, \tag{9}$$

Here, RSS is the sum of the residuals squared; the subscripts r and u refer to the restricted and unrestricted versions of equations (6) or (7), respectively; T is the number of observations; k is the number of regressors in the unrestricted version of the equation; and s is the number of coefficients restricted to zero in equation (8). The test statistic can be evaluated against an F

distribution with s and $T-k$ degrees of freedom in the numerator and denominator respectively, in order to evaluate the null hypothesis that the sunshine duration does not Granger cause the Hadley cell. The full description of Granger Causality is documented in Granger (1969) and Wang (2004).

3. RESULTS AND DISCUSSION

3.1 Stationarity

Before the links between the Hadley cell and sunshine are investigated, linear trends for the individual series at each grid point were examined and are displayed in Figure 1. During DJF, there is a tendency towards decrease in downward massflux over the central and north eastern parts of South Africa and a tendency towards increase over the southern parts of South Africa (Figure 1a). Concurrently a tendency towards a decrease in sunshine for most parts of South Africa is observed (Figure 1b). In JJA there is evidence of increase in downward massflux over the country (Figure 1c) as well as slight decrease in sunshine duration for most parts of South Africa (Figure 1d).

The suitability of each time series to be used in the Granger causality methodology was investigated using the ADF test. Results of the ADF test for the two time series are shown in table 1; the test was applied to each grid point for sunshine duration and the massflux. The test rejected the hypothesis of stationarity for the two time series. The two time series were then first differenced, and tested for stationarity and it was found that the first difference time series contained no unit roots (Table 1), hence making them suitable for Granger causality analysis.

3.2 Lag Correlation and Information Criterion

Interactions between two time series can be tested by lagged correlations. To this end, Mosedale et al. (2005) have used the lagged correlation analysis to check if there is similarity between two time series. Although such a method does not necessarily indicate the presence or direction of Granger causality, it could be useful to give insight about the association between the time series and the determination of the lag value that could give the best links in the time series. This could serve as the verification of the criterion used to determine the maximum number of lags to be used. In this study daily time steps were used to construct the Hadley cell and sunshine duration time series for both DJF and JJA, a lag length of one thus indicates the previous day, a lag length of two implies two previous days, and so on. The AIC and BIC for the links between the Hadley cell and sunshine duration is shown in Fig. 2a and Fig. 2b for DJF and JJA respectively. High values of both AIC and BIC are evident over the first week for both DJF and JJA. The AIC indicates a lag length of one day as the most suitable to be used in Granger causality, whereas the BIC has the highest lag length on day six for DJF and JJA.

The lag relationship between the Hadley cell and sunshine duration daily time series were investigated; temporal correlation coefficient was used to examine the strength and significance of the relationships. Lagged correlations between the Hadley cell and sunshine duration, averaged over South Africa for DJF and JJA, are shown in Fig. 2a and Fig. 2b. Higher correlations are found over the first week. Peak correlations are 0.43 for DJF and 0.54 in JJA, with both of these established on the first day, meaning a lag length of one day is most suitable for predicting sunshine duration from the Hadley cell, or vice versa. A decrease in Lag correlation is evident as the lag lengths increase. Hence, as timescales increase (e.g. weeks to months), so the prediction of sunshine duration using the Hadley cell, or vice versa, may become more difficult.

Zonal gradients of lag correlations between sunshine duration and the Hadley cell are shown in Fig. 3 and Fig. 4 (a-d) for DJF and JJA respectively. Correlations greater than 0.1 are indicated as blue shading, whereas negative correlations of less than -0.1 are indicated as red dots. In DJF (Fig. 3 a-d), negative correlations between the massflux and sunshine duration over South Africa dominate for lag lengths of one to three days. This is due to the fact that as negative massflux increases, so sunshine duration is expected to increase. Negative massflux means subsidence and consequently less cloud formation and more sunshine duration. A lag length of four days seems to have a stronger positive correlation between the Hadley cell and sunshine duration, which suggests that it may be difficult to use a lag length of four days to predict the Hadley cell using sunshine duration, and vice versa. In JJA, a lag length of one day shows greater negative correlation. While a balance between negative and positive correlations is evident for lags of two and three days, the lag of four days is dominated by positive correlations in JJA. Based on the information criterion tests and lagged correlations, it seems that the first day offers the best lag length which could be used in granger causality analysis between the Hadley cell and sunshine duration over South Africa.

3.3 Granger Causality

The investigation on whether the variability in sunshine duration is caused by the Hadley cell was performed using a bivariate VAR model. The F statistics and critical values of the bivariate model were established at each grid point. The presence of Granger causality is denoted by values of an F statistic greater than the critical value and conversely values of F statistics less than the critical value shown by the absence of Granger causality. The strength of Granger causality from sunshine duration to the Hadley cell and Hadley cell to sunshine duration is indicated in Fig. 5a and Fig. 5b respectively for DJF, and Fig. 6a and Fig. 6b in JJA. These interactions are

denoted as SUND-HC for sunshine duration to the Hadley cell and HC-SUND for the Hadley cell to sunshine duration interactions. In DJF, the SUND-HC interaction over South Africa shows very weak Granger causality (Fig.5a). A strong HC-SUND causality is established over the interior of South Africa in DJF, with maximum values of causality found from the Northern Cape toward the south eastern parts of South Africa. There is no discernable causality for the SUND-HC interaction over South Africa in JJA (Fig. 6a). However, a strong HC-SUND causality is present over South Africa, and is strongest over the central interior (Fig.5b).

4. CONCLUSIONS

Granger causality time series modelling approach has been employed to analyse the influence of sunshine duration on the Hadley cell. Bivariate vector autoregressive time series models for the period 1980-2015 were fitted to sunshine duration and the Hadley cell. The optimum lag length was established from the AIC and BIC statistics as well as the lagged correlation analysis. A lag length of one day was found most suitable for Granger causality analysis between two time series for both DJF and JJA.

Granger Causality from the Hadley cell to sunshine duration has been established for both summer and winter over South Africa; however, there is no discernable Granger causality from sunshine duration to the Hadley cell for both seasons. The strength of the HC-SUND causality is seasonal. In DJF, areas of strong causality are located over the interior of South Africa, but extend to the north-western parts as well as to the south-eastern parts. In JJA, the area of strong HC-SUND causality is located over the central parts of South Africa, where the subtropical high pressure cell is located. The seasonal angular momentum conserving limit plays a major role in the links between the Hadley cell and sunshine duration (Merlis et al., 2013). During DJF,

when insolation is at its maximum, the Hadley circulation is close to the angular momentum conserving limit and thus responds directly to radiative changes. This then contributes positively to links between the Hadley circulation and sunshine duration, which could have led to the strong HC-SUND causality.

In JJA when insolation is lowest, the Hadley circulation is mostly affected by momentum flux rather than the angular momentum conserving limit and hence does not respond to local to regional radiative changes (Merlis et al., 2013). This then renders the links between the Hadley circulation and sunshine duration weaker in JJA than in DJF. The results suggest that it is possible to use both present and past values of the Hadley cell, to predict sunshine duration over South Africa. However, it is near impossible to use past and present values of sunshine duration to predict the Hadley cell. The Hadley cell could then be used as a proxy for sunshine duration projections and furthermore for solar energy generation over South Africa. Thus, the next scientific step should be to establish the potential impact of changes in the Hadley cell under climate change on solar energy generation in southern Africa.

REFERENCES

Attanasio, A. 2012. Testing for linear Granger causality from natural/anthropogenic forcings to global temperature anomalies. Theoretical and Applied Climatology 110: 281-289.

Bugaje, I.M. 2006: Renewable energy for sustainable development in Africa: a review. Renewable and Sustainable Energy Reviews 10: 603-612.

CBN. 2016. The largest solar farm in Africa, Middle East and the Southern Hemisphere opens. Retrieved February 18 2019 from $https://www.cnbcafrica.com/news/southern-africa/2016/03/18/the-largest-solar-farm-in-africa/$

Chen, J., Carlson, B., Del Genio, A. 2002. Evidence for strengthening of the tropical general circulation in the 1990s. Science. 295: 838–841.

Clement, A.C. and Soden, B. 2005. The sensitivity of the tropical-mean radiation budget. Journal of Climate 18: 3189-3203.

DEA, 2018. South Africa's low emission development strategy 2050. Department of Environmental Affairs,Pretoria South Africa

Dee, D.P., Uppala, S.M., Simmo, A.J., Berrisford, P., Poli, P., Kobayashi, S., Andrae, U., Balmaseda, M.A., Balsamo, G., Bauer, P. and others. 2011. The ERA-Interim reanalysis: Configuration and performance of the data assimilation system. Quarterly Journal of the Royal Meteorological Society 37: 553-597.

Dickey, D. and Fuller, W. 1981. Likelihood Ratio Statistics for Autoregressive Time Series with a Unit Root. Econometrica 49: 1057-1072.

Edkins, M., Marquard, A. and Winkler,H, 2010. Assessing the effectiveness of national solar and wind energy policies in South Africa.Energy Research Center.University of Cape Town. Cape Town.South Africa.

Engelbrecht, F.A., McGregor, J.L. and Engelbrecht, C.J. 2009. Dynamics of the Conformal- Cubic Atmospheric Model projected climate-change signal over southern Africa. International Journal of Climatology 29: 1013-1033.

Falayi, E.O., Adepitan, J.O. and Rabiu, A.B. 2008. Empirical models for the correlation of global solar radiation with meteorological data for Iseyin, Nigeria. International Journal of Physical Science 3: 210-216.

Granger, C.W.J. 1969. Investigating causal relations by econometric models and cross spectral methods. Econometrica 37: 424-438.

He, W. 2008. Model selection for cointegrated relationships in small samples. MSc dissertation .Nelson Mandela Metropolitan University, Port Elizaberth.

Herweijer, C., Seager, R. and Winton, M. 2005. Why ocean heat transport warms the global mean climate. Tellus. 57A: 662-675.

Hoskins, B. 1996. On the existence and strength of the summer subtropical anticyclones. Bulletin of the American Meteorological Society 77: 1287-1292.

IRENA. Renewable energy auctions: analyzing 2016. IRENA. 2017.
$https://www.irena.org/-/media/Files/IRENA/Agency/Publication/2017/IRENA_REAuctio$

Kruger, A. and Esterhuyse, D. 2005. Climate of South Africa: Sunshine and cloudiness. South African Weather Service 35.

Mahlobo, D.D., Ndarana, T., Grab, S. and Engelbrecht, F. 2018. Integrated climatology and trends in the subtropical Hadley cell, sunshine duration and cloud cover over South Africa. International Journal of Climatology. 39.1805-1821.

Merlis, T.M., Schneider, T., Bordoni, S. and Eisenman, I. 2013. Hadley Circulation to Orbital Precession part II; Subtropical Continent. Journal of Climate 26: 754-771.

Mosedale TJ, Stephenson DB, Collins M, Mills TC. 2006.Granger causality of coupled climate processes: Ocean feedback on the North Atlantic Oscillation. Journal of Climate. ; 19: 1182-1194. https://doi.org/10.1175/JCLI3653.1

Schwendike, J., Govek, P., Reeder, M.J., Wardle, R, Berry, G.J. and Jakob, C. 2014. Local partitioning of the overturning circulation in the tropics and the connection to the Hadley and Walker circulations. Journal of Geophysical Research 119: 1322-1339.D020742.

Trenberth, K.E. and Stepaniak, D.P. 2003. Seamless poleward atmospheric energy transports and implications for the Hadley Circulation. Journal of Climate 16: 3706-3722.

Triacca, U. 2001. On the use of Granger causality to investigate the human influence on climate. Theoretical and Applied Climatology 69: 137-137.

Wang, W., Anderson, B.T., Kaufmann, R.K. and Myneni, R.B. 2004. The relation between the North Atlantic Oscillation and SSTs in the North Atlantic Basin. Journal of Climate 17: 4752-4759.

Zawilska, E., Brooks, .MJ., Meyer, A.J. 2012. A review of solar resource assessment initiatives in South Africa. The case for national network. In Proceedings:

The World Renewable Energy Forum. Denver. Colorado. USA

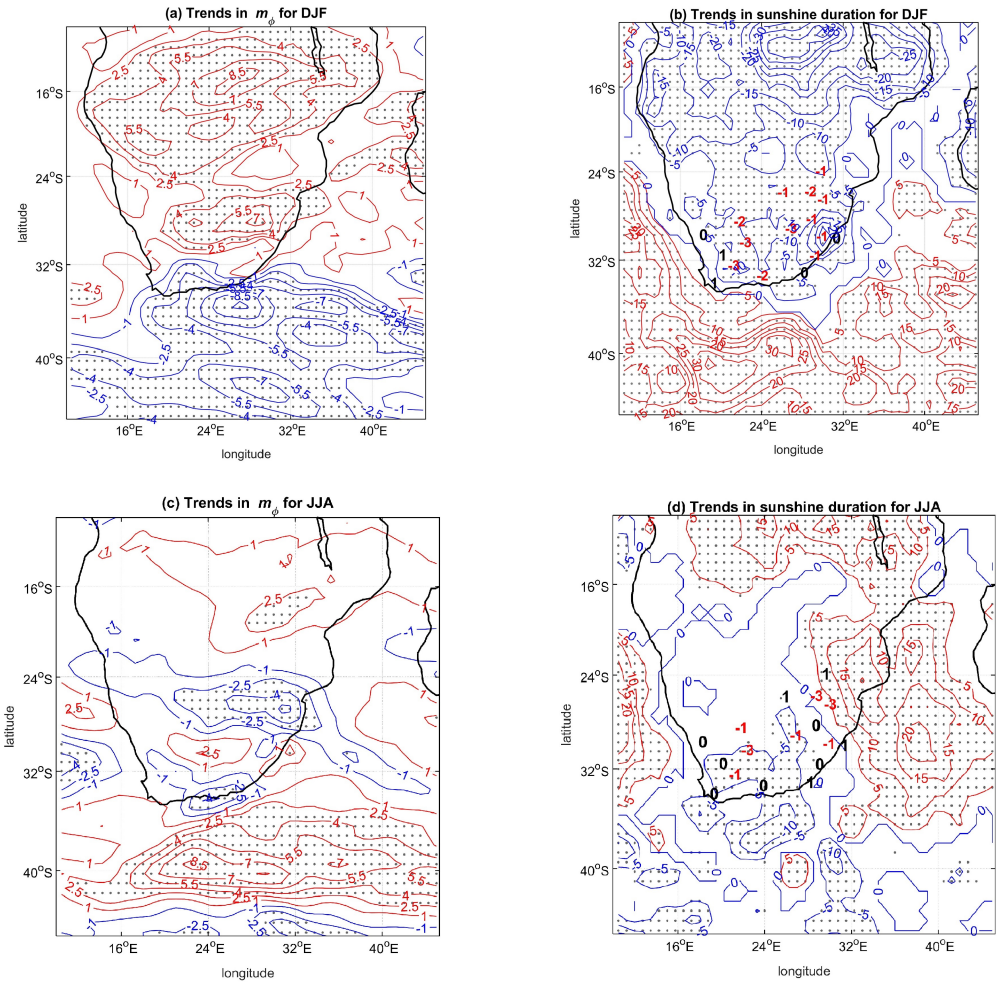

Fig.1 Trends in massflux (10^{-5} kgm^{-2}s^{-1} per 35 years) for (a) DJF, (c) JJA and sunshine duration(%) for (b) DJF and (d) for JJA. The red and blue contours represent positive and negative trends respectively. Sunshine duration trends from SAWS station observations are represented as red values (positive trends) and black values (negative trends). The dotted regions represent 95% statistical significance greater than 0.5.

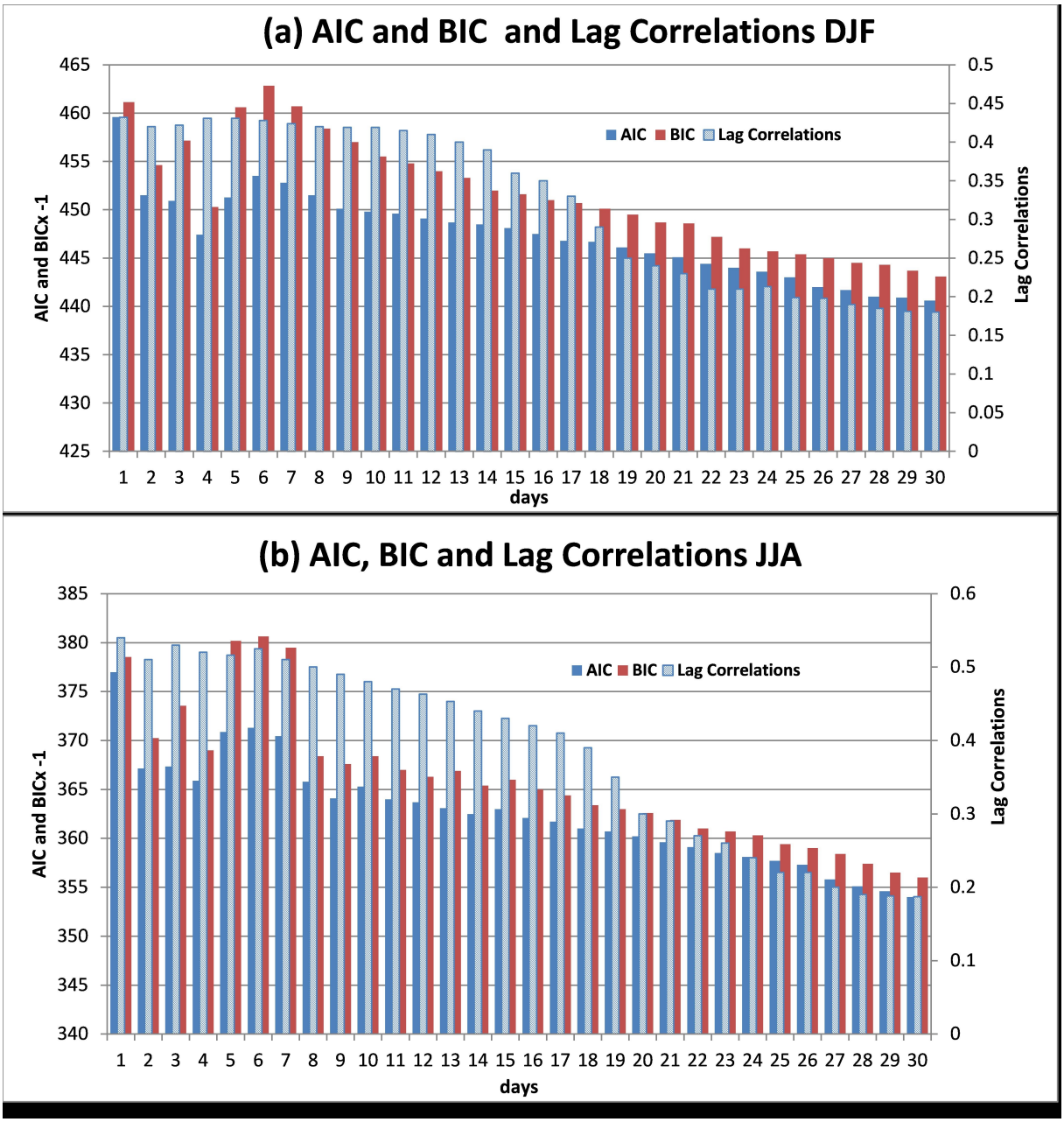

Fig. 2. Fig.2 AIC, BIC information criteria as well as lag correlations for the Hadley cell and sunshine duration for 1 to 30 lag days in (a) DJF and (b) JJA.

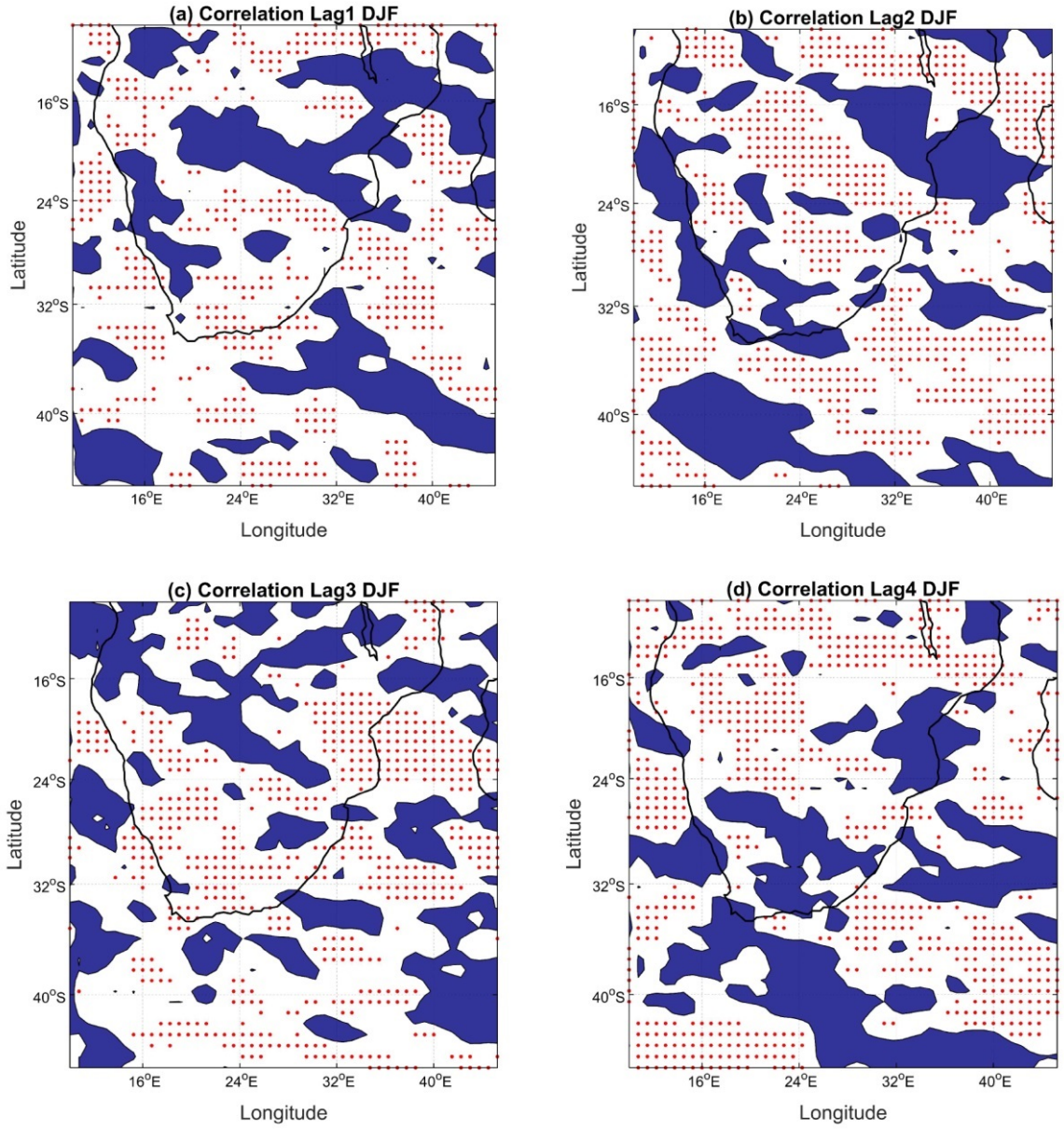

Fig. 3. Fig.3. Correlation Coefficients for the Hadley cell and sunshine duration in DJF for (a) Lag 1, (b) Lag 2, (c) Lag 3 and (e) Lag 4. Blue shading denotes correlation coefficients greater than 1 and red dots indicate correlation coefficients less than -1.

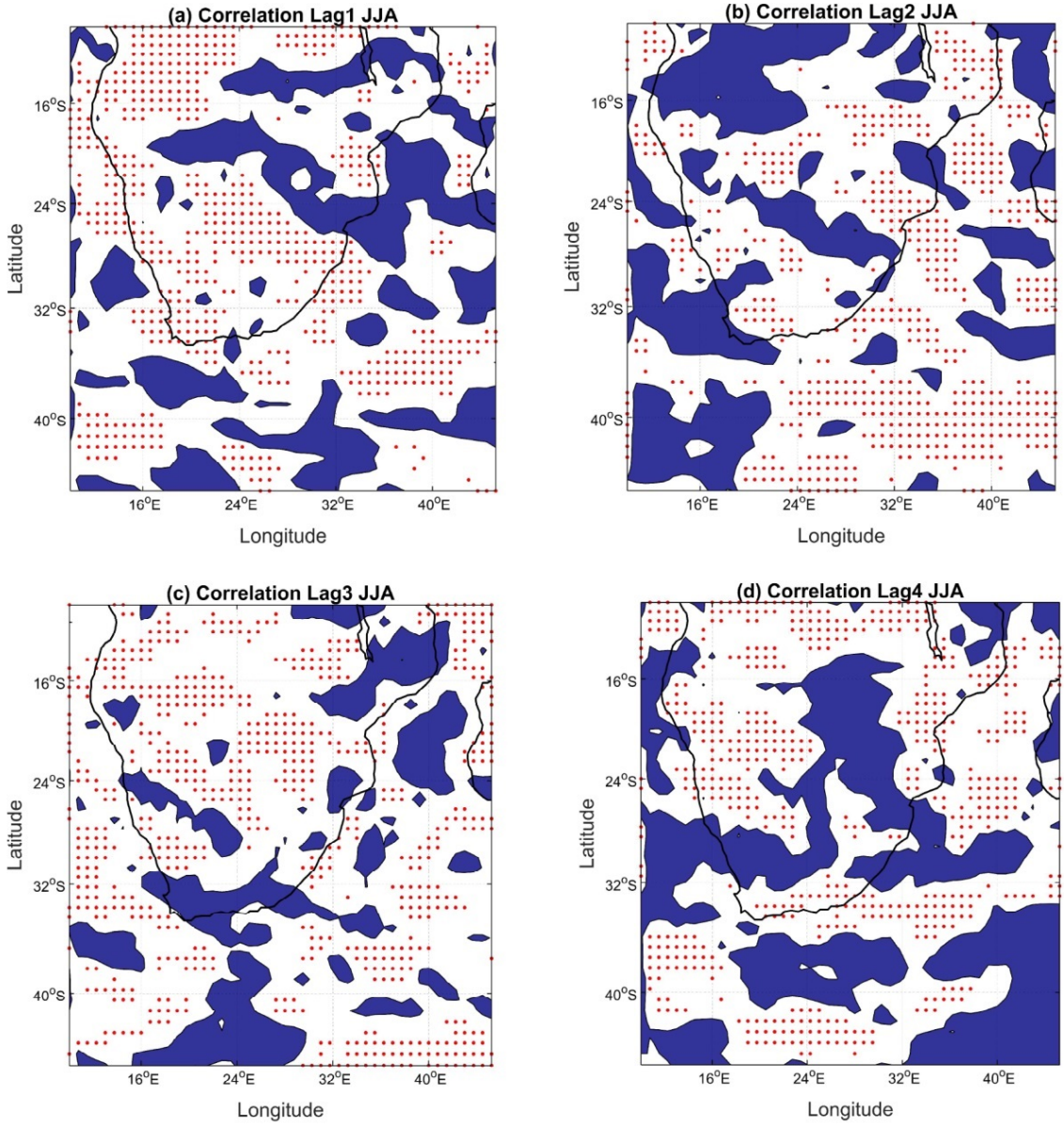

Fig.4. Correlation Coefficients for the Hadley cell and sunshine duration in JJA for (a) Lag 1, (b) Lag 2, (c) Lag 3 and (d) Lag 4. Blue shading denotes correlation coefficients greater than 1 and red dots indicate correlation coefficients less than -1.

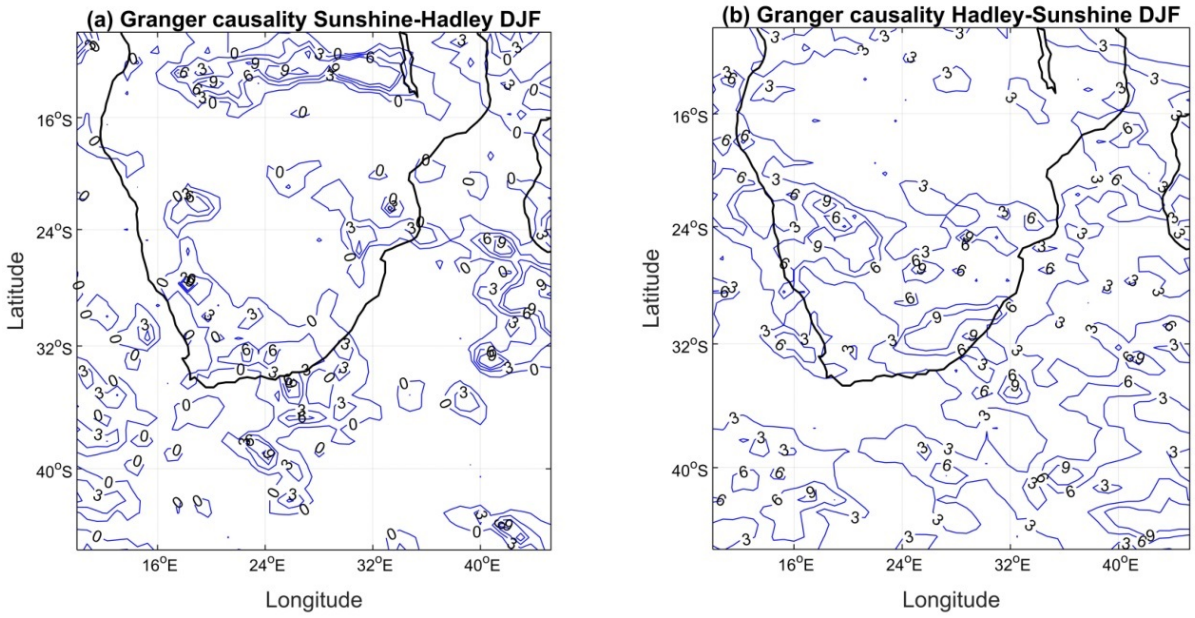

Fig.5. (a) Granger causality of sunshine duration to the Hadley cell; (b) Hadley cell to sunshine duration in DJF..

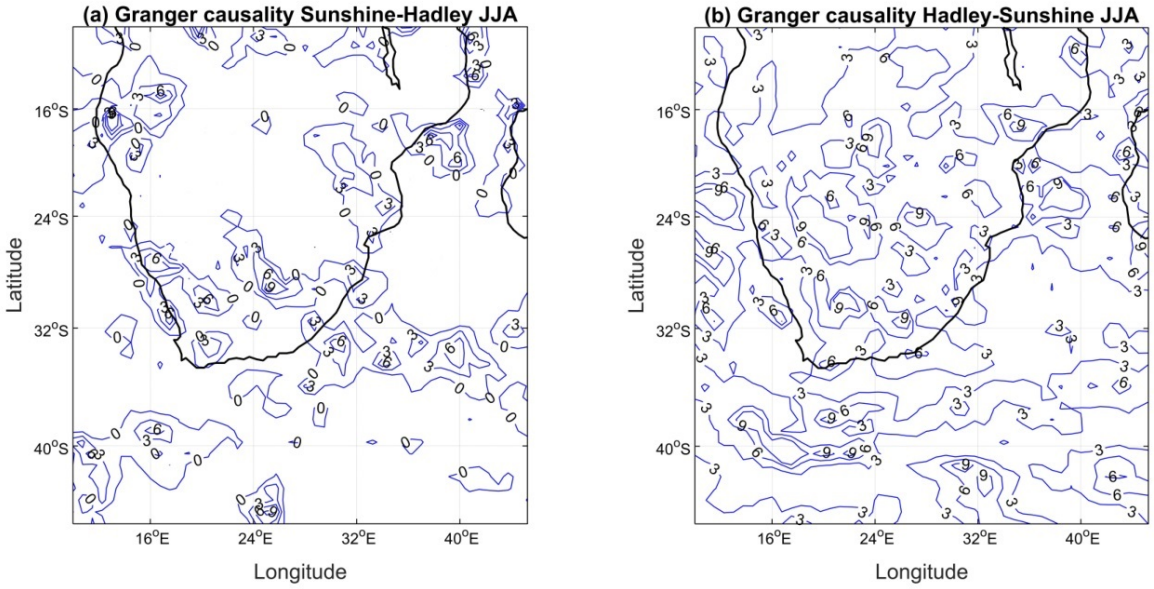

Fig.6. (a) Granger causality of sunshine duration to the Hadley cell; (b) Hadley cell sunshine duration in JJA.

Table 1: Table 1: The Dickey Fuller Test for the Hadley cell, sunshine duration, differenced Hadley cell and first differenced sunshine duration.

Time Series	DF Value	P value	Decision
HC	0	0.1	Do not reject hypothesis
SUND	0	0.1	Do not reject hypothesis
HC'	1	0.001	Reject hypothesis
SUND'	1	0.001	Reject hypothesis

Chapter 5
Link between the local Hadley circulation and energy generation in South Africa
Preface

This chapter consists of a paper to be submitted to the journal of Theoretical and Applied Climatology

This study addresses objective 4 of the thesis. The evolution of the Hadley cell under the RCP 8.5 is investigated and its likely impact on rainfall and temperature over South Africa. Furthermore the impact of the Hadley cell in electricity generation is examined. The Long-range Energy Alternatives Planning system (LEAP) is introduced and used to analyse the impact of climate change on energy generation.

Link between the local Hadley circulation and energy generation in South Africa

ABSTRACT: This paper examines the behaviour of the Hadley cell, rainfall and temperatures over South Africa under the RCP 8.5 setting and its implication on energy generation. The statistical downscaled data from a regional climate model CCAM is used. The Hadley cell has been strengthening and is projected to strengthen for all seasons except DJF. Consequently, rainfall is projected to decrease during all seasons. In DJF, the projected decrease in rainfall is only over the western parts, while the expected increase is over the central and eastern regions of South Africa. Mean temperatures are projected to increase during all seasons. Changes in the Hadley cell, rainfall and temperature, have strong implications to the electricity generation in South Africa. A further advantage in understanding the Hadley cell is that it could also be used to locate areas with solar potential in South Africa.

Keywords: Hadley circulation, RCP 8.5, massflux, CCAM

1. INTRODUCTION

The Hadley cell is a large scale atmospheric circulation, resulting from differential heating of the earth's surface (Wallace and Hobbs, 2006). Its main characteristics are the ascending motion in the tropics and descent in the subtropics. The Hadley cell is situated in the tropical-subtropical belt of each hemisphere (Ceppi and Hartman, 2013) and is the most protruding feature of the atmospheric circulation (Kang and Lu, 2012). The climates of tropical and subtropical regions are therefore informed by the meridional extent of the Hadley cell. For example, the descending branch of the Hadley cell is the main cause for arid to semi-arid conditions in the subtropical

regions. The zonally asymmetric diagnosis of the Hadley cell can be presented in terms of a massflux stream function (Keyser et al., 1989; Schwendike et al., 2014; Mahlobo et al., 2018). Areas of negative massflux coincide with positive vertical velocity meaning downward motion or descent. Conversely areas of positive massflux coincide with negative vertical velocity and vertical ascent (Schwendike et al., 2014; Mahlobo et al., 2018).

Several studies have documented the connection between the Hadley circulation and rainfall (Kanamitsu and Krishnamurti, 1978; Nicholson, 1981; Hou and Lindzen, 1992; Yin, 2005). Some of the earliest work found a positive correlation between the intensification and equatorward displacement of the Northern Hadley circulation, and dry conditions over the northern tropical regions (Kanamitsu and Krishnamurti, 1978). Nicholson (1981) suggested that changes in the Hadley circulation have a major impact on rainfall fluctuations over West Africa. The effect of the Hadley circulation on rainfall is stronger when there are no other rainfall producing systems, such as for instance the easterly waves (Hou and Lindzen, 1992). The poleward edge of the Hadley circulation has been expanding polewards, resulting in subtropical dry zones expanding and becoming even drier (Johanson and Fu, 2009). The Hadley cell overturning is associated with convective intensity over southern Africa, anticyclonic ridging and moist inflows from the Indian Ocean. During summer, cloud bands play a major role in the production of synoptic rainfall over the subcontinent (Harrison, 1984). South Africa in particular, is positioned in the descending branch of the Hadley cell and the expansion of the Hadley cell may lead to even drier conditions in southern Africa (Mahlobo et al., 2018). The mean positions of storm tracks, high and low pressure systems, jet streams and associated precipitation patterns, are also projected to change owing to the expansion of the Hadley cell (Seidel et al., 2008). The Hadley cell is normally associated with enormously wet summer months over the eastern parts of southern Africa (Manabe and Holloway, 1975), with particularly high rainfall over the

eastern coasts during summer (Tyson and Preston-Whyte, 2000).

Apart from links between the Hadley cell and rainfall, links between the Hadley cell and solar radiation are also strong (Chen et al., 2002; Trenberth and Stepaniak, 2003). The relatively clear skies in the subsiding branch in the subtropics means that solar radiation is abundant at the surface (Trenberth and Stepaniak, 2003). The subtropics are characterized by relatively high outgoing long-wave radiation and low reflected short-wave radiation (Clement and Soden, 2005), which is caused by dynamical induced drying in the subtropics (Herweijer et al., 2005). Chen et al. (2002) demonstrated that decadal trends in tropical mean radiative fluxes are linked to the strength of the Hadley circulation. Changes in insolation have a greater impact upon the Hadley circulation during summer, as opposed to winter, given the seasonality of the angular momentum-conserving limit (Merlis et al., 2013). In the descending branch of the Hadley cell, energetics do not have direct implication to the strength of the Hadley cell during winter. Conversely, in the ascending branch during summer, the Hadley cell reacts to the thermodynamic and energetic changes as it is close to the angular-momentum conserving limit (Merlis et al., 2013). These energetic changes are mainly due to insolation variations near the uppermost parts of the earth's atmosphere. During summer when there is more insolation, the massflux of the Hadley circulation increases and this affects the annual-mean Hadley circulation.

According to the "total actual renewable water resources" (TARWR) per person per year, South Africa is classified as a water-scarce country (Muller et al., 2009). According to the defining attributes of TARWR, South Africa was found to be the 29th driest country out of 193 countries, with an estimated 1110 cubic metres (m^3) of water per person in 2005 (Muller et al., 2009). Annual rainfall over most parts of South Africa is projected to decrease as the subtropical high pressure intensifies over time (Engelbrecht et al., 2009). Such projected decreases

in rainfall may have serious consequences for an already water stressed country where water consumption continues to increase over time (de Lange, 2010). However, there could be an increase in rainfall during summer over the central and eastern regions; associated with a possible increased frequency of extreme rainfall events (Engelbrecht et al., 2009; Shongwe et al., 2009; Engelbrecht et al., 2015). Furthermore temperatures are projected to increase under low mitigation climate change futures. (Engelbrecht et al., 2009; Christensen et al.,2007; Niang et al., 2014; Engelbrecht et al., 2015)

South African electricity generation is primarily supplied by the state-owned national utility-Eskom. Coal is the main source of electricity generation in South Africa. Hydro, pumped storage and nuclear energy also contribute toward electricity generation in South Africa, albeit a small percentage. The South African government aims to diversify its energy generation from coal-fired electricity to an energy mix in which renewable energy contributes 30% (DoE, 2013).

The Hadley cell is thus an important climate attribute to southern Africa, given its influence on energy generation. Its continued expansion under the low mitigation setup namely the Representative Concentration Pathway (RCP) 8.5 (Johanson and Fu, 2009) and continued intensification under RCP 8.5 (Engelbrecht et al., 2009; 2011) is the reason for the projected decrease in rainfall and increase in mean temperatures over southern Africa (Engelbrecht et al., 2009; 2015). While the above discussion is true it is based on the zonally averaged diagnostics of the Hadley cell and some of the regional features resulting from the expansion and intensification of the Hadley cell may be missed due to zonally averaging. To this end, it is important to establish how the Hadley cell has been evolving over southern Africa during the recent past, and how it will continue to evolve in future. Using zonally asymmetric diagnosis of the Hadley cell, this paper aims to examine the Hadley cell evolution based on the RCP 8.5 pathway. The

RCP 8.5 is a worst case climate change scenario and assumes that globally, very low mitigation efforts are undertaken to deal with climate change. The effect of the Hadley cell under such drastic levels of climate change is likely to affect future rainfall and temperature over South Africa and consequently energy generation. The study will further demonstrate energy generations scenarios that can be implemented locally to meet energy demand given factors that the local authorities cannot control (low mitigation efforts globally).

2. DATA AND METHODS

2.1 Data

The study is based on high-resolution simulations of present-day (1980–2018) and future (2030–2060) and (2070-2100) climate over southern Africa, as obtained from a variable resolution GCM. Monthly outputs from a Regional Climate Model (RCM) known as the Conformal-Cubic Atmospheric Model (CCAM) were used. The spatial resolution of the RCM used $0.5^{\circ} \times 0.5^{\circ}$ and has 18 vertical levels. The full description of the CCAM is provided by Engelbrecht et al. (2011). For the dynamically downscaled CCAM, data used include rainfall, temperature and vertical velocity at 500hPa, all of which were provided by the Council for Scientific and Industrial Research (CSIR). The downscaled CCAM data based on RCP 8.5 comprises five Global Climate Models (GCMs) namely the Australian Community Climate and Earth System Simulator (ACCESS1-0); the Geophysical Fluid Dynamics Laboratory Coupled Model (GFDL-CM3); the National Centre for Meteorological Research Coupled Global Climate Model, version 5 (CNRM-CM5); the Max Planck Institute Coupled Earth System Model (MPI-ESM-LR); and the Community Climate System Model (CCSM4). Vertical velocity was used to calculate the massflux, which was used to represent the asymmetric Hadley circulation. The full derivation of the massflux is provided by Schwendike et al. (2014) and Mahlobo et al. (2018). In this study,

the massflux, Hadley cell and Hadley circulation are used interchangeably. Energy consumption data were obtained from the Department of Energy, while population data, population growth rates and Gross Domestic Product (GDP) values were provided by Statistics South Africa.

2.2 Methods

The consistencies between the Hadley cell, rainfall and mean temperatures across South Africa are examined in this study. In so doing, linear trends of the historical massflux, rainfall and temperatures as well as future climate anomalies are provided. The Student t- test is used to test trends for statistical significance at the 95% level. To demonstrate energy generation scenarios that could be implemented a result of the Hadley cell evolution, the Long-range Energy Alternatives Planning system (LEAP) is used. The LEAP system was developed by the Stockholm Environment Institute, Boston (SEI-B). The LEAP model uses both bottom–up and top–down approaches collectively to assess total system impacts (Song et al., 2007). All phases of the energy flow from the demand-side to supply-side are analysed holistically (SEI, 1995). The LEAP system includes the Technology and Environmental Database (TED), which was jointly developed by SEI-B, and the United Nations Environment Programme (UNEP) (SEI, 2008). TED provides information describing the technical characteristics, costs, and environmental impacts of different energy technologies. As such, TED allows for the tracking of pollution resulting from each stage of the fuel chain.

In this study, LEAP is used to examine current energy generation and to simulate alternative energy futures for different scenarios for the period 1990-2099. Energy in South Africa is supplied through a single national grid, to which different technologies across South Africa make a contribution. To this end, energy demand for South Africa is used to calculate the required energy supply to meet current and future projected demands. The following equation

(SEA, 2015) was used to perform this calculation.

$$Cp(MW) = \frac{Dm(MWh)}{Hrs(365 * 24)}) \times (RM + 1) \quad (1)$$

Where Cp is the capacity, Dm the demand, Hrs hours in a year and RM is the reserve margin.

2.2.1 LEAP Scenario Design

Three electricity generation scenarios that can be implemented to meet energy demand given the evolution of the Hadley cell under the RCP 8.5 pathway are demonstrated. First, the business as usual (BAU) scenario is based on the weathering the storm scenario as set out in the IRP 2010 policy adjusted case. According to electricity planning experts this scenario represents the "most likely" new build path. Under the BAU scenario, fossil fuels remain the dominant part of the primary energy. The second scenario is renewables (REN) it follows the IRP strategy to diversify energy generation from South Africa's current primary dependence on coal-fired electricity, to an energy mix in which a third is generated by renewable energy technologies (DoE, 2013). This is achieved by introducing large-scale renewable electricity while both fossil fuel and nuclear sources are gradually phased out. The third scenario namely ($REN_PV_embeded$) considers the impact of large scale solar technologies as well as embedded solar PV. Embedded solar PV refers to solar PV installed on residential, commercial or industrial buildings' rooftops.

3. RESULTS AND DISCUSSION

3.1 Correlations between the Hadley cell, rainfall and temperature

Links between the massflux and rainfall are quantified using correlation coefficients and these are displayed in Figure 1. Positive correlation coefficients are established for all seasons over South Africa and this implies that strengthening (weakening) of the Hadley cell is associated

with rainfall decrease (increase). Correlation coefficients between the massflux and mean temperatures are shown in Figure 2. Negative correlation coefficient is observed in DJF for most parts of South Africa (Figure 2a), with the exception of the western and south western parts of South Africa. High correlation values are over the north western parts of South Africa. In MAM negative correlation coefficients dominates for the entire country, with the exception of the south western parts (Figure 2b). High values of correlations are still found over the north western parts. During JJA negative correlations are evident over the northern half of South Africa, while over the south, positive correlation is evident. High values of correlation are confined to the north western parts of the country (Figure 2c). In SON, negative correlation between the massflux and temperature is still evident, however high correlation values are found over the central interior of South Africa (Figure 2d).

3.2 Linear Trends of the Hadley cell, rainfall and temperature and implications to electricity generation

3.2.1 Trends

Linear trends of mean temperatures, Hadley cell and rainfall for an ensemble average of five GCM's for the period 1980-2018 are shown in Figures 3, 4 and 5 respectively. Areas of statistical significance are shown as grey dots. Red contours indicate an increasing trend while blue contours represent a decreasing trend. A statistical significant increase in mean temperatures for the period 1980-2018 is evident over South Africa for all the seasons (Figure 3). Maximum increase for all seasons is confined to the western and north western parts of the country. The highest increase of mean temperatures for all seasons is in SON (Figure 3d). Statistically significant negative rainfall trends for most parts of Southern Africa are evident during DJF (Figure 4a). However, the central and eastern parts of South Africa show an increasing rainfall trend. During MAM (Figure 4b), JJA (Figure 4c) and SON (Figure 4d), a tendency towards a decrease

in rainfall is established over the country. In SON the statistical significance of the negative trend is confined to the eastern parts of South Africa. However a small region over the south eastern parts shows a statistical significant tendency towards an increase in rainfall in SON.

During (December to February) DJF, a statistically significant increase in downwards massflux is observed over most parts of South Africa (Figure 5a). Simultaneously, an increase in upward massflux is established over the western and southern parts of South Africa. The increase in downward massflux and upward massflux implies the strengthening and weakening of the Hadley cell respectively. In March to May (MAM)(Figure 5b), the increase in downwards massflux is still persistent and cover a wider area than in DJF, an increase in upward massflux is only confined to the south western the country. During June to August (JJA) (Figure 5c), a tendency towards an increase in downwards massflux is dominant over northern parts of the South Africa; while over the central interior and southern parts of South Africa an increase in upwards massflux is evident. For JJA the strengthening of the Hadley circulation over the South Africa is attributed to an increase in the formation of midlevel-highs enhancing subsidence over the country (Engelbrecht et al., 2009). In September to November (SON) (Figure 5d), statistically significant increase in downwards massflux is located further northwards than in JJA, while the southern half of South Africa has a tendency towards an increase in upward massflux. The above discussion is in agreement with massflux trends informed by the ERA-Interim for the period 1980-2015 documented in Mahlobo et al. (2018).

3.2.2 Projected Changes

To examine projected changes of mean temperatures, the Hadley cell and rainfall and for an ensemble average of five GCM's two periods i.e. 2030-2060 and 2070-2100 were used. Fu-

ture climate anomalies for the period 2030-2060 and 2070-2100 relative to the current climate (1980–2018) are presented in Figures 6 and 7 for mean temperatures, Figures 8 and 9 for rainfall and Figures 10 and 11 for the massflux for the time slabs 2030-2060 and 2070-2100 respectively. Areas of statistical significance are shown as grey dots. Red contours indicate an increasing trend while blue contours represent a decreasing trend.

A statistical significant increase in mean temperature is evident in all season (Figures 6 and 7). Maximum increase in mean temperatures is in SON and is around 2.4 and 5.8°C for the 2030-2060 (Figure 6d) and 2070-2100 (Figure 7d) time-slabs respectively. This is way above the 2°C limit recommended by the IPCC (Hoegh-Guldberg et al., 2008). Maximum increase in mean temperatures for all seasons is mainly over the north-western to south-eastern regions. The south-western regions show lowest rates of temperature increase for all seasons.

An increase in rainfall is expected over the central to eastern parts of South Africa in DJF (Figure 8a). Over the central parts of the country, increase in rainfall goes up to 6% and 11% for the 2030-2060 (Figure 8a) and 2070-2100 (Figure 9a) periods respectively. The projected rainfall increase in DJF may be attributed to the projected southern expansion of the subtropical high-pressure belt that results in an increase in the frequency of trough formation, which leads to anomalously high rainfall over the eastern parts of South Africa in DJF (Engelbrecht et al., 2009). A tendency towards a statistical significant decrease in rainfall over South Africa is evident in MAM (Figure 8b), JJA (Figure 8c) and SON (Figure 8d), maximum decrease in rainfall is in JJA and is projected to reach rainfall decrease of 30% and 60% for the 2030-2060 (Figure 8b) and 2070-2100 (Figure 9b) time-slices respectively.

In the case of the Hadley cell, negative anomalies imply, a decrease in upward massflux

and hence the strengthening of the subtropical Hadley cell. Consequently positive anomalies symbolises an increase in upward massflux and hence weakening of the subtropical Hadley cell. A generally statistically significant weakening of the Hadley cell is evident in DJF (Figure 10a) for both time steps, maximum weakening is found over the southern and south-western interior of South Africa for both time steps. The weakening is more during the 2070-2100 (Figure 11a) than in the 2030-2060 timestep. The strengthening of the Hadley cell is also evident in DJF, but confined to the north-western parts of the country and this intensification is more for the latter time step. During MAM (Figure 10b), JJA (Figure 10c) and SON (Figure 10d), strengthening of the Hadley cell is evident for most past of the country, however the southern and south-western regions show weakening of the Hadley cell. Maximum strengthening of the Hadley cell is evident in SON and JJA and reaches 30 and 50kgm^{-2}s^{-1} for the 2030-2060 (Figure 10) and 2070-2100 (Figure 11) respectively. The strengthening (weakening) of the subtropical Hadley cell means more subsidence (ascent) over southern Africa and consequently less (more) opportunity for cloud formation (Mahlobo et al., 2018).

The general weakening of the Hadley cell coincides with increase in rainfall in DJF, although the spatial extent is not exactly the same. Similarly, the strengthening of the Hadley cell during MAM, JJA and SON coincide with the decrease in rainfall during these months. The exception being the south-western and southern parts, which consistently show weakening of the Hadley cell. The strengthening of the Hadley cell during austral winter months results from the formation of mid-level highs that enhance subsidence over southern Africa (Engelbrecht et al., 2009). Consistency between massflux and rainfall changes is more pronounced in austral winter than in austral summer. This is owing to winter subsidence mainly being informed by the Hadley cell. In summer, other rainfall producing systems have an impact in the ascent/subsidence over southern Africa. This makes the connection between the Hadley cell and rainfall stronger in

JJA than DJF in southern Africa (Hou and Lindzen, 1992).

The intensification of the subtropical cell is associated with increase in the subtropical dry zones (Seidel et al., 2008; Mahlobo et al., 2018) and is evident in all seasons except for DJF. According to Lu et al. (2007) the increase in subtropical dry zones means the spatial extent of limited cloud cover and more sunshine hours will increase (Tselioudis et al. 2016; Mahlobo et al., 2018) and this is attributed to the increasing greenhouse gases (GHGs) (Lu et al., 2007). South Africa has high levels of solar radiation varying between 4.5 and 6.5 $kWhm^2$ and the highest values are confined to the Northern Cape Province and this is where the Hadley cell is strongest (Mahlobo et al., 2018). High levels of solar radiation over this region may even be higher due to the strengthening of the Hadley cell under the RCP 8.5 pathway (Figures 8 and 9) and this has a huge impact on electricity generation in South Africa. Most large scale solar PV technologies are located over areas where the Hadley cell is strongest.

Different scenarios may be used to illustrate electricity generation in South Africa (Figures 12, 13, 14). The LEAP model is used to show such scenarios. First the business as usual (BAU) scenario is shown in Figure 12. The BAU scenario follows a low mitigation pathway and considers fossil fuel as the main contributor to electricity generation in South Africa. This may not be a viable option, since the dependence of electricity generation from coal threatens the energy security of South Africa and this is caused by issues related to internal supply and the rise in coal prices internationally. Local efforts to meet the electricity demand through natural resources other than the coal are hence necessary.

Increasing GHG's and hence intensification of the Hadley cell offers opportunities to South Africa's renewable energy industry since this would influence the country's ability to generate

electricity from the solar energy resource. This is demonstrated in the second (Figure 13) and third (Figure14) scenarios. In the second scenario (REN), fossil fuels are gradually phased out, the remaining demand for electricity generation is met through massive increase in large scale on-grid solar technologies (Figure 13). This scenario increases the share of electricity produced from renewables to more than 16%.

The third scenario namely $(REN_PV_embeded)$ considers the impact of large scale solar technologies as well as embedded rooftop solar PV. The increase in share of solar energy in the electricity generation process could be done by the addition of solar water heaters by different municipalities across the country. A mass roll out of these solar waters heaters has already been implemented by a number of municipalities' e.g. city of Cape town, city of Joburg, Ekurhuleni municipality etc. (SEA, 2011). This is demonstrated in the third scenario $(REN_PV_embeded)$, fossil fuels are gradually phased out, and the remaining demand for electricity generation is met through massive increase in large scale solar technologies as well as embedded solar PV (Figure 14). Embedded solar PV denotes to solar PV installations on residential, commercial or industrial buildings rooftops. In this third scenario the share of solar based renewable energy technologies for electricity generation exceed a third.

4. CONCLUSIONS

This paper examines the links between the Hadley cell and rainfall over South Africa and showed how the changes in the Hadley cell under the RCP 8.5 setting could affect electricity generation in South Africa. An evidence of the strengthening of the Hadley cell and projected decrease in rainfall and increase in temperatures under the RCP8.5 settup over most parts of the country in MAM, JJA and SON was found. In DJF, the weakening of the Hadley was found

and successively a tendency towards an increase in rainfall over the central and eastern parts of South Africa. The strengthening of the Hadley cell in general, has positive implications on electricity generation through renewable energy technologies especially solar technologies. Renewable energy technologies play a major role in the energy security. Therefore the Hadley cell can be also used as a proxy to identify regions which have more solar energy resources. Over South Africa, Hadley cell maximum intensification was found to be exactly over the areas where sunshine duration is more, and this was found to be over the north western parts of South Africa (Mahlobo et al., 2018). It is over these regions that solar energy technologies are located. The promotion of solar energy resource in South Africa will have economic, social and environmental benefits. The associated benefits include improved health due to the reduction of carbon emissions. More business opportunities in the renewable energy sector will lead to more jobs which is a current crisis in South Africa.

REFERENCES

Ceppi P, DL Hartman, 2013. On the speed of the Eddy-Driven Jet and the width of the Haley Cell in the Southern Hemisphere, Journal of Climate. 26.3450-3465.

Chen J, Carlson B, Del Genio A, 2002. Evidence for strengthening of the tropical general circulation in the 1990s. Science. 295. 838–841.

Clement AC, Soden B, 2005. The sensitivity of the tropical-mean radiation budget. Journal of Climate 18: 3189-3203.

Christensen JH, Hewitson B, Busuioc A, Chen A, Gao X,Held I, Jones R, et al., 2007. Regional climate projections. In: Climate Change 2007: The Physical Science Basis. Contribution of Working Group I to the Fourth Assessment Report of the Intergovernmental Panel on Climate Change [Solomon S, Qin D, Manning M, Chen Z, Marquis M, Averyt KB, et al. (eds.)]. Cambridge University Press, Cambridge.

DEA, 2018. South Africa's low emission development strategy 2050. Department of Environmental Affairs,Pretoria South Africa

De Lange W, 2010. The water situation in South Africa: Some inconvenient truths, in A CSIR perspective on water in South Africa. CSIR. 2010.

Dickey D, Fuller W, 1981. Likelihood Ratio Statistics for Autoregressive Time Series with a Unit Root. Econometrica 49: 1057-1072.

DoE, 2013. Integrated Resource Plan For Electricity (IRP) 2010-2030 Update Report 2013. Department of Energy. Pretoria South Africa.

Engelbrecht FA, McGregor JL, Engelbrecht CJ, 2009. Dynamics of the Conformal-Cubic Atmospheric Model projected climate-change signal over southern Africa. International Journal of Climatology 29: 1013-1033.

Engelbrecht FA, Landman WA, Engelbrecht CJ, Landman S, Bopape MM, Roux B, McGregor JL, Thatcher M, 2011. Multi-scale climate modelling over Southern Africa using a variable-resolution global model. Water S.A. 37. 647-658

Engelbrecht F, Adegoke J, Bopape M, Naidoo M, Garland R, Thatcher M, et al., 2015. Projections of rapidly rising surface temperatures over Africa under low mitigation. Environmental Research Letters 10, https://doi.orgi:10.1088/1748-9326/10/8/085004.

Harrison MSJ, 1984. A generalized classification of South African rain-bearing synoptic patterns systems. International Journal of Climatology. 4. 547-560.

Herweijer C, Seager R, Winton M, 2005. Why do ocean heat transport warms the global mean climate. Tellus. 57. 662-675.

Hoegh - Guldberg O, Jacob D, Taylor M, Bindi M, Brown S, Camilloni I, et al,2018. Chapter 3: Impacts of 1.5°C global warming on natural and human systems. In: Global Warming of 1.5°C an IPCC special report on the impacts of global warming of 1.5°C above pre-industrial levels and related global greenhouse gas emission pathways, in the context of strengthening the global response to the threat of climate change. Intergovernmental Panel on Climate Change.

Hou AY, Lindzen RS, 1992. The influence of concentrated heating on the Hadley Circulation. Journal of Amospheric Science. 49. 1233-1241.

Johanson CM, Fu Q, 2009. Hadley cell widening: model simulations versus observations. Journal of Climate, 22, 2713–2725.

Kanamitsu M, Krishnamurti TN, 1978. Northern summer tropical circulations during drought and normal rainfall months. Monthly Weather Review. 106. 331-347.

Kang SM, Lu J, 2012. Expansion of the Hadley cell under Global Warming: Winter versus Summer, 25. Journal of Climate. 25. 8387-8393.

Keyser D, Schmidt BD, Duffy DG, 1989. A technique for representing three-dimensional vertical circulations in baroclinic disturbances. Monthly Weather Review. 177. 2463-2494.

Lu J, Vecchi GA, Reichler T, 2007. Expansion of the Hadley cell under global warming. Geophysics Research Letter, 34, L06805. https://doi.org/10.1029/2006GL028443.

Mahlobo DD, Ndarana T, Grab S, Engelbrecht F, 2018. Integrated climatology and trends in the subtropical Hadley cell, sunshine duration and cloud cover over South Africa. International Journal of Climatology. 39. 1805-1821.

Manabe S, Holloway JL, 1975. The seasonal variation of the hydrological cycle as simulated by a global model of the atmosphere, Geophysics Research Letters. 80. 1617-1649.

Merlis TM, Schneider T, Bordoni S, Eisenman I, 2013. Hadley circulation to orbital precession part II; Subtropical continent. Journal of Climate. 26. 754-771.

Muller M, Schreiner B, Smith L, van Koppen B, Sally H, Aliber M, Cousins B, Tapela B, van der Merwe-Botha M, Karar E, Pietersen K.2009: Water security in South Africa. development Planning Division. Working Paper Series No.12, DBSA: Midrand

Niang I, Ruppel OC, Abdrabo MA, Essel A, Lennard C , Padgham J , et al. Africa, 2014. In: Climate Change 2014: Impacts, Adaptation, and Vulnerability. Part B: Regional Aspects. Contribution of Working Group II to the Fifth Assessment Report of the Intergovernmental Panel on Climate Change [Barros VR, Field CB, Dokken DJ, Mastrandrea MD, Mach KJ, Bilir TE, et al.(eds.)]. Cambridge University Press, Cambridge.

Schwendike J, Govekar P, Reeder MJ, Wardle R, Berry GJ, Jakob C, 2014. Local Partitioning of the overturning circulation in the tropics and the connection to the Hadley and Walker circulations, Journal of Geophysical Research. Atmopshere, 119,1322-1339.

Seidel DJ, Fu Q, Randel WJ, Reichler TJ, 2008. Widening of the tropical belt in a changing climate. Nature Geoscience. 1, 21-24.

SEA-Sustainable Energy Africa, 2011. State of energy in South African: Technical Report. Cape Town. South Africa

SEA-Sustainable Energy Africa, 2015. Energy scenarios for Cape Town. Energy Scenarios for Cape Town: Technical Report. Cape Town. South Africa

SEI–Stockholm Environment Institute, 1995. Version 95.0, LEAP User Guide Stockholm Environment Institute, Boston.

SEI-Stockholm Environment Institute, 2008. Long Range Energy Alternatives Planning System, Tellus Institute, Boston.

Shongwe ME, van Oldenborgh GJ, van den Hurk BJJM, de Boer B, Coelho CAS, van Aalst MK, 2009. Projected changes in mean and extreme precipitation in Africa under global warming. Part I: Southern Africa. Journal of Climate, 22, 3819-3837.

Song HJ, Lee S, et al., 2007. Environmental and economic assessment of the chemical absorption process in Korea using the LEAP model. Energy Policy. 35. 5109-5116.

Tselioudis G, Lipat BR, Konsta D, Grise KM, Polvani LM, 2016. Midlatitude cloud shifts, their primary link to the Hadley cell, and their diverse radiative effects. Geophysics Research Letter, 43(9), 4594–4601.

Trenberth KE, Stepaniak DP, 2003. Seamless poleward atmospheric energy transports and implications for the Hadley Circulation. Journal of Climate. 16. 3706-3722.

Tyson PD, Preston-Whyte RA, 2000. The Weather and Climate of Southern Africa, Oxford University Press, pp396.

Wallace JM, Hobbs PV, 2006. Atmospheric Science: An Introductory Survey. 2nd ed. Academic Press, 483pp.

Yin JH, 2005. A consistent poleward shift of the storm tracks in simulations of 21st century climate. Geophysics Research Letters. 32. L18701

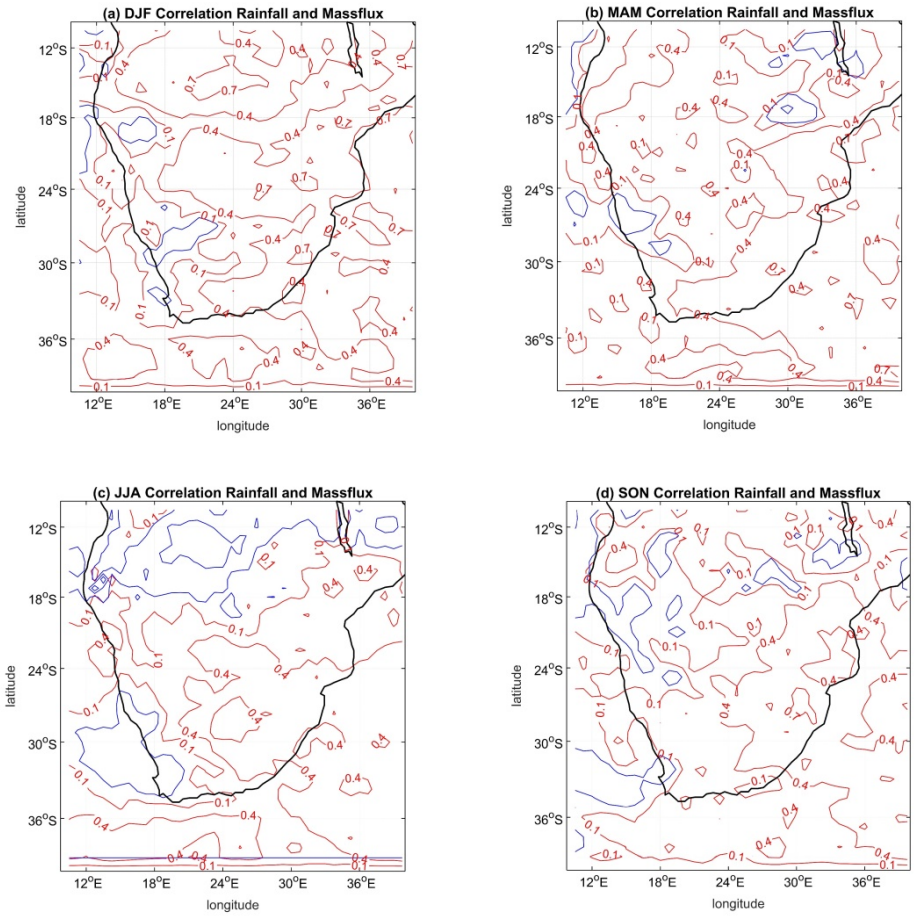

Figure 1: Correlations between rainfall and massflux for (a) DJF, (b) MAM, (c) JJA and (d) SON, red contours represent positive correlation while blue contours represent negative correlation.

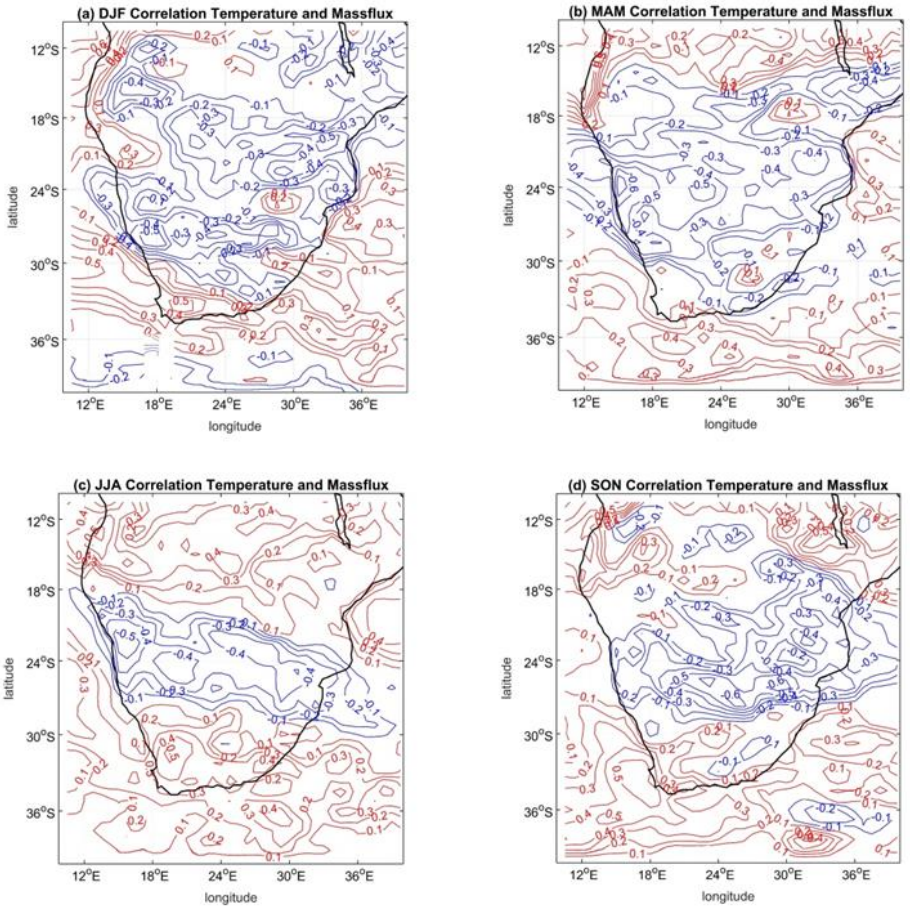

Figure 2: Correlations between temperature and massflux for (a) DJF, (b) MAM, (c) JJA and (d) SON, red contours represent positive correlation while blue contours represent negative correlation.

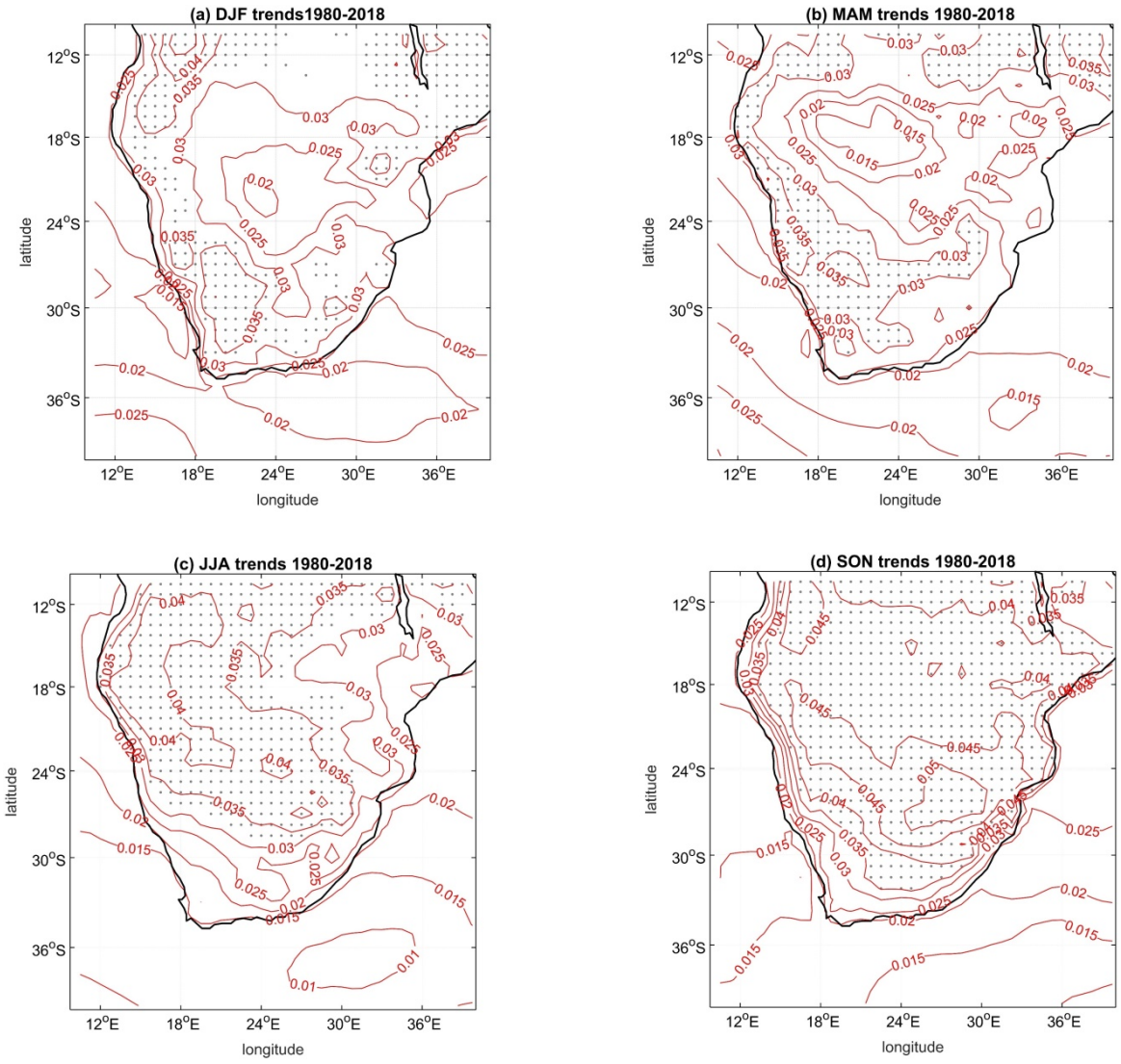

Figure 3: Linear trends seasonal mean of the mean temperatures and the units are °C for (a) DJF, (b) MAM, (c) JJA and (d) SON. Negative anomalies of the mean temperatures are represented by the blue contours and positive anomalies are represented by red contours. Regions of 95% statistical significance is represented using the grey dots and where there are no grey dots, trends are not significant.

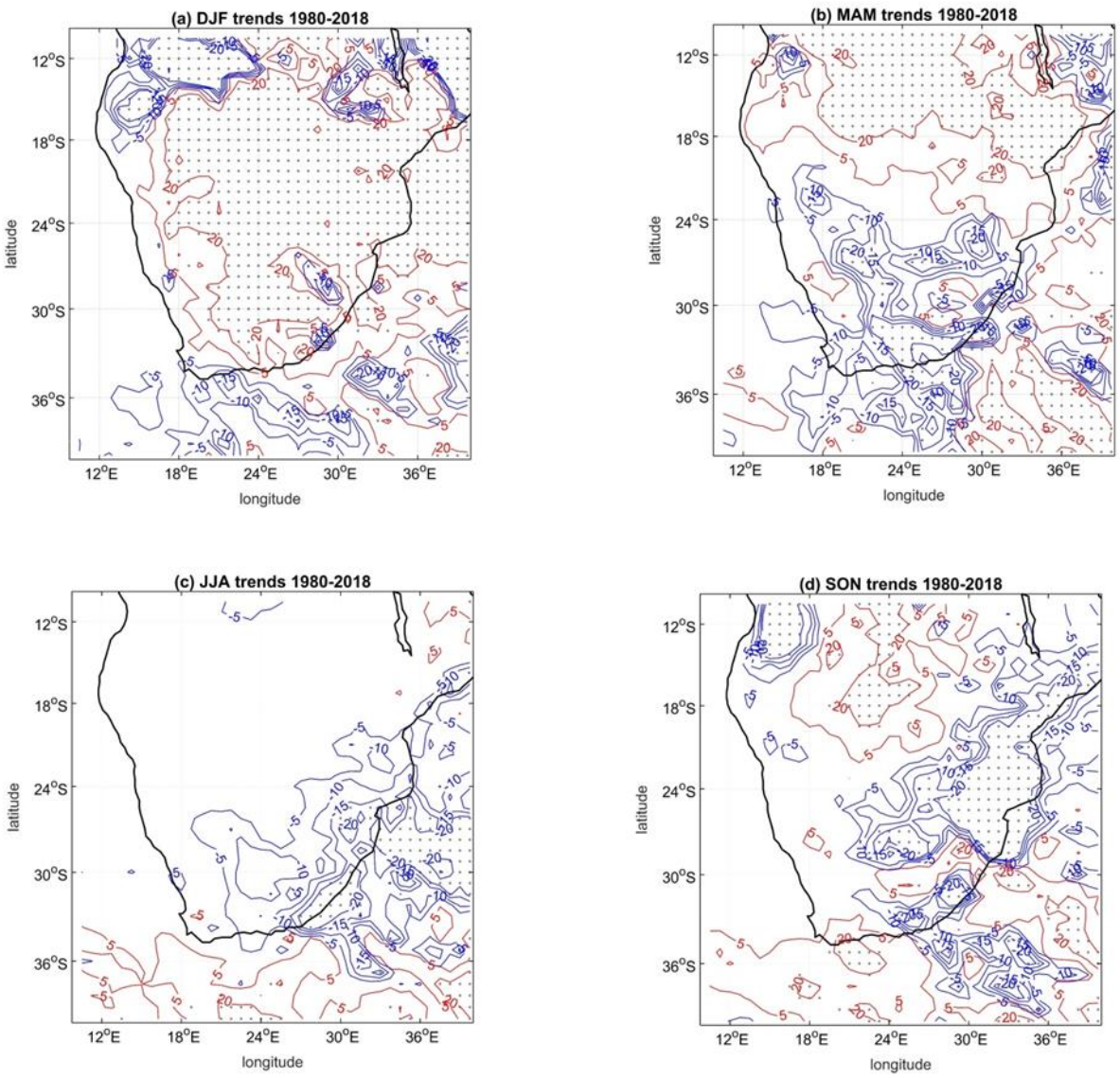

Figure 4: Linear trends in seasonal mean of rainfall and the units are mm for (a) DJF, (b) MAM, (c) JJA and (d) SON. Negative (positive) trends of the rainfall are represented by the blue (red) contours. Regions of 95% statistical significance is represented using the grey dots and where there are no grey dots, trends are not significant.

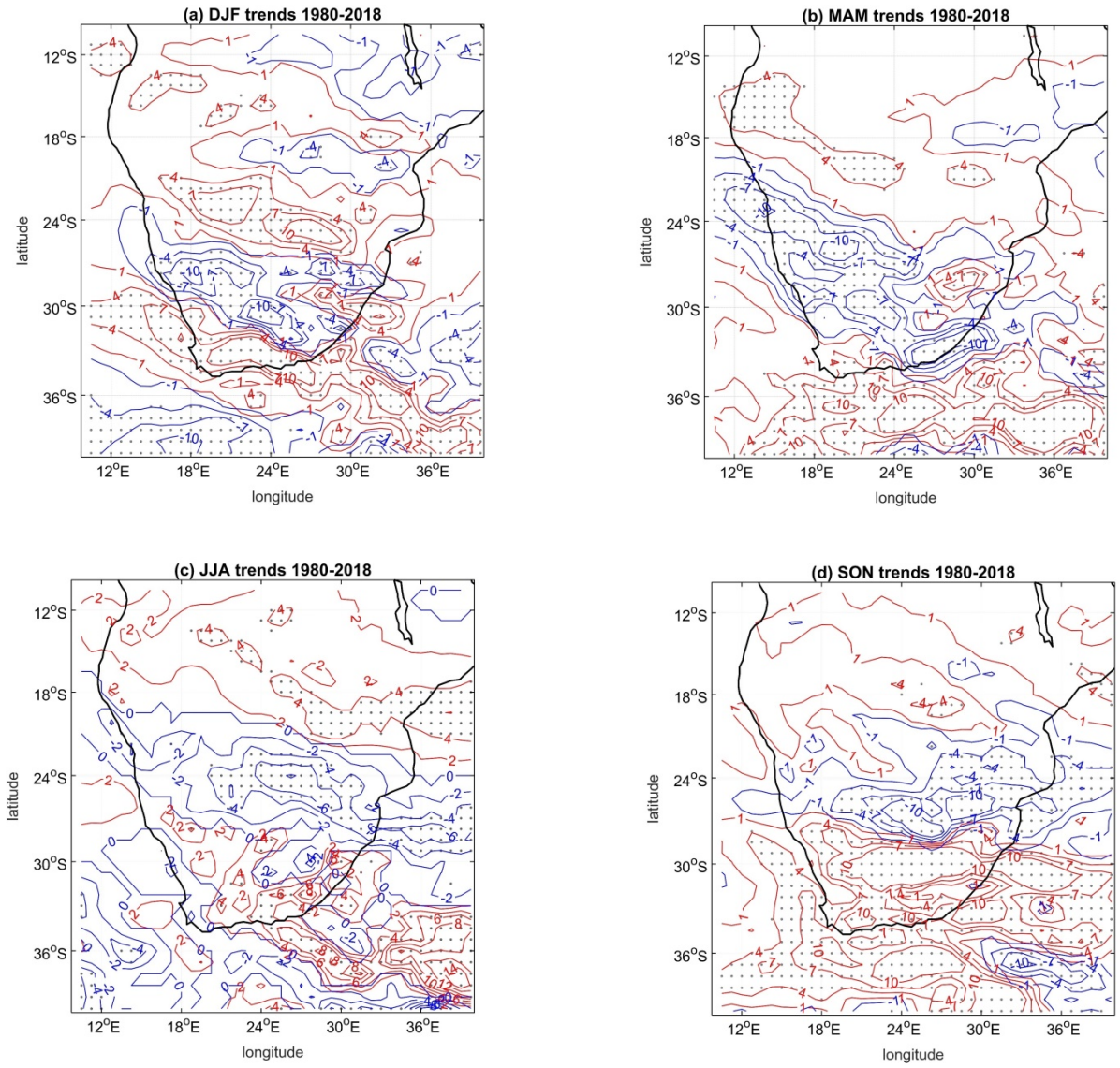

Figure 5: Linear trends in seasonal mean of the massflux for the period 1980-2018 and the units are $\mathrm{kgm^{-2}s^{-1}}$ for (a) DJF, (b) MAM, (c) JJA and (d) SON. Negative (positive) trends of the massflux are represented by the blue (red) contours. Regions of 95% statistical significance is represented using the grey dots and where there are no grey dots, trends are not significant.

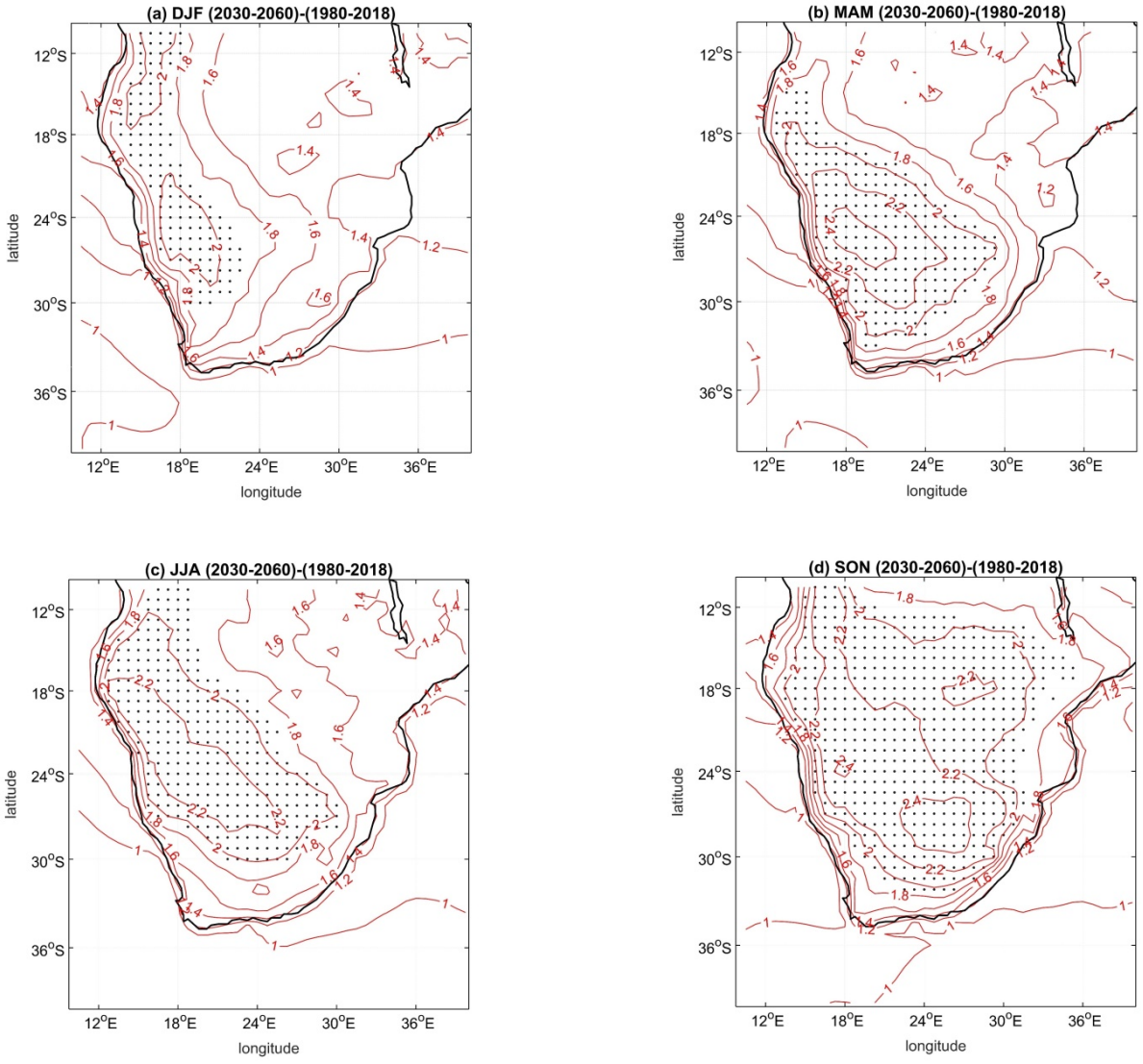

Figure 6: Projected changes in seasonal mean of the mean temperatures for the period 2030-2060 and the units are °C for (a) DJF, (b) MAM, (c) JJA and (d) SON. Negative anomalies of mean temperatures are represented by the blue contours and positive anomalies are represented by red contours. Regions of 95% statistical significance is represented using the grey dots and where there are no grey dots, trends are not significant.

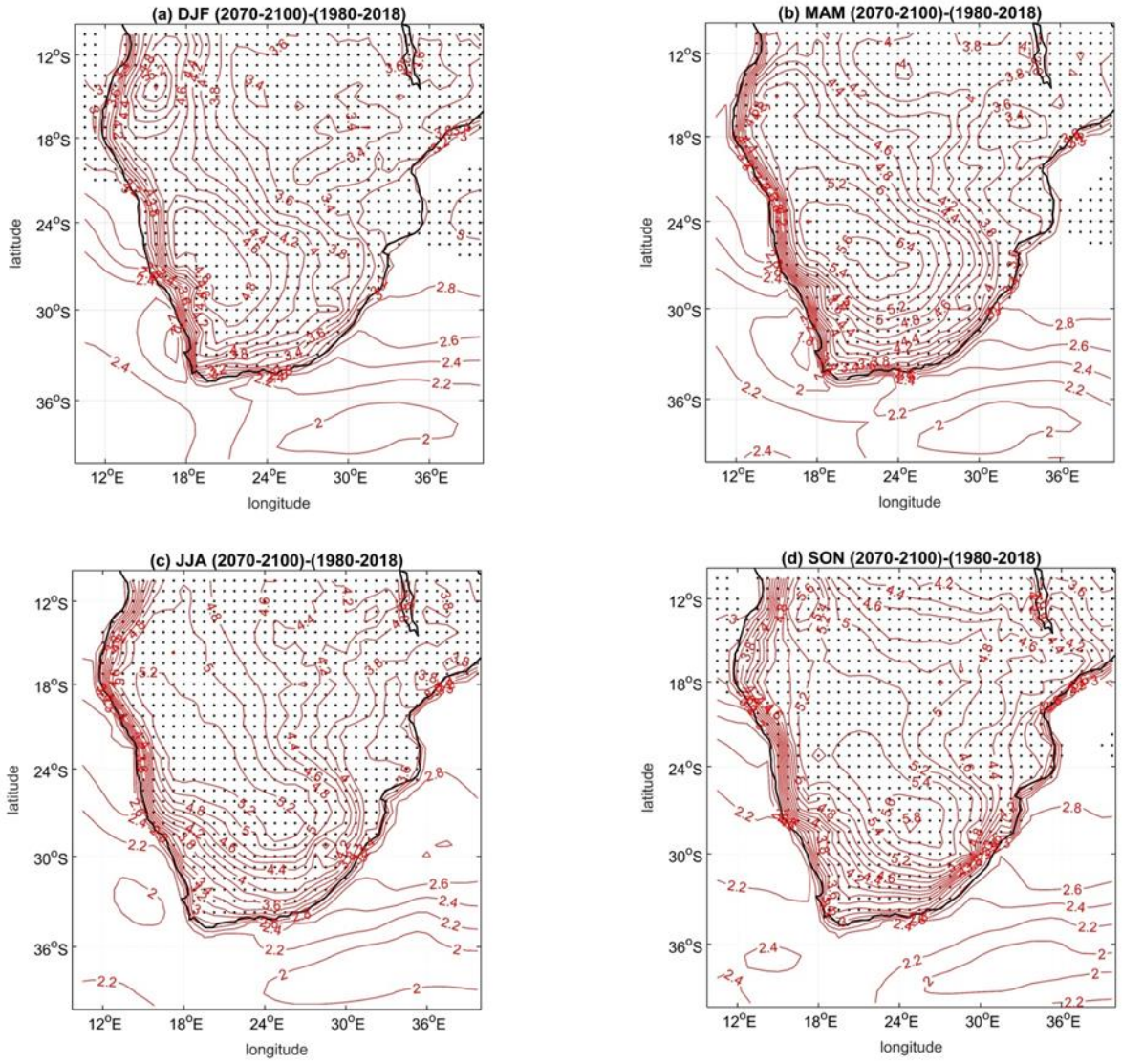

Figure 7: Projected changes in seasonal mean of mean temperatures for the period 2070-2100 and the units are °C for (a) DJF, (b)MAM, (c) JJA and (d) SON. Negative anomalies of mean temperatures are represented by the blue contours and positive anomalies are represented by red contours. Regions of 95% statistical significance is represented using the grey dots and where there are no grey dots, trends are not significant.

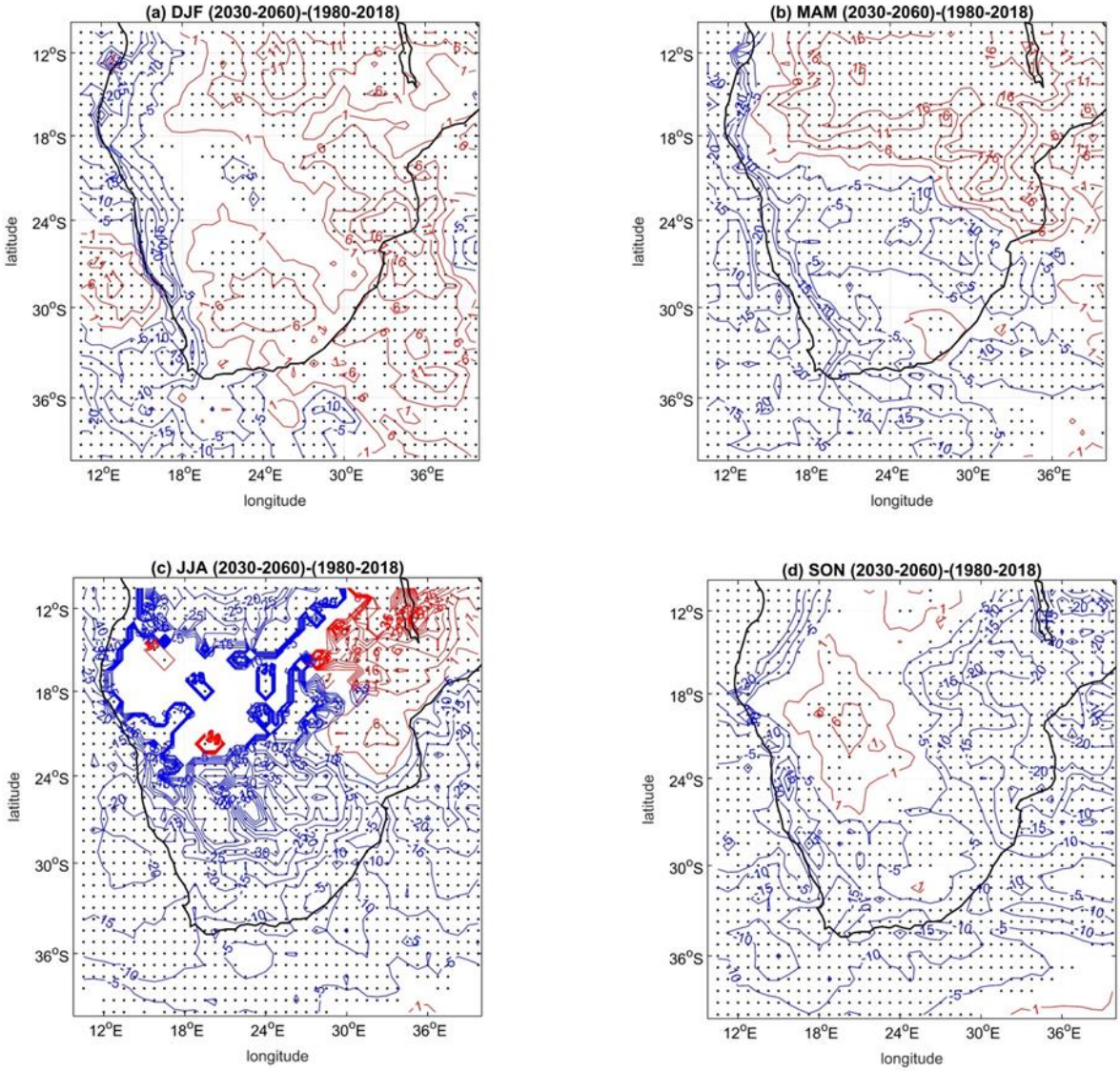

Figure 8: Projected changes in seasonal rainfall for the period 2030-2060 and the units are mm for (a) DJF, (b) MAM, (c) JJA and (d) SON. Negative anomalies of rainfall are represented by the blue contours and positive anomalies are represented by red contours. Regions of 95% statistical significance is represented using the grey dots and where there are no grey dots, trends are not significant.

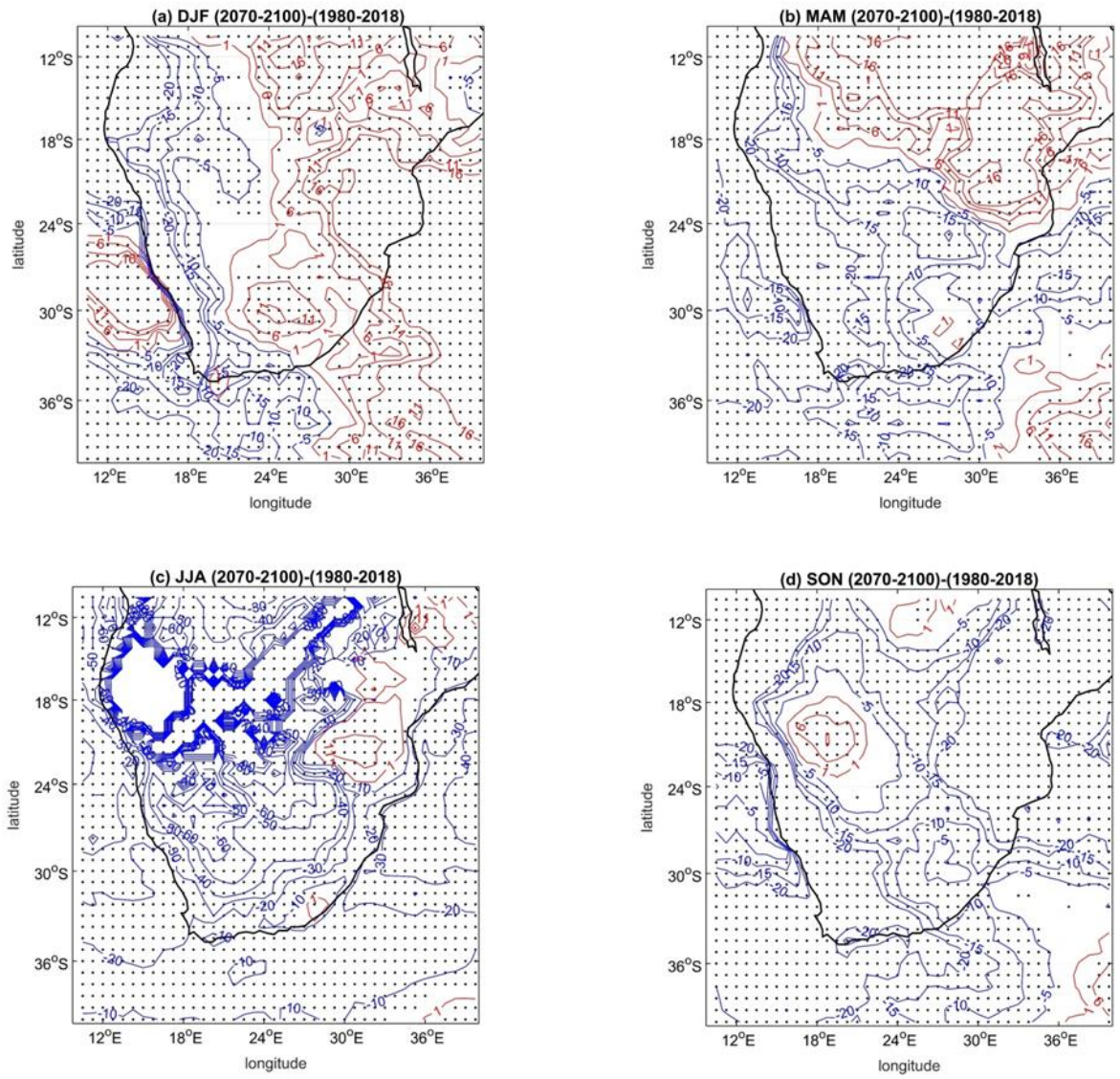

Figure 9: Projected changes in seasonal rainfall for the period 2070-2100 and the units are mm for (a) DJF, (b) MAM, (c) JJA and (d) SON. Negative anomalies of the rainfall are represented by the blue contours and positive anomalies are represented by red contours. Regions of 95% statistical significance is represented using the grey dots and where there are no grey dots, trends are not significant.

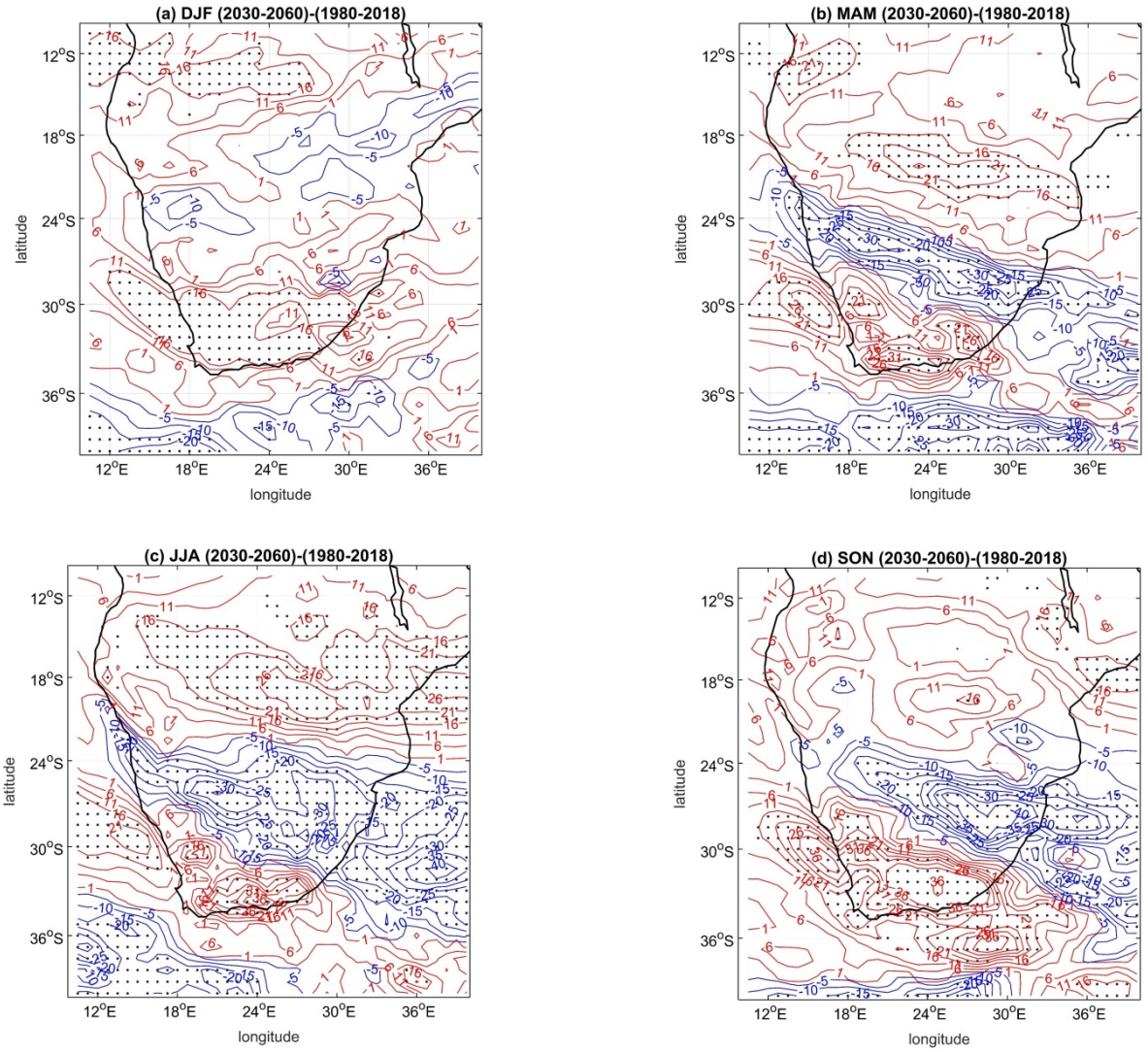

Figure 10. Projected changes in seasonal mean of the massflux for the period 2030-2060 and the units are $kgm^{-2}s^{-1}$ for (a) DJF, (b) MAM, (c) JJA and (d) SON. Negative anomalies of massflux are represented by the blue contours and positive anomalies are represented by red contours.Regions of 95% statistical significance is represented using the grey dots and where there are no grey dots, trends are not significant.

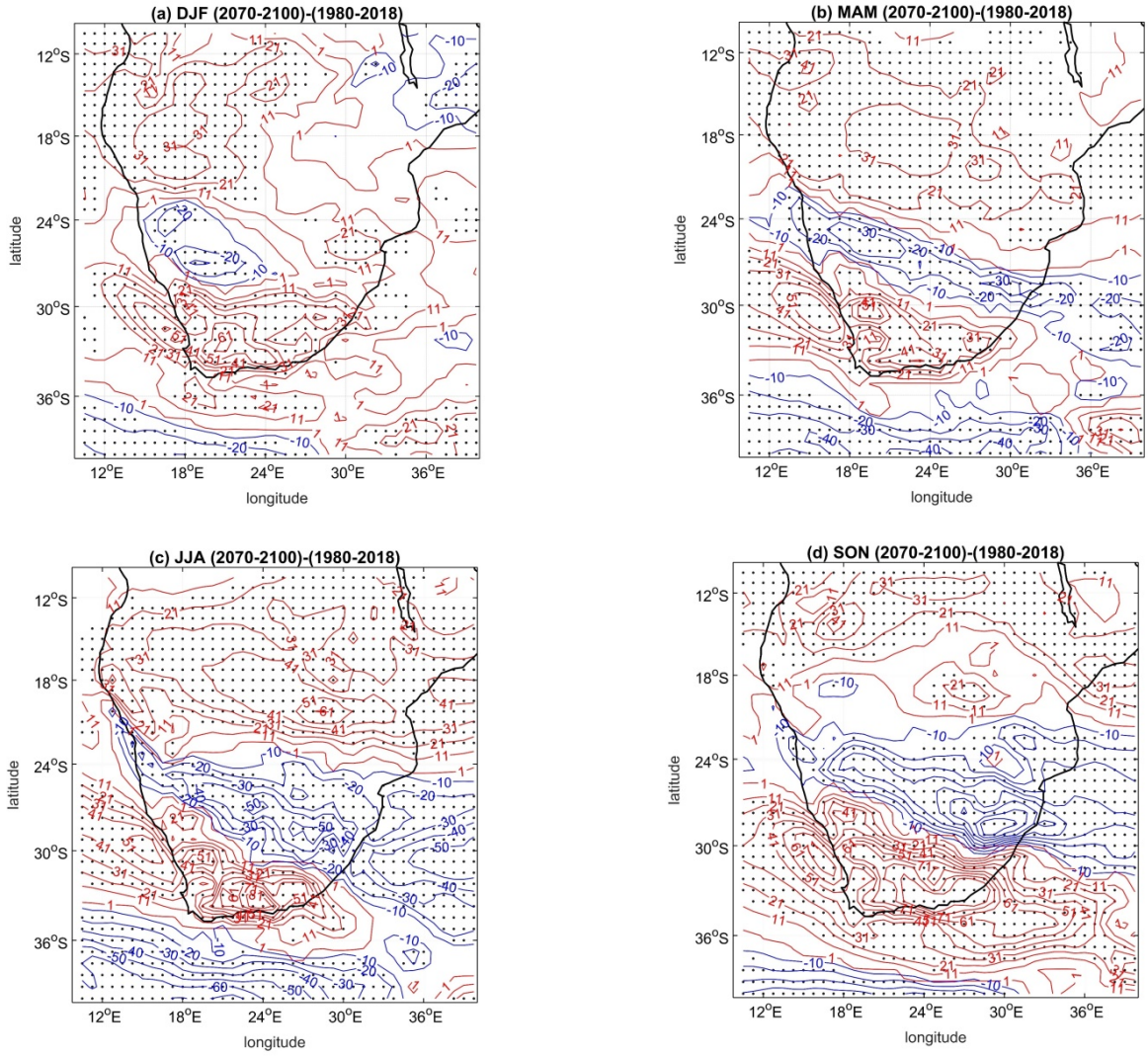

Figure 11. Projected changes in seasonal mean of the massflux for the period 2070-2100 and the units are kgm^{-2}s^{-1}for (a) DJF, (b) MAM, (c) JJA and (d) SON Negative anomalies of massflux are represented by the blue contours and positive anomalies are represented by red contours. Regions of 95% statistical significance is represented using the grey dots and where there are no grey dots, trends are not significant.

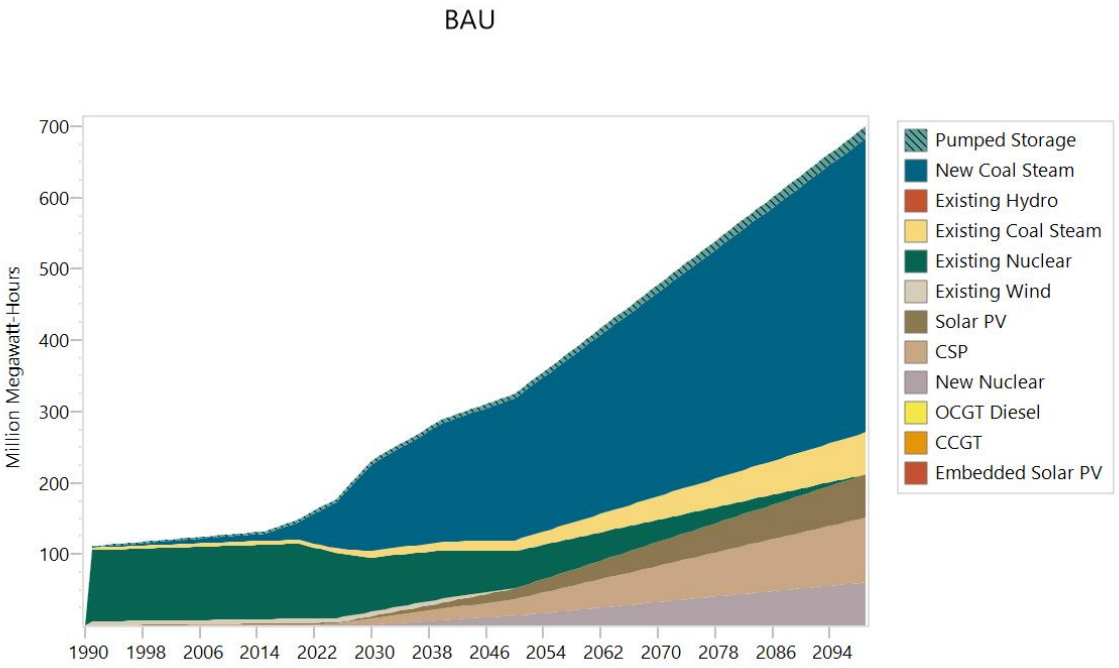

Figure 12: The energy mix of annual electricity generation for the BAU scenario.

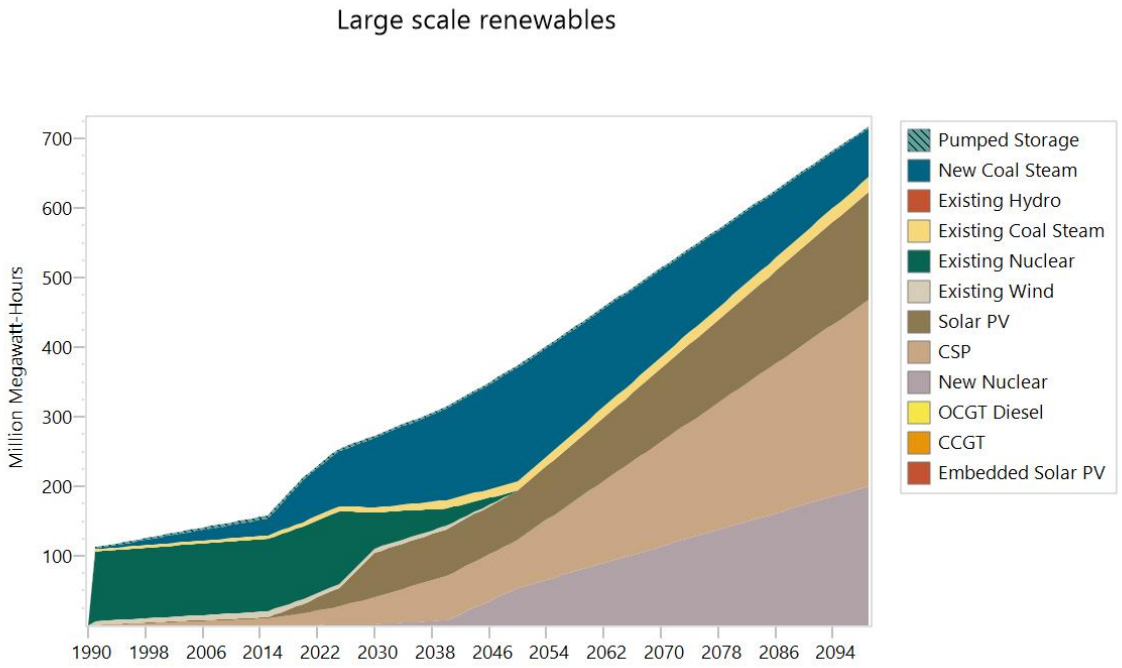

Figure 13: The energy mix of annual electricity generation for the largescale renewables scenario.

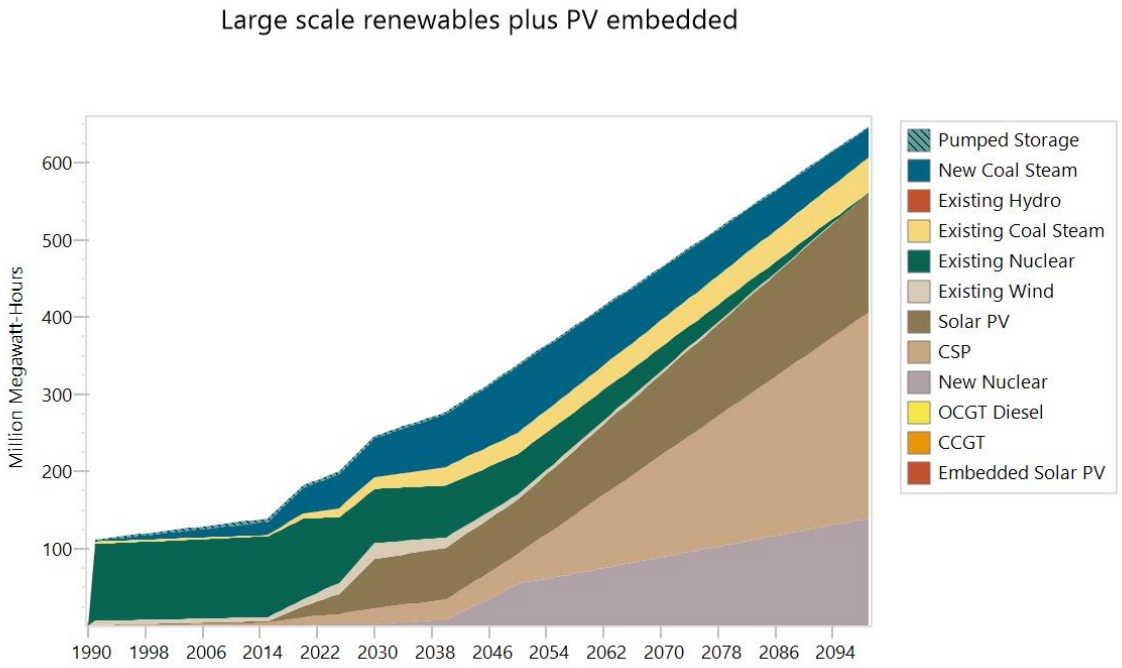

Figure 14: The energy mix of annual electricity generation for the large scale scale renewables plus embedded solar PV scenario.

Chapter 6
Summary

1. Background

This study was inspired by the Integrated Resource Plan (IRP) 2010 of South Africa, in which a number of renewable energy options were identified to inform the country's energy mix on the 2030 horizon and beyond. Solar energy was identified as one of the options. Solar energy is mostly influenced by large scale cloud formation and the latter could be linked with the subtropical Hadley cell. The study thus focused on the local behaviour of the Hadley cell and how it relates to cloud cover and sunshine duration over South Africa and how it affects energy generation. The primary aim of the research was to establish a causal chain reaction that begins with changes on the Hadley cell upstream and ends with energy generation downstream. To achieve this aim, the following objectives were to be addressed:

- To establish an integrated climatology of the Hadley cell, cloudiness and sunshine duration and associated trends over South Africa.

- To establish the influence and associated causality of observed changes in the subtropical branch of the Hadley cell on trends in cloudiness over South Africa.

- To establish the influence of changes on the Hadley cell on sunshine duration over South Africa.

- To determine the implications of the changes in the Hadley cell caused by climate change on energy generation over South Africa.

The success of this study depended on the proper diagnosis of the Hadley cell, which is the focal point of this study. The Hadley circulation is a fundamental process in the general circulation; it is the main reason for the ascending motion in the tropics and descent in the subtropics. It plays an integral role in the context of climate change and associated changes in the atmospheric circulation. The Hadley cell is defined by Wallace and Hobbs (2006), as a large scale atmospheric circulation that is caused by differential heating of the earth's surface and it is rendered as the most protruding feature of the atmospheric circulation (Kang and Lu, 2012). Weather and climate in both the tropics and subtropics are thus informed largely by the Hadley circulation. South Africa is situated in the subtropics and so its weather and climate are affected by circulation systems that prevail in the tropics, subtropics as well as the temperate latitudes to the south (Tyson and Preston-Whyte, 2002). The edge of the Hadley cell is related to the movement of the ITCZ and the expansion of the Hadley cell increases as the ITCZ moves farther from the equator (Kang and Lu, 2012). The Hadley cell boundaries are characterized by a pole-ward extent of subsidence in the subtropical zones as well as the location of subtropical jet boundaries (Seidel et al, 2008). The Hadley circulation has important implications for the solar energy resource along the subtropical belts, and over South Africa in particular. The abundance and increase in solar radiation and sunshine over South Africa is due to the fact that the country is located in the subtropical belt, where the

Hadley cell descending branch is located. However, it should be noted that solar radiation reaching the surface has a strong longitudinal gradient, which is also the case with cloud cover (Loeb and Schuster, 2008) and sunshine duration.

The above discussion suggests that there might be links between the descending branch of the Hadley cell, cloudiness and solar radiation (as a renewable energy resource) over South Africa. In order to have a better understanding of these issues, we hypothesised in Chapter 1 that a combined climatology and trends analysis will elucidate some issues embedded in this complex interplay. The combined climatology has been missing over South Africa because, for one thing, the diagnostics used to represent the Hadley cell have traditionally been zonally symmetric. In Chapter 2, a framework that will diagnose the Hadley cell asymmetrically was developed. These diagnostics laid a foundation of this study and they formed part of the integrated climatology and trend analysis as detailed in Chapter 2. The diagnostics were also used for causality analysis detailed in Chapters 3 and 4 for meeting objectives 2 and 3 respectively. The Hadley cell zonally asymmetric diagnostics were further used in Chapter 5 to examine future scenario of the Hadley cell caused by climate change and how this can be exploited to secure electricity generation in South Africa.

The method by Schwendike et al. (2014) and Keyser et al. (1989) was used for the asymmetric diagnosis of the Hadley cell. Using this method, the irrotational part of the three dimensional flow was partitioned into a pair of orthogonal two-dimensional circulations. This method resulted in a vertical flow field that can be decomposed into longitudinal and latitudinal parts, which in turn are used to define

two zonally varying vertical fluxes that can be used to define the local Hadley and local Walker circulations, respectively. Using the Hadley diagnostics, an integrated climatology and trend analysis of the descending branch of the Hadley cell cloud cover was established for South Africa. Simultaneously, the widely used zonally averaged mass stream function was used to generate zonally symmetric diagnostics of the Hadley cell. Although there is some form of consistency between the two diagnoses, a contrast was also established. A weaker and more poleward Hadley cell was found in DJF, while a stronger and more equatorward Hadley predominated in JJA. Consistently, the subtropical dry zones in the Southern Hemisphere are located further southwards in DJF and further northwards in JJA. Associations between the Hadley cell, cloud cover and sunshine duration has been established from both diagnostics. Minimum total cloud cover, maximum sunshine duration, and the Hadley cell edges were found to be located poleward in DJF, and equatorward in JJA. Both diagnoses showed maximum weakening of the Hadley in DJF. The maximum intensification of the subtropical Hadley according to the zonally symmetric diagnosis was found to be in JJA; however the zonally asymmetric diagnosis indicated maximum intensification of the Hadley cell over South Africa to be in SON. This is consistent with the decrease in total cloud cover and increase in sunshine duration (although the increase in sunshine duration is limited to the eastern parts of the country) in JJA, as well as the increase in total cloud cover and decrease in sunshine hours in DJF over the subtropics and over South Africa in particular. Similarly, maximum intensification in SON coincides with maximum decrease in cloud cover and increase in sunshine over South Africa.

A quantitative correlation of the Hadley cell (for both zonally-symmetric and zonally-

asymmetric diagnostics), total cloud cover as well as the sunshine duration was also achieved for all the seasons. It is clear that the strength of the subtropical Hadley cell intensity is positively correlated with sunshine duration and negatively correlated with total cloud cover. Results from Chapter 2 suggest that the general behaviour of the Hadley cell can be attained from zonally symmetric diagnostics; however, regional implication can be easily missed from such a framework. Therefore, the zonally-asymmetric method provides a useful way to explore regional implications of the Hadley cell and could be further used for impact studies on solar energy.

The study has demonstrated in Chapter 2 that large scale cloudiness over South Africa is linked to the dynamics of the Hadley circulation over the country. Chapter 3 (objective 2), investigates whether the changes in cloudiness over South Africa are directly caused by the changes in the Hadley circulation or vice versa. The Granger causality time series modelling was used to quantitatively diagnose the influence of the seasonal Hadley cell between cloud cover in both directions. Bivariate vector autoregressive time series models for the period 1980 to 2015 were fitted to the seasonal Hadley cell and total cloud cover.

According to the AIC and BIC statistics, the optimum lag used in the Hadley cell-cloud cover bivariate model was two days. The highest correlation coefficient of the lag correlations from averaged data was also two days. The lag correlations calculated from each grid point indicates lag lengths of one to two days for strongest correlation. The strength of these correlations is seasonally dependent and advocates linkage between the northwards-southwards shift of the Hadley cell and the

seasonal migration of the Inter-Tropical Convergence Zone (ITCZ) (Kang and Lu, 2012). The lag correlation seemed to be stronger in DJF than in JJA. This may be owing to the synoptic systems (e.g. tropical temperate troughs and cut-off-lows) leading to cloud formation, dominating in the DJF period. Such systems have life spans of one to several days (Hart et al., 2010: Singleton and Reason, 2007).

It was further established that the Hadley cell can Granger cause cloud cover for both DJF and JJA. This causality is associated mostly with limited cloud cover. For example, causality is found over the interior of South Africa, where the subtropical high pressure cell dominates. In DJF, the western parts of South Africa experience cloudlessness, and this is mostly where causality is established. Weak causality from cloud cover to the Hadley cell was also established. This is a typical case of spurious causality in bivariate systems caused by the exclusion of a third variable in the Granger causality analysis.

Further analysis has shown that vertical velocity is the main variable that could have led to the causality of cloud cover to the Hadley cell. Finally, although it was shown that Granger causality is a useful tool in establishing causality from the Hadley cell to cloud cover. The study further recommended that for Granger causality to be employed in climate science, the scientific background of the variables being analysed should be well understood before correct interpretations of the causality results can be made. Strong links between sunshine duration over the subtropics and the strength of the Hadley circulation over the country were established in Chapter 2. In Chapter 4, the causal direction and strength of the links between the Hadley cell and sunshine duration were investigated. This was done by employing the Granger

causality procedure, as was done in Chapter 3. The presence of Granger causality in both directions was established between the sunshine duration and the Hadley cell.

In Chapter 5 the links between the Hadley cell, mean temperatures and rainfall over South Africa and their evolution under the RCP 8.5 were investigated. An evidence of the strengthening of the Hadley cell and projected decrease in rainfall and increase in temperatures under the RCP8.5 settup over most parts of the country in MAM, JJA and SON was found. In DJF, the weakening of the Hadley was found and successively a tendency towards an increase in rainfall over the central and eastern parts of South Africa. The strengthening of the Hadley cell in general, has positive implications on electricity generation through solar based renewable energy technologies. Renewable energy technologies play a major role in the energy security. Therefore the Hadley cell can be also used as a proxy to identify regions which have more solar energy resources. Over South Africa, Hadley cell maximum intensification was found to be over the areas where sunshine duration is more, and this was found to be over the north western parts of South Africa (Mahlobo et al., 2018). It is over these regions that solar plants are located.

The LEAP model was used to demonstrate electricity generation scenarios that could be implemented as a result of the evolution of the Hadley cell under the RCP 8.5 pathway. The first scenario is the business as usual (BAU), it follows a low mitigation pathway and considers fossil fuel as the main contributor to electricity generation in South Africa. In the second and third scenarios fossil fuels are gradually phased out, while the share of renewables is increased through solar based

technologies. Electricity demand is therefore met by increasing the share of renewables through large scale solar technologies. The share of renewables is further increased by the supplementing the large scale solar PV technologies by embedded solar rooftops through the third scenario. The promotion of solar energy resource in South Africa will have economic, social and environmental benefits. The associated benefits include improved health due to the reduction of carbon emissions. Moreover business opportunities in the renewable energy sector will lead to more jobs which is a current crisis in South Africa.

In conclusion, local diagnosis of the Hadley cell that could be used to illustrate the local behaviour of the Hadley cell over South Africa were produced. Links between the local Hadley and cloud cover as well as sunshine duration were observed. Furthermore, the impact of the Hadley cell to rainfall and further to energy resources was shown. The local Hadley cell could then further be used as proxy to show areas that are resourceful for solar energy generation.

2. Scientific Contributions of the Study /Contribution to Knowledge

A significant contribution made by this study was to implement local diagnostics of the Hadley cell over South Africa that could be used for assessing the spatial distribution of the Hadley cell. The diagnostics could be further used in a number of impact studies. The key points worth mentioning are as follows.

1. This study was able to implement zonally asymmetric diagnostics that could be used to represent the Hadley cell over South Africa. This is the first study in South Africa whereby the Hadley cell is analysed across different spatial gradients. The diagnostics used to represent the Hadley cell have traditionally been zonally symmetric.

2. Most studies using zonally symmetric diagnosis have defined the strength of the Hadley cell in each hemisphere by taking the maximum mass stream function in each hemisphere, however this study has further qualified this definition by taking the maximum stream function and dividing it by the difference in latitude (latitude corresponding to the maximum stream function minus latitude corresponding to the minimum stream function) to cater for the maximum expansion of the Hadley cell.

3. This is the first study to establish Granger causality between the Hadley cell and cloud cover as well as between the Hadley cell and sunshine duration. Formally establishing the causality of anomalously strong regional Hadley cell circulation in terms of cloud cover and sunshine duration over southern Africa is of profound importance within the context of future climate change over the region.

4. To our knowledge, no study has linked the local Hadley circulation to energy generation. Using the zonally asymmetric diagnostics the study managed to show that there is a link between the Hadley cell

and energy generation in the country. The Hadley cell can further be used as a proxy in identifying places with solar potential in the generation of energy over South Africa.

3. Future Work

1. In Chapter 2 diagnostics for the asymmetric Hadley cell which could be used in South Africa were established. From the diagnostics of the Hadley cell links between the Hadley cell and cloud cover were established over South Africa. These links were stronger in JJA than DJF and this is attributed to the dominance of weather systems (Hou and Lindzen, 1992) that account for weather in the summer rainfall region of South Africa. It is therefore obvious that in DJF, the Hadley circulation cannot fully account for the South African weather; weather systems also have a role to play in this interplay. A diagnostic that could be used as a proxy to rainfall producing systems in South Africa is therefore proposed. Such diagnostics could be used, to examine links between the Hadley cell and weathers systems.

2. Momentum flux is used as a proxy to storm tracks (Wettstein and Wallace, 2010). Variations in storm tracks are mainly equivalent barotropic and are caused by changes in momentum fluxes (Trenberth and Stepaniak 2003). Storm tracks of the Southern Hemisphere play an integral role in defining the weather and climate of

the hemisphere (Hoskins and Hodges, 2005). As a matter of fact they are actually weather systems that often pass in the SH midlatitudes disrupting the westerly flow. Storm tracks are often called storms (including both low and high pressure perturbations centers) (Trenberth and Stepaniak, 2003) and they include the axis of the surface frontal frequency maximum, the axis of minimum frequency of cyclone centers (Tyson and Preston-Whyte, 2000).

In South Africa, maximum values of momentum flux are located southwards of South Africa at latitudes 30-40°S in winter and further southwards in summer and these are the regions where storm tracks are also located. Storm tracks in the form of midlatitude cyclones move along the southern coast of Africa during winter (Apr-Sep) resulting in rainfall (Majodina and Jury, 1996). Another example of the effect of momentum flux to South African weather is the increase in monthly rainfall totals over the central interior of South Africa due to the strong poleward momentum flux brought by temperate tropical troughs over the subcontinent (Harrison, 1984). Temperate troughs are responsible for the poleward migration of the mean meridional circulation of momentum and they are the main contributor of rainfall over the summer rainfall region (Harrison, 1984) and are channels for large scale transfer of momentum from the tropics to the midlatitudes. In the light of the above, we propose a construction of momentum flux diagnostics that could be used as proxy for all weather systems over the South Africa. The momen-

tum diagnostics could be further used to show the effect of weather systems to the Hadley circulation in South Africa.

3. In Chapter 4, causality between the Hadley cell and sunshine was investigated. A strong causality of the Hadley cell to sunshine duration was found in DJF and weak in JJA; this is attributed to seasonality of the angular momentum-conserving limit. According to Merlis et al. (2013), changes in insolation have a greater effect in the Moonsonal Hadley circulation during summer as opposed to winter because of the seasonality of the angular momentum-conserving limit. During winter in the descending branch of the Moonsonal Hadley cell, the energetics do not have direct implication to the strength of the Hadley cell. Conversely, in summer in the ascending branch, the Moonsonal Hadley cell reacts to the thermodynamic and energetic changes since it is close to the angular-momentum conserving limit (Merlis et al., 2013). These energetic changes are mainly due to the top of the atmosphere insolation variations. During summer when there is more insolation, the massflux of the Moonsonal Hadley circulation increases and this affect the annual-mean Hadley circulation (Merlis et al., 2013). We propose that the role of angular momentum conserving limit to the Hadley cell and solar radiation over South Africa be fully investigated.

4. In Chapter 5 links between the Hadley cell, rainfall and temperatures were presented. As the Hadley cell is projected to strengthen,

rainfall and temperature are projected to decrease and increase respectively. Decrease in rainfall will affect water resources over South Africa. Therefore a study on future projections of the Hadley cell and its impact and water supply across South Africa is proposed.

4. CONCLUSIONS

This paper examines the links between the Hadley cell and rainfall over South Africa and showed how the changes in the Hadley cell under the RCP 8.5 setting could affect electricity generation in South Africa. An evidence of the strengthening of the Hadley cell and projected decrease in rainfall and increase in temperatures under the RCP8.5 settup over most parts of the country in MAM, JJA and SON was found. In DJF, the weakening of the Hadley was found and successively a tendency towards an increase in rainfall over the central and eastern parts of South Africa. The strengthening of the Hadley cell in general, has positive implications on electricity generation through renewable energy technologies especially solar technologies.

Renewable energy technologies play a major role in the energy security. Therefore the Hadley cell can be also used as a proxy to identify regions which have more solar energy resources. Over South Africa, Hadley cell maximum intensification was found to be over the areas where sunshine duration is more, and this was found to be over the north western parts of South Africa (Mahlobo et al., 2018). It is over these regions that solar energy technologies are located. The promotion of so-

lar energy resource in South Africa will have economic, social and environmental benefits. The associated benefits include improved health due to the reduction of carbon emissions. More business opportunities in the renewable energy sector will lead to more jobs which is a current crisis in South Africa.

REFERENCES

Abakumova GM, Feigelson EM, Russak V , Stadnik VV, 1996. Evaluation of long term changes in radiation, cloudiness and surface temperature on the territory of the Formar Soviet Union, Journal of Climate. 9. 1319-1327.

Bergman and Salby, 1996. Diurnal variations of cloud cover and their relationship to climatological conditions, Journal of Climate. 9. 2802-2820.

Bergman and Salby, 1997. The role of cloud diurnal variations in the time-mean energy budget, Journal of Climate. 10. 1114-1124.

Ceppi P, DL Hartman, 2013. On the speed of the Eddy-Driven Jet and the width of the Haley Cell in the Southern Hemisphere, Journal of Climate. 26.3450-3465.

Choi J, Sun S-W, Lu J, Min S-K. 2014: Further observational evidence of Hadley cell widening in the Southern Hemisphere, Geophysics Research Letters. 41. 2590-2597.

Crook JA, Jones LA, Forster PM , Crook R, 2011. Climate change impacts on future photovoltaic and concentrated solar power energy output, Energy Environ.Science. 4. 3101-3109.

D'Abreton, PC, Tyson, PD, 1995. Divergent and non-divergent water vapour transport over southern Africa during wet and dry conditions. Meteorology and Atmospheric Physics. 55. 47–59.

Engelbrecht FA, Landman WA, Engelbrecht CJ, Landman S, Bopape MM, Roux B, McGregor JL ,Thatcher M, 2011. Multi-scale climate

modelling over Southern Africa -using a variable-resolution global model. Water S.A. 37. 647-658.

Falayi EO, Adepitan JO, Rabiu AB, 2008. Empirical models for the correlation of global solar radiation with meteorological data for Iseyin, Nigeria. International Journal of Physical Science. 3. 210-216.

Fu Q, Johanson CM, Wallace JM, Reichler T, 2006. Enhanced mid latitude tropospheric warming in satellite measurements. Science, 312, 1179..

Granger CWJ. 1969. Investigating causal relations by econometric models and cross spectral methods. Econometrica.. 37. 424-438. https://doi.org/10.2307/1912791

Grenfell JI, Shindell DT, Grewe V, 2003. Sensitivity studies of oxidative changes in the troposphere in 2100 using the GISS GCM, Atmospheric Chemistry and Physics. 3. 1267-1283.

Hamdy KE, 2007. Experimental and theoretical investigation of diffuse solar radiation: Data and models quality tested for Egyptians sites. Renewable Energy. 32. 73-82.

Harrison MSJ, 1984. A generalized classification of South African rain-bearing synoptic patterns systems. International Journal of Climatology. 4. 547-560.

Hart NCG, Reason CJC, Fauchereau N, 2010. Tropical- Extratropical interactions over southern Africa: Three cases of heavy summer season rainfall. Monthly Weather Review. 138. 2608-2623.

Hoskins BJ, Hodges KI, 2005. A new perspective on Southern Hemisphere storm tracks. Journal of Climate. 18. 4108-4129.

Hou AY, Lindzen RS, 1992. The influence of concentrated heating on the Hadley circulation. Journal of Atmospheric Science. 49. 1233-1241.

Hu Y, Fu Q, 2007. Observed poleward expansion of the Hadley circulation since 1979. Atmospheric Chemistry and Physics. 7. 5229-5236.

Hudson RD, Frolov AD, Andrade MF, Follette MB, 2003. The total ozone field separated into meteorological regimes. Part 1: Defining the regimes. Journal of Atmospheric Science. 60. 1669-1677.

IPCC, 2007. Climate Change 2007:Synthesis report: Contribution of working group I,II and III to the fourth Assessment Report of the Intergovernmental Panel on Climate Change IPCC, Geneva Switzerland, 104pp (Core writing Team, Pachauri RK, Resinger A (Eds)

Johanson CM, Fu Q, 2009. Hadley Cell Widening: Model Simulations versus Observations. Journal of Climate, 22, 2713-2725.

Kang SM, Lu J, 2012. Expansion of the Hadley Cell under Global Warming: winter versus summer, 25. Journal of Climate. 25. 8387-8393.

Karl TR, Steurer PM, 1990. Increased cloudiness in the United States during the 1st-half of the 20th century-Fact or Fiction. Geophysics Research Letters. 17. 1925-1928.

Keyser D, Schmidt BD, Duffy DG, 1989. A technique for representing three-dimensional vertical circulations in baroclinic disturbances. Monthly Weather Review. 177. 2463-2494.

Kruger AC, 2007. Trends in cloud cover from 1960 to 2005 over South Africa. Water SA. 33. 603-608.

Kruger AC , Esterhuyse DJ, 2005. Climate of South Africa: Sunshine and cloudiness, South African Weather Service,pp35.

Lau NC , Crane MW, 1995. A satellite view of the synoptic-scale organisation of cloud properties in midlatitude and tropical circulation system. Monthly Weather Review. 123. 1984-2006.

Liepert BG, 2002. Observed reductions of surface solar radiation at sites in the United States and worldwide from 1961 to 1990, Geophysics Research Letters. 29. 1421.

Loeb NG, Schuster GL, 2008. An observational study of the relationship between cloud, aerosol and meteorology in broken low-level cloud conditions, Journal of Geophysical Research. 113, D14214,doi:10.1029/2007JD009763

Loeb NG, Rutan DA, Seiji S, Wang W, 2014. Observing interannual variations in Hadley circulation atmospheric heating and circulation strength, Journal of Climate. 27. 4139- 4158.

Lorente, J, Redano A, De Cabo X, 1996. Influence of urban aerosol on spectral solar irradiance. Journal of Applied Meteorology and Climatology. 33, 406-415.

Lu J, Vecchi GA, Reichler T, 2007. Expansion of the Hadley Cell under global warming. Geophysics Research Letters. 34. L06805, doi:10.1029/2006GL028443.

Mahlobo, D.D., Ndarana, T., Grab, S. and Engelbrecht, F. 2018. Integrated climatology and trends in the subtropical Hadley cell, sunshine duration and cloud cover over South Africa. International Journal of Climatology. 39. 1805-1821.

Majodina M, Jury MR. 1996. Composite winter cyclones south of Africa:

evolution during eastward transit over the Agulhas warm pool .South African Journal of Marine Science, 17. 241-252.

Merlis TM, Schneider T, Bordoni S, Eisenman I, 2013. Hadley circulation to orbital precession part II; Subtropical continent. Journal of Climate. 26. 754-771.

Nicholson, S.E., 1981: Rainfall and Atmospheric Circulation during Drought Periods and Wetter Years in West Africa. Monthly Weather Review. 109, 2191–2208.

Norris JR, Wild M, 2007. Trends in aerosol radiative effects over Europe inferred from observed cloud cover, solar"dimming" and "brightening", Journal of Geophysical Research. 112. DO8214.

Pfister G, McKenzie RL, Liley JB, Thoas A, Forgan BW, Long CN, 2003. Cloud coverage based on all-sky imaging and its impacts on surface solar irradiance, Journal of Applied Meteorology and Climatology. 42, 1421-1434.

Qian T, Dai A, Trenberth KE, Oleson KW, 2006. Simulation of Global Land Surface Conditions from 1948 to 2004. Part I: Forcing Data and Evaluation. International Journal of Hydrometeorology. 7, 953-975.

Salby ML, Hendon HH, Woodberry K, Tanaka K, 1991. Analysis of global cloud imagery from multiple satellites. Bulletin of the American Meteorological Society. 72, 467-475.

Schwendike J, Govekar P, Reeder MJ, Wardle R, Berry GJ, Jakob C, 2014. Local Partitioning of the overturning circulation in the tropics and the connection to the Hadley and Walker circulations, Journal of

Geophysical Research. 119.

Seidel DJ, Randel WJ, 2007. Recent widening of the tropical belt: Evidence from tropopause observations. Journal of Geophysical Research. 112. D20113

Seidel DJ, Fu Q, Randel WJ, Reichler TJ, 2008. Widening of the tropical belt in a changing climate. Nature Geoscience. 1, 21-24.

SEI–Stockholm Environment Institute, 1995. Version 95.0, LEAP User Guide Stockholm Environment Institute, Boston.

SEI-Stockholm Environment Institute, 2008. Long Range Energy Alternatives Planning System, Tellus Institute, Boston.

Singleton AT, Reason CJC, 2007. Variability in the characteristics of cut-off low pressure systems over subtropical southern Africa. International Journal of Climatology. 27. 295-310.

Swarztrauber, PN, 1974. The direct solution of the discrete Poisson equation on the surface of a sphere. Journal of Computational Physics, 15, 46-54.

Trenberth KE, Stepaniak DP, 2003. Seamless poleward atmospheric energy transports and implications for the Hadley Circulation. Journal of Climate. 16. 3706-3722.

Tyson PD, Preston-Whyte RA, 2000. The Weather and Climate of Southern Africa, Oxford University Press, pp396.

van Heerden J, Taljaard JJ, 1998. Africa and Surrounding Waters. In: Karoly D.J., Vincent D.G. (eds) Meteorology of the Southern Hemi-

sphere. Meteorological Monographs. American Meteorological Society, Boston, MA

Wallace JM, Hobbs PV, 2006. Atmospheric Science: An Introductory Survey. 2nd ed. Academic Press, 483pp.

Wang X, Key JR, 2003. Recent trends in Arctic surface, cloud and radiation properties from space. Science, 299, 1725-1728.

Wang X, Key JR, 2005a. Arctic surface, cloud and radiation properties based on the AVHRR Polar Pathfinder dataset. Part 1: Spatial and temporal characteristics. Journal of Climate, 18, 2558-2574. Wang X, Key JR, 2005b. Arctic surface, cloud and radiation properties based on the AVHRR Polar Pathfinder dataset. Part 1: Recent trends. Journal of Climate, 18, 2575-2593.

Warren SG, Hahn CJ, London J, Chervin RM, Jenne RL. 1986. Global Distribution of total cloud cover and cloud type over land. NCAR Tech Note NCAR/TN-273+ST, 29 99,199 maps [Available from National Center for Atmospheric Research, PO Box 3000, Boulder, CO 80307]

Wettstein JJ, Wallace JM, 2010. Observed Patterns of Month-to-Month Storm-Track Variability and Their Relationship to the Background Flow. Journal of Atmospheric Science. 67. 1420-1437.

Wild M, Gilgen H, Roesch A, Ohmura A, Long CN, Dutton EG, Forgan B, Kallis A, Rassak V , Tsvetkov A , 2005. From dimming to brightening, Decadal changes in solar radiation at Earth's surface, Science, 308, 847-850.

Young GHF, McCarrol D, Loader NJ, Gagen MH, Kirchhefer AJ, Demm-

ler JC, 2012. Changes in Atmospheric circulation and the Arctic Oscillation preserved within a millennial length reconstruction of summer cloud cover from northern Fennoscandia. Climate Dynamics, 39, 495-507.